

# A feasibility study for the installation of 10 MW offshore wind turbines with an SSCV

## Master Thesis

M. van Beek

Delft University of Technology



“Front cover: Graphical representation of a single-lift installation with the Thialf, where the wind turbine components are supplied per barge.”

# A feasibility study for the installation of 10 MW offshore wind turbines with an SSCV

## Master Thesis

by

M. van Beek

to obtain the degree of Master of Science

at the Delft University of Technology,

to be defended on Tuesday May 29, 2018 at 3:00 PM.

Student number: 4109198

Thesis committee:	Prof. Dr. Ir. A. Metrikine,	TU Delft, Chairman
	Ir. J.S. Hoving,	TU Delft, Daily supervisor
	Dr. Ir. K.N. van Dalen,	TU Delft
	Ir. R. van Dijk,	Heerema Marine Contractors, Senior supervisor
	Ir. M. Bolk,	Heerema Marine Contractors, Daily supervisor

*This thesis is confidential and cannot be made public until May 29, 2023.*

An electronic version of this thesis is available at <http://repository.tudelft.nl/>.





# Preface

This thesis has been submitted in the partial fulfillment of the requirements for the degree of 'Master of Science' in Offshore and Dredging Engineering at the Delft University of Technology. The research was done in cooperation with Delft University of Technology (TU Delft) and Heerema Marine Contractors (HMC) in Leiden, where the research was performed. In this master thesis the feasibility was analyzed for the use of a SSCV for the installation of 10 MW offshore wind turbines.

First of all, I would like to thank Andrei Metrikine, the chairman of my graduation committee, for his pertinent observations and support during the meetings we had. Second, I would like to thank Jeroen Hoving, my daily supervisor from TU Delft, for the interesting conversations we had and for helping me with the structure of my thesis. He consistently allowed this paper to be my own work, but steered me in the right the direction whenever he thought I needed it. I consider myself fortunate to have Radboud van Dijk and Mattijs Bolk as my supervisors from HMC, without your attention, enthusiasm and guidance, my work would not have been productive. Thank you Radboud, for your valuable inputs and suggestions during the modeling process of the project. Thank you Mattijs, for your moral support and always reminding me of the 'rode draad' of the thesis. Furthermore, I would like to express my gratitude to all other HMC employees who have taken an interest in my thesis topic and for making my stay at HMC even more special. For the guidance on the use of the ECN Install Tool, I would like to thank Ashish Dewan.

I must express my very profound gratitude to my parents and to Floris, for providing me with unfailing support and continuous encouragement throughout my years of study and through the process of researching and writing this thesis. And finally, last but by no means least, it was great sharing the daily struggles of the thesis life with my fellow graduation students at HMC. Thank you, Sophie, Gijs-jan, Jonathan, Bob, Bastiaan, Anner, Christiaan, and Kris for your friendship and for making my time at HMC more enjoyable.

*M. van Beek  
Leiden, May 2018*



# Abstract

Since the oil price collapse at the end of 2014, operators in the offshore industry experience a decline in revenues and a need for downsizing. Simultaneously, the wind industry is growing every year, as an increasing amount of companies and consumers are investing in green energy. This creates opportunities for Heerema Marine Contractors (HMC), as they have ample experience in offshore installations, operations and maintenance. Currently, in most cases a Jack-Up Vessel (JUV) is used to install offshore Wind Turbine Generators (WTGs). With the exception of Hywind, a wind farm of floating wind turbines commissioned with a Semi-Submersible Crane Vessel (SSCV) near shore and thereby protected from large waves, there is little experience in installing large WTGs with a floating vessel in offshore sea states. Current trends in Offshore Wind Farm (OWF) development are the upscaling of WTGs and installations in deeper waters, both resulting in more complex operations. In the current market however, there are many installation operators with lower priced JUVs. Therefore, to compete and make it economically viable for HMC to enter this industry, HMC must be able to install WTGs at a faster rate than the rate of conventional installation vessels.

The main objective of this master thesis is to determine the economic and technical feasibility for HMC to enter the offshore wind industry as an installation operator. First, the attractiveness of the offshore wind market is analyzed. For the analysis of the offshore wind market as a business environment the theoretical framework 'PESTLE' is applied. Through the application of the 'Porter's Five Forces' model, the competitive position of HMC as a potential entrant to the offshore wind market is analyzed. Second, insight is gained under which conditions it is economically feasible to use a SSCV for the installation of 10 MW WTGs. Different logistical methods are compared in terms of installation time and installation costs, as a function of site particularities, and by comparing the use of a JUV, a purpose-build installation vessel and a SSCV. As the installation of WTGs makes up a significant percentage of the total costs of a project, the workability of the installation vessel is of great importance. To address the technical feasibility, this thesis aims to quantify the influence of wave forecast on the workability of installing a fully-assembled 10 MW WTG with a SSCV.

The offshore wind market in the North Sea as a business environment is evaluated to be attractive. Additionally, there is a large potential for building new OWFs in the North Sea and governmental support is significant and assumed to be stable in the future. The trends that OWF development moves into deeper waters and further offshore, as well as the increase in size of wind turbines are all positive for floating installation vessels with larger crane capacity, as many JUVs have reached their maximum capacities. Although the barriers to enter the OWE industry are high, the power of the OWF developers is significant and the price competition among installation operators is fierce, the threat of alternative WTGs becoming mainstream is small due to economies of scale and the enormous potential of new OWF development. It is recommended to enter the market with a HMC SSCV and focus on the installation of extra-large WTGs ( $\geq 10$  MW) and thereby succeed in the offshore wind market by specialization.

Based on the current ECN Tool (version 2.1) and the assumptions made, it is economically feasible to use an SSCV for the installation of completely pre-assembled wind turbines in a large OWF ( $> 1500$  MW). In the scenario used in the ECN Tool, the duration of the WTG lift, installation and the SSCV sailing to the next TP should be less than six hours. According to the industry, a great concern is the movement of the SSCV during the set-down, and thereby making it a complex operation with impact loads that are more difficult to predict.

Wave forecasting is the key that can take away this concern, however it is still an 'unproven innovation' in the industry. With the use of a 2 minute wave and motion forecast, the waiting on weather for the 'WTG lift' and 'WTG set-down' on the TP can be reduced from 28 hours per turbine to 7 hours for the 'WTG lift' and 48 minutes for the 'WTG set-down' (on an average of 5 months). Subsequently, based on a 2 minute wave and motion forecast, the impact load on the bottom of the tower and the TP can be reduced by 13 % by choosing an optimal sea elevation for the set-down moment. As the average waiting on weather time is relative high for installing the third blade and lifting the WTG, it is furthermore recommended to investigate the influence on wave radar forecast on these steps. The implementation of wave radar technology during the installation process, is to be investigated further. The estimation of step durations and operational limits, has a large influence on the analysis of installation time and accompanying costs. Additionally, a closer and more detailed cooperation with industry experts is required to estimate new durations more accurately.

# Abbreviations

BFLOW	Bottom Fixed Offshore Wind
COG	Centre of Gravity
DCV	Deepwater Construction Vessel
DP3	Dynamic Positioning 3
DTU	Danish Technical University
EC	European Commission
ECN	Energy research Center of the Netherlands
EOM	Equation of Motions
EPIC	Engineering, Procurement, Installation & Construction
ETS	European Trading System
EU	European Union
FID	Final Investment Decision
HMC	Heerema Marine Contractors
JUV	Jack-Up Vessel
MW	Mega Watt
O&M	Operations & Maintenance
OWE	Offshore Wind Energy
OWF	Offshore Wind Farm
R&D	Research & Design
RWT	Reference Wind Turbine
SDA	Significant Double Amplitude
SSCV	Semi-Submersible Crane Vessel
TP	Transition Piece
WTG	Wind Turbine Generator



# Sign conventions

## LiftDyn

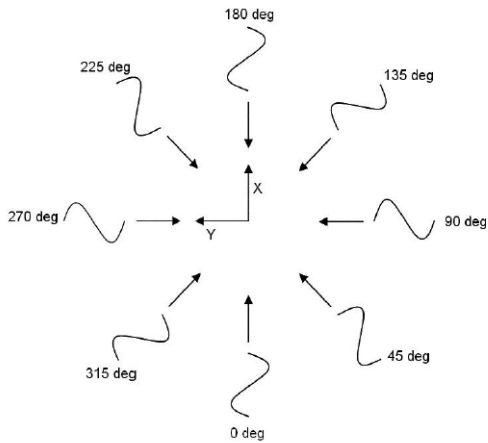


Figure 1: Sign convention LiftDyn: Wave direction coming from, counter clock wise w.r.t. local body axis, 0 deg wave following vessel

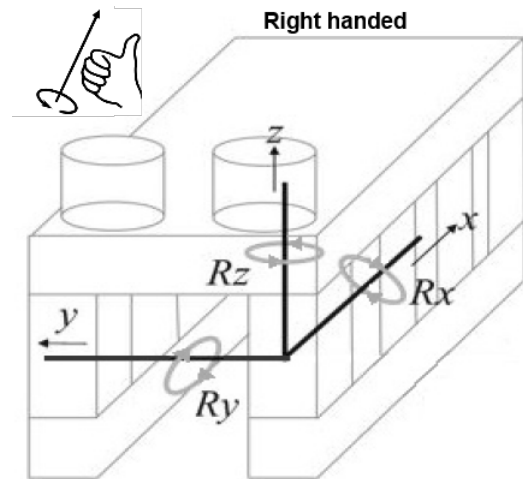


Figure 2: Sign convention LiftDyn: Right handed coordinate system, Positive: Z up, x to bow, y to PS, yaw counter clock wise, roll SB down, Pitch bow down

## OrcaFlex

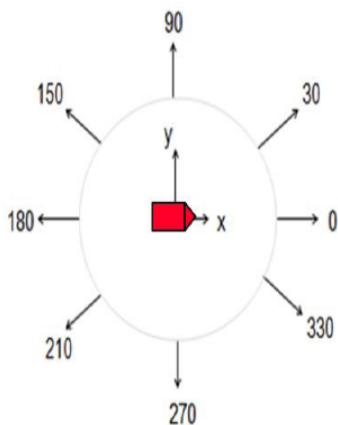


Figure 3: Sign convention OrcaFlex: Wave direction going to, counter clock wise w.r.t. local body axis, 0 deg wave following vessel



# Contents

<b>Preface</b>	<b>iii</b>
<b>Abstract</b>	<b>v</b>
<b>Abbreviations</b>	<b>vii</b>
<b>Sign conventions</b>	<b>ix</b>
<b>1 Research definition</b>	<b>1</b>
1.1 Company profile . . . . .	1
1.2 Research relevance . . . . .	2
1.3 Motivation . . . . .	2
1.4 Scope and objectives . . . . .	3
1.5 Thesis lay-out. . . . .	4
<b>2 Offshore wind energy in the North Sea</b>	<b>5</b>
2.1 Status quo European offshore wind market. . . . .	6
2.2 External factors influencing the offshore wind energy industry . . . . .	7
2.2.1 Political and legislative support . . . . .	8
2.2.2 Technological development . . . . .	9
2.2.3 Economic growth . . . . .	10
2.2.4 Environmental policies . . . . .	11
2.2.5 Public opinion. . . . .	13
2.3 Competitive position as installation operator . . . . .	13
2.3.1 Intensity of competition. . . . .	13
2.3.2 Power of wind farm developers as consumers . . . . .	15
2.3.3 Power of wind turbine manufacturers as suppliers . . . . .	15
2.3.4 Threat of substitutes . . . . .	16
2.3.5 Barriers to entry. . . . .	17
2.4 Conclusion . . . . .	17

<b>3</b>	<b>Installation phase in the development of an offshore wind farm</b>	<b>19</b>
3.1	Focus of the supply chain . . . . .	19
3.2	Capacities of installation vessels . . . . .	20
3.3	Pre-assembly and re-supply strategies . . . . .	21
<b>4</b>	<b>Comparison of installation costs depending on pre-assembly and re-supply strategies</b>	<b>23</b>
4.1	Set-up of analysis . . . . .	23
4.1.1	Relevance to the existing literature . . . . .	23
4.1.2	Scope of the analysis. . . . .	23
4.1.3	ECN Install Tool. . . . .	24
4.1.4	Scenarios based on installation vessel, pre-assembly and re-supply strategy . . . . .	24
4.1.5	Model characteristics for the ECN Install Tool. . . . .	25
4.2	Trends installation costs per vessel . . . . .	26
4.2.1	Installation costs for varying offshore wind farm size and distance to port . . . . .	26
4.2.2	Sensitivities on step duration and day-rate vessel . . . . .	28
4.3	Challenges for the single-lift installation with a floating vessel . . . . .	30
<b>5</b>	<b>Analysis on resonance risk and impact loads on the offshore wind turbine</b>	<b>31</b>
5.1	Operational limits and weather restrictions during the installation phase . . . . .	31
5.2	Constructing the offshore wind turbine . . . . .	32
5.2.1	Sequence of critical path . . . . .	32
5.2.2	Crane position . . . . .	33
5.3	Free-hanging wind turbine in the installation phase . . . . .	34
5.3.1	Frequency domain analysis . . . . .	35
5.3.2	Radii of gyration of offshore wind turbine . . . . .	36
5.3.3	Resonance risk . . . . .	37
5.3.4	Influence mass and wires on operability. . . . .	40
5.4	Set-down moment of the wind turbine in the installation phase . . . . .	41
5.4.1	Time domain analysis . . . . .	41
5.4.2	Mating technique . . . . .	41
5.4.3	OrcaFlex model. . . . .	41
5.4.4	Impact loads during set-down moment in one sea state . . . . .	43

---

5.4.5	Impact load during set-down moment in multiple sea states . . . . .	46
5.4.6	Impact load during optimal set-down moment . . . . .	50
5.5	Impact load reduction with a docking system of 3 units . . . . .	51
<b>6</b>	<b>Optimization of workability by reducing required time-frame for set-down</b>	<b>53</b>
6.1	Sequence tool . . . . .	53
6.2	Waiting on weather for installation of entire wind farm . . . . .	54
6.3	Uptime analysis. . . . .	54
6.3.1	Wave radar forecast . . . . .	54
6.3.2	Semi-deterministic Matlab model . . . . .	55
6.3.3	Increase in uptime percentage by reducing time-frame for set-down moment. . . . .	56
6.4	Average waiting on weather with new time-frame . . . . .	58
6.5	Total installation time for installation entire wind farm. . . . .	58
<b>7</b>	<b>Conclusions and recommendations</b>	<b>61</b>
7.1	Conclusions. . . . .	61
7.1.1	Offshore wind market. . . . .	61
7.1.2	Economic feasibility . . . . .	62
7.1.3	Technical feasibility. . . . .	62
7.2	Recommendations . . . . .	62
<b>A</b>	<b>Appendix A</b>	<b>65</b>
A.1	Vessel characteristics . . . . .	65
A.1.1	Deck configuration of pre-assembly strategies . . . . .	65
A.1.2	Bolted connections . . . . .	66
A.1.3	Vessel costs . . . . .	66
A.1.4	Step duration for a jack-up vessel . . . . .	67
A.1.5	Sailing route from port to site location . . . . .	68
A.2	Dimensions offshore wind turbine and lift-frame . . . . .	69
A.3	Mode shapes computed with LiftDyn . . . . .	71
A.4	Impact loads on buckets during set-down. . . . .	72
A.5	Tension hoist wires . . . . .	74

---

A.6	Unity check for modified environment . . . . .	75
<b>B</b>	<b>Appendix B</b>	<b>77</b>
B.1	Matlab codes . . . . .	77
B.1.1	Matlab code: generate data files as input for OrcaFlex. . . . .	77
B.1.2	Matlab code: Uptime analysis . . . . .	78
B.1.3	Matlab code: Modify environment as input for Sequence Tool. . . . .	84
B.1.4	Matlab code: Generate dataset from result of OrcaFlex simulations . . . . .	85
B.1.5	Matlab code: Function for post-retrieving data of OrcaFlex simulations . . . . .	86
B.1.6	Matlab code: Generate scatterplot from OrcaFlex simulations. . . . .	88
B.1.7	Matlab code: Used script for IFF. . . . .	89
B.1.8	Matlab code: Used script genwave . . . . .	92
	<b>List of Figures</b>	<b>97</b>
	<b>List of Tables</b>	<b>103</b>
	<b>Bibliography</b>	<b>105</b>

# Research definition

## 1.1. Company profile

Heerema Marine Contractors is a company specialized in the design, construction, transporting and installation of offshore facilities for the oil and gas industry. It started in 1948 as a small construction company in Venezuela. In the 1960s it expanded to the North Sea oil and gas industry and started operating crane vessels. Together with the commissioning of the world's first semi-submersible crane vessels, Balder and Hermod, and with an innovative dual-crane feature, Heerema acquired the position of the industry leader. With the Aegir, a deep water construction vessel, Heerema is capable of executing complex infrastructure and pipeline projects in ultra-deep water. Heerema built up considerable expertise with Engineering, Procurement, Installation and Construction (EPIC) contracts, which achieved cost reductions for their clients. Currently, Heerema is an international organization specialized in the engineering and fabrication of large and complex structures for the offshore oil and gas and energy-related business. Heerema is specialized in producing large one of a kind projects with high precision [1].



Figure 1.1: Aegir



Figure 1.2: Balder



Figure 1.3: Thialf



Figure 1.4: Sleipnir

The fleet is consisting of Deepwater Construction vessel (DCV) Aegir (Fig.1.1), DCV and Semi-Submersible Crane Vessel (SSCV) Balder (Fig.1.2), SSCV Thialf (Fig.1.3) and anchor handling

tugs, cargo barges and launch barges. A new Semi-Submersible Crane Vessel, the Sleipnir (Fig.1.4), is under development and will be operational in 2019.

## 1.2. Research relevance

Since the oil price collapse in the end of 2014, barrels are currently sold at about \$64 [2]. Even though the average crude oil price per barrel is volatile last years, there is an overall rise started in July 2017 from \$48 [3]. According to executives in the industry it is uncertain if and when oil returns to \$90 or \$100 a barrel [4]. Investments in upstream operations in the oil and gas industry are decreasing every year and this trend will continue next year, which will represent the longest investment decline period in the history of the industry according to the International Energy Agency [5][6]. Subsequently, the amount of new projects contracted for the coming years is decreasing for Heerema. As most of the company's operating in the oil and gas industry, they experience a decline in revenues and a need for downsizing [7].

More than 90% of the power that is currently used in Europe, is obtained by the processing of fossil fuels like coal, natural gas, and oil [8]. Besides that the extraction of these sources is limited,  $CO_2$  on a large scale is released during combustion. Thereby, it poses possible environmental concerns [8]. Although producing the materials for and constructing of wind turbines also leads to  $CO_2$  emissions, the  $CO_2$  release due to combustion of fossil fuels is much more significant [8]. In a European context it has been agreed that the target for 2020 is that 14% of total Dutch energy consumption must come from renewable sources. One of these options is wind energy, onshore as well as offshore [9]. The wind industry is growing every year, especially since a growing amount of companies and consumers are interested to invest in green energy. This can create opportunities for companies that have experience in offshore installation and offshore operations and maintenance [10].

There are many companies that made the transition from the oil and gas industry to the offshore wind industry. On the one hand, there are energy supply companies that switch from coals, oil and gas to renewables and on the other hand there are operators in the offshore industry having experience in installation and maintenance works. Mostly energy suppliers, like Vattenfall, made the transition to be a project developer of an entire wind farm and operators providing a certain technique, equipment or service, like A2SEA, made the transition to be an operator in the offshore wind industry [11]. Other companies, like Van Oord and Ørsted became both; they are responsible for the development of an entire wind farm but they are also an integrated operator with in-house engineers. The resemblance in these transitions is the adaptation to a completely different type of project development. From big yields and one-of-a kind projects in the oil and gas industry to an aim for cost reduction, dependency on subsidies and batch production per project in the wind industry [11].

For HMC it could be interesting to investigate the feasibility of an SSCV as a new possible installation vessel for installing large wind turbine generators (WTG). Besides Hywind, a wind farm of floating wind turbines commissioned with the SSCV Saipem 7000 near shore, protected from large waves, it is never done before in offshore sea states [12]. This study adds to the existing literature by comparing installation strategies, including the use of a SSCV, taking trends in increased size of wind turbines, and development further offshore and in deeper waters into account [13].

## 1.3. Motivation

As mentioned before, there are less projects for Heerema to perform because of the declining oil and gas industry[7]. With its vessels and engineering expertise, it can be an opportunity for Heerema to enter the growing offshore wind market. Ten years ago the discussion started

about which role Heerema can play in this rising industry. Even though the company gained some experience in installing converter stations for offshore wind farms [14], serious attempts were never made to conquer a position in the offshore wind market. Now the debate is triggered again because the niche market of ten years ago has developed itself into one of the fastest growing industrial segments of the world [13]. Additionally, the trend in the upscaling of turbines, resulting in more complex installation projects can be interesting for Heerema. Therefore, Heerema wants to know if and how they should enter the offshore wind market as an installation operator.

Despite the cost reduction trend in the wind industry, most wind assets are still unable to cover the cost of plant over their asset lifetime through today's price levels in the energy market [15]. It is a challenge to make profit during the development of a wind farm, and also during the engineering and construction phase. In the current market there are enough installation operators with lower priced jack-up vessels, so to compete economically Heerema should install turbines at a faster rate or the installation vessels should have unique capacities. To be able to do this some challenges have to be overcome: gain a position in the offshore wind industry as an installation operator, optimize the supply chain, ensure a safe transportation and installation of components of the wind turbine, analyze the wind loading and impact loads during the installation of the wind turbine on the foundation, optimizing the vessel operability limits during the installation.

## 1.4. Scope and objectives

The main objective of this master thesis is to determine the economic and technical feasibility for Heerema to enter the offshore wind industry.

Due to the limited duration of this master thesis, two specific challenges were chosen within the feasibility framework. By comparing different installation strategies for installing an offshore wind turbine, insight is gained under which conditions it is economically feasible to use an SSCV for the installation of a wind turbine. Although there are many technical challenges related to the installation phase, the soft landing of the wind turbine on the transition piece is a crucial and most concerning operation when utilizing a floating installation vessel. The goal of the second section therefore, is to determine the influence of wave forecast on the workability for installing a fully-assembled 10 MW WTG with a SSCV.

Therefore, the following sub-objectives are set to attain the main objective:

1. To analyze the attractiveness of the offshore wind market, and identify the factors influencing the competitive position of Heerema entering and operating in this market.
2. To increase the transparency in logistical methods for installing offshore wind turbines in terms of installation time and installation costs, as a function of site particularities, and by comparing the use of a jack-up vessel, a purpose-build installation vessel and a SSCV.
3. To quantify the influence of a smaller step duration of the most weather restricted operation, the set-down of a completely pre-assembled WTG with a SSCV, on the workability.

This thesis is focusing on the installation of three bladed offshore WTGs with a capacity of 10 MW in the North Sea. According to WindEurope, an association based in Brussels, promoting the use of wind power in Europe and analyzing wind market trends, the North Sea has the greatest economically attractive potential compared to the Baltic Sea and the Atlantic Sea [16]. Because of this potential, and to narrow down the scope, only the developments in the North Sea are analyzed.

The scope excludes the installation of the substructure and the transition piece (TP). It is

assumed that the transition piece is connected on a fixed substructure, as they represent 99% of all installed substructures in Europe [17].

## 1.5. Thesis lay-out

This report consists of seven chapters that will contribute to the research of this thesis. Chapter 1 contains the motivation and objective of this research. In Chapter 2 the current trends in the offshore wind market are analyzed to understand the competition between installation operators. The following part of this thesis consists of two sections; an economical part researching the installation phase of the development of an offshore wind farm and a technical part focusing on two specific operations during the installation phase: the free-hanging and the set-down.

Chapter 3 elaborates on the supply chain in the transportation and installation phase, and capacities of different types of installation vessels. In Chapter 4 three installation strategies are compared in terms of installation time and installation costs as a function of site particularities. The chapter ends with some of the technical challenges occurring during installation with a SSCV, of which the soft-landing is assumed to be a potential bottleneck for a single-lift installation. This operation will be the focus of the technical feasibility study. Chapter 5 focuses on building a general model of a free-hanging wind turbine that is completely assembled. Once the mode shapes of the model in the frequency domain are checked for a risk for resonance, impact loads during the set-down of the wind turbine on the transition piece are analyzed. In Chapter 6 the workability is optimized by taking a shorter time frame for the set-down moment. The final chapter, Chapter 7, answers the research question by concluding the two sections. For these conclusions, all retrieved information of this research is used. Furthermore several recommendations are provided in Chapter 7. These recommendations will focus on identifying opportunities for further research. Figure 1.5 shows the report structure and synergy between the seven chapters.

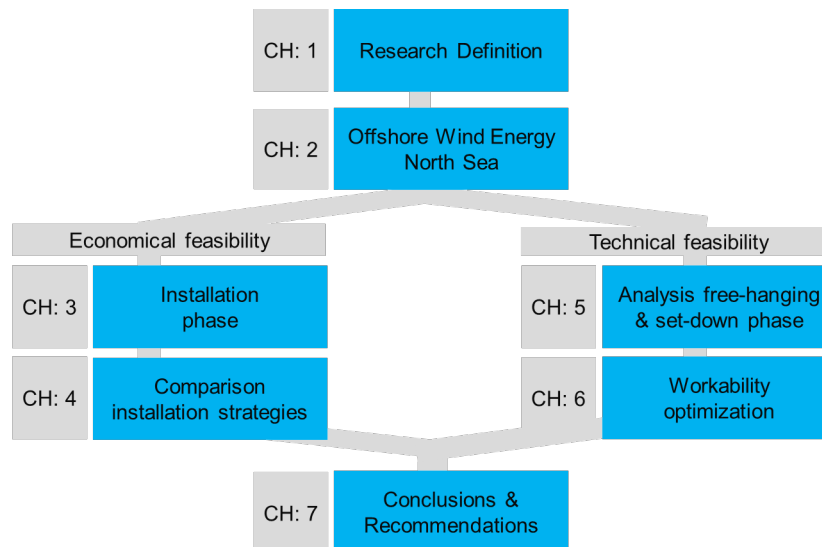


Figure 1.5: Structure of report

# 2

## Offshore wind energy in the North Sea

The main question in this chapter aims to answer is whether the Offshore Wind Energy (OWE) industry is attractive for Heerema to operate in. First, significant factors influencing the industry's further development and deployment in the North Sea are identified, to attain an understanding of the business environment of the OWE industry. Second, the intensity of competition in the market for installation operators of Wind Turbine Generators (WTGs) is evaluated, by looking at the power of substitutes, buyers, suppliers and barriers to enter the industry.

### **Method**

To analyze the offshore wind market as a business environment a theoretical framework called 'PESTLE' is applied. Political, Economic, Social, Technological, Legislative, and Environmental factors are influencing the development and current state of the offshore wind industry, indicated in the outer circle in Fig. 2.1. It offers insight into the main drivers in the energy sector and the dependency of a wind turbine installation operator on changes at a macro level. This analysis will also help understanding market movement towards growth or decline, and its potential and direction for operations. Through the application of the 'Porter's Five Forces' model the competitive position of Heerema as a potential entrant to the offshore wind market is analyzed in section 2.3. The model identifies and analyses how the following five forces determine the balance of power in a situation: supplier power, buyer power, competitive rivalry, threat of substitution and threat of new entry (represented in red circles in Fig. 2.1).

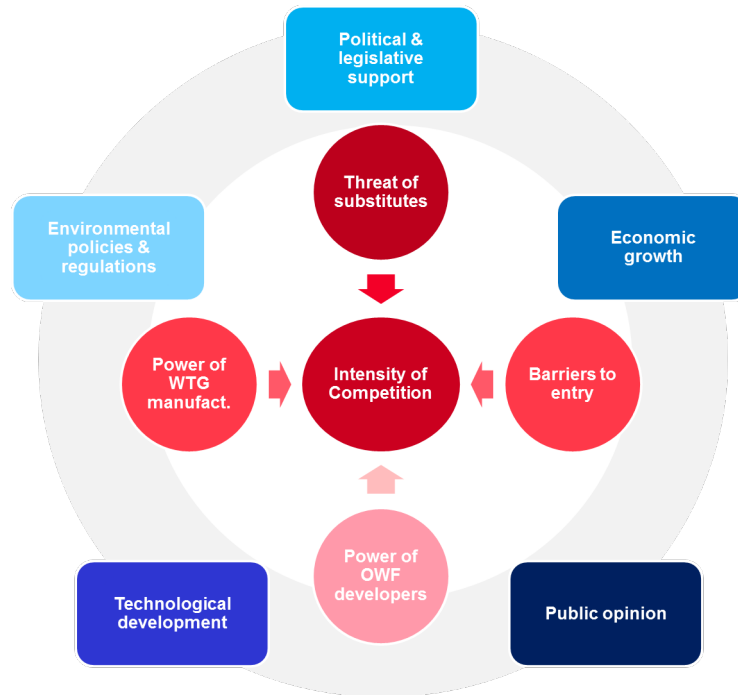


Figure 2.1: Theoretical framework of Porter's Five Forces (red) and PESTLE model (blue)

## 2.1. Status quo European offshore wind market

According to WindEurope, the cumulative installed offshore wind capacity reached 15.78 GW at the end of 2017 [17]. In the last year, a record of 3.148 GW of net additional installed capacity was seen, corresponding to 560 new offshore wind turbines across 17 wind farms (Fig. 2.2). Eleven projects are under construction in Germany and the UK. This will increase the total installed grid connected capacity by a further 2.9 GW, bringing the cumulative capacity to in Europe to 18.7 GW [17].

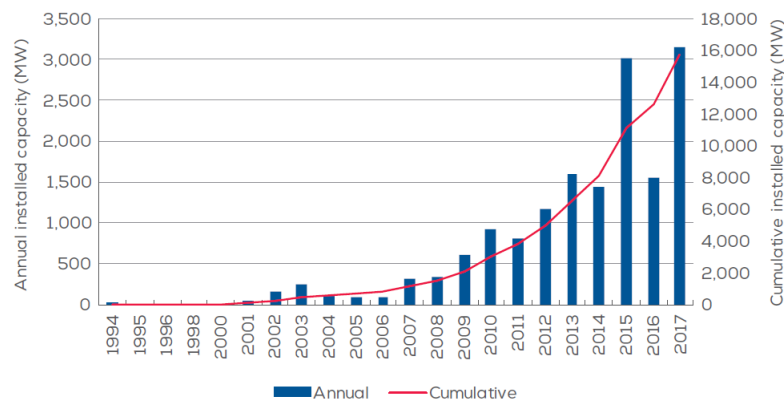


Figure 2.2: Cumulative and annual offshore wind installations in Europe (MW) [17]

A remarkable development in 2016 was the dramatic reduction in offshore wind prices. The Dutch Borssele 1 & 2 was auctioned at EUR 72/MWh in June, followed by a Danish nearshore tender in September at EUR 64/MWh. In November the winning bid for the Danish Krieger's Flak was EUR 49/MWh and then Borssele 3 & 4 in the Netherlands coming in at EUR 54.50/MWh in December. In March 2018 the first non-subsidized offshore wind tender was awarded by the Dutch government for the Hollandse Kust Zuid I & II. For the first time, in some circumstances, offshore wind energy is cheaper than onshore. The reasons for these reductions are the advances in technology and management, such as the deployment of new generation 8-10 MW WTGs [18]. The maturing of the industry results in a growing confidence of investors. Also the current low steel price has an influence on the tender offers. Much of the state of the steel industry can be tied to the rate of Chinese production. An overall economic slowdown in China results in a reduction of its steel production by 20%. This will cause demand outweigh supply for the first time in over a decade. This is expected to cause a sharp rise in steel prices during 2018 and lasting at least to 2020. It could result in a significant rise of offshore wind price in the near future or even a shift to foundations containing less steel, such as gravity based, in the long term [19].

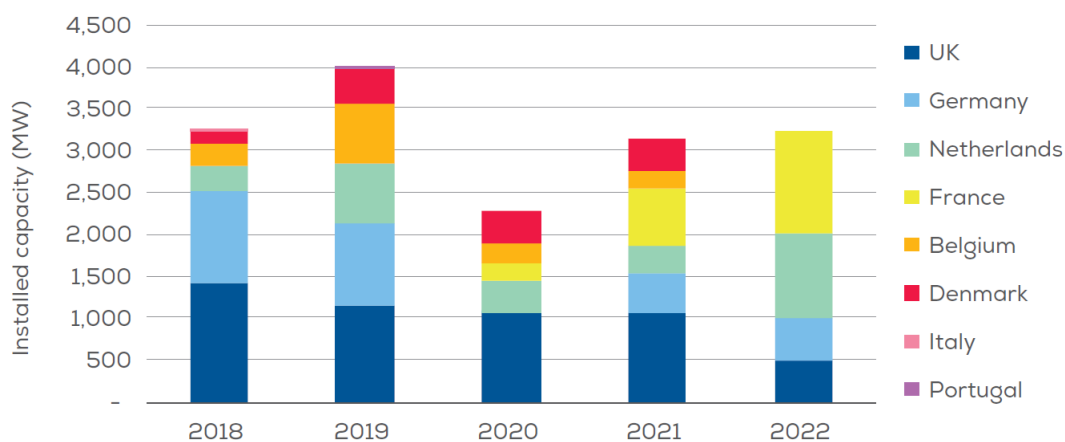


Figure 2.3: European market outlook for next five years [17]

By 2020 WindEurope expects a total installed European offshore wind capacity of 25 GW. As depicted in Figure 2.3, it is predicted that by 2022 another 16.1 GW of offshore wind energy will be commissioned. These are projects under construction and awaiting grid connection (2.9 GW), projects with a Final Investment Decision (FID) or projects awarded in auctions but without FID (together 13.2 GW).

## 2.2. External factors influencing the offshore wind energy industry

The OWE industry is currently influenced by political, environmental, economic and social factors, some to a greater extent than others. All these factors together determine market movement towards growth or decline, its potential and direction for operations.

Given the current subsidies, tax exemptions and allowances for development of offshore wind project, the governmental support is significant. Governments possess strong interest in offshore wind power because of  $CO_2$  reduction targets and thus, political and legislative changes are implemented to impact development and movement of the industry. However, this support from politicians is not certain in the future. Neither the speed and path of further development of offshore wind is certain.

Even though the energy production of OWFs is sustainable in an overall manner, the construction of wind farms may have a negative impact on marine wildlife through underwater noise emissions. Ongoing research is monitoring and technological solutions are designed to mitigate these effects. Nonetheless, concern for greenhouse gas emissions has already

resulted in implementation of various environmental policies and regulations establishing taxation on  $CO_2$  emissions, where all renewable energy sources are referred as environmental friendly. Together with the targets for climate change and a steadily increasing demand for electricity, a search for new alternatives is triggered. From an economic point of view offshore wind is believed to be capable of meeting energy demands in the near future. Still, the biggest obstacle for developers of new offshore wind projects is credit accessibility. Finally, public opinion has a significant influence on actions of some states and operations of various players in the market. Opinions that offshore wind is causing visual horizon pollution may trigger political intentions to assist the industry financially and legally to move into deeper waters. Logically, one of the incentives for the government to mitigate with the public is because the subsidies are paid with tax money.

### 2.2.1. Political and legislative support

Renewable energy sources are promoted by politicians because they can ensure security of energy supply, efficient utilization of resources, a sustainable development of cities and regions, and especially support to reach climate policy targets. These targets were set during the climate conference in Paris in 2015 between 195 countries. The main target is to stay below a temperature incline of 2 degree Celsius compared to 1990 levels, meaning a reduction in greenhouse gas emissions by 80-95% [20]. This will have a large impact on the current energy system.

According to the yearly progress report about the climate policy of the Member States the Commission concluded that targets for 2020 seems to be realistic they will succeed. This year a special report will be produced by the IPCC, the VN-panel for climate science, about the consequences of an increase of 1,5°C and the required emission reduction to reach that target. From 2023 on there will be an evaluation 'Global Stocktake' every five years to measure the reduction in carbon emissions worldwide [20]. The targets for 2030 are revised in a new Framework for climate and energy in June 2017 by the European Council [21]:

- A 40% cut in greenhouse gas emissions compared to 1990 levels
- At least a 27% share of renewable energy consumption
- At least 27% energy savings compared with the business-as-usual scenario

The European Commission presented a roadmap suggesting that, by 2050, the EU should cut its emissions to 80% through domestic reductions alone rather than relying on international credits. The accompanying milestone is 60% by 2040. All sectors need to contribute to the low-carbon transition according to their technological and economic potential. Figure 2.4 shows the  $CO_2$  emissions of the power sector almost totally have to be eliminated by 2050 [22]. Large investments in smart power grids are necessary for the transition to renewable sources, in order to transport wind energy from where it is produced to where it is consumed over large distances.

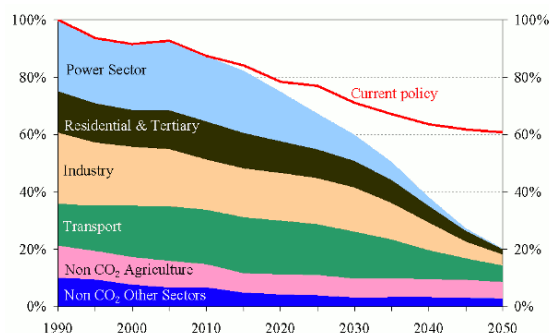


Figure 2.4: Possible 80% cut in greenhouse gas emissions in the EU (100%=1990) [22]

The question if these targets are realistic is difficult to answer. The Commission concludes with its roadmap that the transition is feasible and affordable, but requires innovation and investments. The EU would need to invest an additional €270 billion over the next 4 decades. However, accountability is missing in the Paris Agreement for the emissions budget nor for quantified emission reductions. The package of targets does not contain obligatory goals per country but only judicial binding targets for the EU as a whole.

To support the offshore wind industry in its development and further integration, various price subsidies, green certificates, tender schemes for the construction of OWFs, tax exemptions or reductions on energy production and quota obligations have been implemented. A feed-in tariff is a price subsidy that is formed to offer extra investment security and guarantee long-term stability to producers. Green certificates oblige the energy suppliers to deliver a portion of their electricity from renewables, and to finance the additional cost of producing green electricity themselves [23].

Decisive policies and clear procedures have boosted the growth of the offshore wind sector in some countries, but a lack of synergy in the EU as a whole prevents the industry from exploiting its full potential. In order to facilitate dynamic trade across borders and efficient sharing of reserves, unified regulation and a unified system operation are to be pursued [24].

### 2.2.2. Technological development

The offshore wind industry has been characterized by its strong focus on R&D, stimulated by a technological race between manufacturers. Supply chain efficiency and cost reduction are achieved not only through emphasis on new technologies but also through a focus on economies of scale and standardization.

The question often arises whether there is one single 'optimum' technology. A certain concept is chosen by the market that will be continuously improved, but it is not necessarily the technically optimal concept. An optimized wind turbine is the outcome of a complex function combining requirements in terms of efficiency, reliability, access, transport and storage, installation, visibility, support to the electricity network, noise emission, cost and so on. Most occurring typology in the industry covering about 99% of all wind turbines installed are horizontal axis turbine with an upstream three-bladed rotor. For foundations, monopiles remained the most popular substructure type in 2017, representing 87% [17]. The initial technology and system design applied for wind turbines offshore has been adapted from onshore-based versions and deployed in shallow waters.

As technology evolves and the most favorable shallow site locations have been commissioned, the OWE industry is moving into deeper waters, further offshore, or to harsher locations that are still shallow and not far offshore (Fig. 2.5, where the size of the bubble indicates the overall capacity of the site). The average water depth of wind farms completed in 2017 was 27.5 m and the average distance to shore was 41 km [17]. The OWFs far from shore are exposed to harsher weather conditions with fewer weather windows for the installation and Operations and Maintenance (O&M) of wind turbines. The electrical infrastructure and the grid connection increase in costs as a direct result. Moreover, offshore wind turbines have gradually increased in size in order to reduce cost and overall improvement in access to wind resources with height. Larger turbines can capture wind more efficiently and taller turbines can reach stronger winds. In 2017, the average size of installed offshore wind turbine was 5.9 MW, a 23% increase on 2016 [17]. Consequently, transportation and installation vessels were developed specifically designed to be operating in deeper waters and installing with larger crane capacity.

There are different opinions about how 'economies of scale' can be reached, by upscaling or farm optimization. Some argue turbines will continue to increase in size up to 15 MW or even 20 MW. A study from ECN concludes a turbine size 20 MW is technically feasible, with a rotor diameter of 250m [25]. The exact consequences are unknown, but the tip of

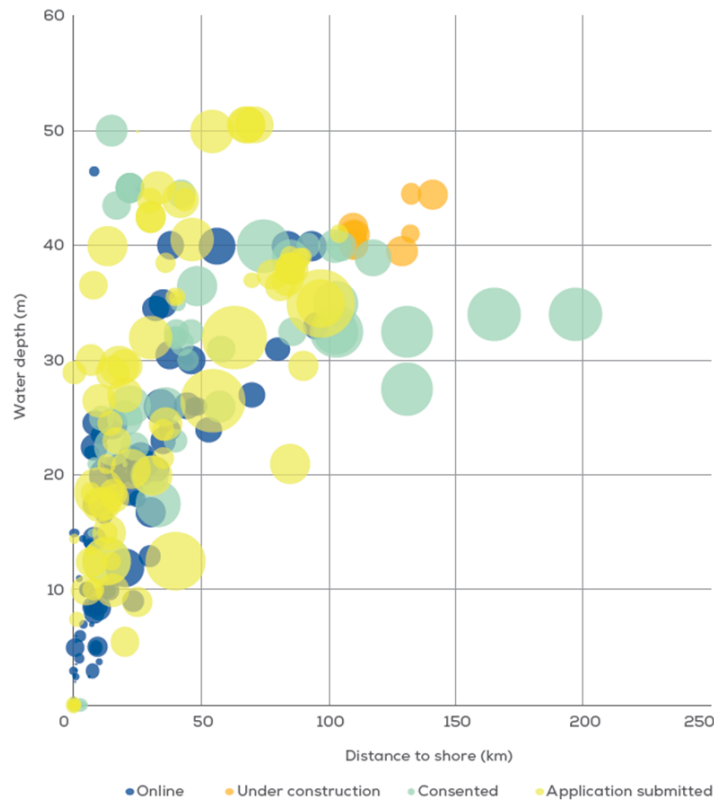


Figure 2.5: Average water depth and distance to shore of bottom-fixed offshore wind farms [17]

the blades of the largest turbines may exceed the speed of sound resulting in additional vibrations and thereby causing extra fatigue of the steel. Others argue 10 MW turbines will become mainstream and the number of turbines in a farm will increase resulting in 5 to 10 GW mega projects[23]. Interaction between turbines and value creation across the supply chain is the focus of optimization.

Shell believes that large integrated projects up to 10 GW are the means to reach the energy targets. With an anchor tenant, a party who takes the biggest risk for about half the project but pays a lower price for the site, a pilot project should be developed in order to gain experience [26]. It is not surprising Shell is promoting giga wind farms since they are one of the few companies with sufficient investment capital.

Ultimately, all research activities, including research regarding upscaling, are focused on reductions of the cost of energy. According to a study done by WindEurope, called 'UpWind', two directions were distinguished, which the industry is taking towards cost reductions [27]:

- Incremental innovation: cost reductions through economies of scale resulting from increased market volumes of mainstream products, with a continuous improvement of manufacturing and installation methods and products;
- Breakthrough innovation: creation of innovative products, including significantly up-scaled dedicated turbines, to be considered as new products.

### 2.2.3. Economic growth

Not only concerns for increasing prices of fossil fuels or wind energy being recognized as a proven source of clean and affordable energy drives European policy makers towards supporting this promising sector, but also the opportunity to realize economic potential plays a

role. The development of a new industrial sector in Europe is considered an innovative motor for regional and local development, creating jobs and facilitating growth of other economic sectors [13].

Not less than ten years ago, financial institutions and banks considered subsidies a commercial risk since any financial aid from the government can be as easily awarded as removed. This made it difficult for wind farm owners to raise capital required for the development of any offshore project in the wind industry. However, cost competitiveness and reduced risk perceptions have brought in market players last years who are looking to diversify their oil and gas portfolios. Many reports from organizations like WindEurope and IRENA provide information about the investment landscape and predict a positive outlook to attract more investors [13, 16]. As can be seen in Figure 2.6, in 2016 eleven projects reached a final investment decision with a combined investment value of €18.2 billion, representing an increase of 39% over 2015. Although a first decrease in investments since 2012 occurred last year, in 2017 six projects worth €7.5 billion reach the final investment decision, representing a decrease of 60% over 2016 [10].



Figure 2.6: New offshore wind investments and capacity financed: 2010 – 2017 (€bn) [17]

To realize the enormous potential of the North Sea, the offshore grid infrastructure is of great significance, with more projects in deeper waters and further offshore. The current offshore electricity grid is not yet suitable for large scale development of offshore wind. Grid connection, comprising onshore connection and international offshore interconnections are key barriers for large scale deployment. The inter-governmental organization The North Seas Countries' Offshore Grid Initiative has been launched, in order to offer a framework for regional cooperation to find common solutions in questions of current and possible future grid infrastructure developments in the North Sea [28]. Together with the EU this initiative is focused on transnational cooperation through exchange of specific experience, lessons learned from other OWE project, cost-efficient installation and industrialization in order to reach benefits of scale.

#### 2.2.4. Environmental policies

The OWE industry is highly supported and prioritized by the European Commission in the energy policy, in order to deliver sustainable, competitive and secure energy. New policies resulted in cutting subsidies from conventional energy sources and allocating these into renewable energy sources. This redistribution of subsidies, the increasing awareness of sustainable development and the European Emission Trading System (ETS) are incentives for companies to innovate in resources they use, known as eco-innovation [29].

The EU ETS is introduced by The Commission in 2005 to reduce the greenhouse gas emissions by letting certain company's pay for the amounts of carbon dioxide, nitrous oxide and perfluorocarbons they emit. There are around 10 000 large  $CO_2$  emitters – power and heat producers, oil refineries, steel manufactures, cement manufacturers, glass manufacturers,

brick and ceramics and the paper industry. A cap is set on the total amount of certain greenhouse gases that can be emitted by installations covered by the system. In time this cap will be reduced so total emissions decrease. Companies can buy so-called emission rights, which are interchangeable between companies. Companies polluting more than the cap, have to purchase additional rights and consequently have higher costs. Companies that deal more efficient with energy or use renewables, can sell their non-used emission rights [30].

The EU ETS system is criticized for several points. First of all the current price per right of five Euro's per ton  $CO_2$  is too low. This way there is no incentive for companies with big capital to reduce their emissions. Secondly, the German Renewable Energy Federation has criticized the European Parliament's propositions for a reform of the EU's ETS for being 'an empty shell' that cements the system's status as 'an ineffective instrument for climate protection'. The federation said the number of issued certificates had to be reduced by 4.7% per year to limit global warming as intended, while the 2.2% the parliament now agreed on they were failing to achieve this goal [31]. Third, the complexity of the EU ETS is experienced as a genuine problem. Particularly for small and medium-sized enterprises, the administrative burden associated with emissions trading is large in proportion to their emissions. That diminishes the cost effectiveness of the system and erodes the support for the system at the same time [32]. It is unknown what the consequences are if the system fails.

In order to understand and evaluate the extent to which offshore wind farms achieve a net carbon emission reduction over their lifetime, life-cycle assessments were made [33]. Variations in cost and carbon emissions estimates are affected by assumptions made in the calculation itself, methodological choices and data uncertainty. Every study differs in what is included, although mostly direct emissions that occur during construction, operation and decommissioning are taken into consideration; and indirect emissions that occur in the manufacture and transport of components such as turbines, foundations, cables etc. These emissions are normalized to the electricity produced over the project's lifetime to produce a 'carbon footprint' for the project [33].

Even though these studies can be seen as subjective, some common conclusions could be drawn. Several carbon life-cycle analysis of wind farms agree that the manufacturing and disposal phase of the life-cycle dominates its footprint. They also conclude that the offshore wind turbine has returned the investment in terms of energy after approximately nine months [34].

Moreover, environmental impacts of OWFs on local biodiversity and habitats are closely monitored. The existing EU legislation highly protects sensitive nature areas, and only grants permission for wind farm operation only when certain conditions have been met. Potential locations for offshore wind farms are to be granted approval and permits, in order to avoid substantial adverse environmental impacts. The EC has established a European Marine Observation and Data Network to facilitate access to data for environmental impact assessments [35]. National governments of Member States are becoming more involved in the site selection for OWF through detailed screenings of wind, water and soil conditions. This is a time consuming process and can take up to five years [36].

## Noise reduction

The construction noise of offshore wind farm foundation can effect marine wildlife in a negative manner. Fistuca's Blue Piling technology demonstrated that noise levels can be reduced when using a large water column to drive the pile in the soil, instead of the steel ram used by conventional hammers. A combustion throws up this water column, which falls back on the pile under the force of gravity, hence delivering two blows. According the Fistuca, the nature of the mechanism ensures quiet piling [37]. Another example is a bubble curtain which is a simple technique to reduce propagation of the noise from the source. To create the bubble curtain, each foundation is first encircled by a perforated tube. The tube is then filled with compressed air which rises toward the surface, forming a circular wall of bubbles

[38]. A disadvantage of the technique is that it is only partially effective. In fact, the high frequencies that are produced during the hammer, tend to 'escape' through the seabed and propagate further in the ocean.

### 2.2.5. Public opinion

Currently, public support is crucial for successful operation of offshore wind projects, which is why many developers make an effort to inform the public and the civilians living near the offshore areas of project development. Press conferences, availability of newsletters and access to information on the internet are drawing attention to the sector's ability to improve energy security, increase employment and economic development, indicating the capability of the industry to power number of households, other industries with reduced greenhouse gas emissions, and contribute towards national and EU commitments.

According to an attitude survey, known as the 2011 Eurobarometer survey, Europeans were more favorable to renewable energy and wind energy in particular (89%) when compared to nuclear or fossil fuels [39]. The use of renewable energy sources instead of fossil fuels has been found to reduce premature mortality and lost workdays; an installed offshore WTG does not pollute drinking water systems or compete with agriculture, while coal mining and natural gas drilling pose significant pollution of water resources. To reduce visual and noise impact of operating offshore WTG, governments established a '12 mile (23 km) zone' as a minimum distance to shore for an OWF [40]. In the future, wind farms will be constructed further offshore and far away from the perception onshore.

Finally, more awareness is created because the end customer gained power to freely choose the preferable source of electricity in their household, and available technologies afford to offer prompt electricity meters and services that help customers to understand and control their electricity usage. The awareness of the public led to the appearance of online crowdfunding platforms, which created additional mechanisms for broader participation and support for industry, and allowing anyone to invest and benefit from the returns.

## 2.3. Competitive position as installation operator

### 2.3.1. Intensity of competition

The market for wind turbine installation in the North Sea is rather undifferentiated and price competition is fierce. Due to the current reduced oil and gas activities, the options for a jack-up vessel with a low day-rate to choose from are numerous. In order to compete in this market, it is imperative to have high productivity. Installing a wind farm includes many repetitions and it is important to know exactly how you do it in the most efficient way.

The foundation is often installed by a different vessel than the WTG itself, because different capacities are required. Although it is likely to change in the future with the increase in wind farm size, the WTG is mostly installed with a single installation vessel. An exception is the construction of the Global Tech I wind farm in the German North Sea. Fred. Olsen Wind-carrier's jack-up vessels, the Brave Tern and the Bold Tern, worked together enabling them to install either four towers and nacelles or two complete rotor stars in a single deployment [41].

The market is currently concentrated in the countries along the shores of the North Sea. As a result, the main actors are based in Denmark, UK, and the Netherlands. Even if the knowhow base and operations are still situated in countries around the North Sea, the ownership of the companies is becoming increasingly global. One of the major operators, Seajacks, is owned by a Japanese equity fund and another major operator, Swire Blue Ocea, is headquartered

in Singapore. Because the list of wind turbine installation vessels is extensive, four types of competition are explained with an accompanying vessel.



Figure 2.7: Sea Installer, A2SEA



Figure 2.8: Aeolus, Van Oord



Figure 2.9: Saipem 7000, Saipem SpA



Figure 2.10: Orion, GeoSea

A2SEA is a company that made a successful transition from pioneer to market leader through specialization. A2SEA has focused exclusively on offshore wind, while many competitors are also engaged in other areas. Installation of windmill foundations, cables, and windmills accounts for approximately 95-98% of the company turnover. The remaining 3-5% include replacement of key components, cargo transfer, maintenance, and accommodation [42]. The Sea Installer (Fig. 2.7) is a purpose-built vessel, designed to transport and install up to eight 4MW turbines or four 8.3MW turbines. This focus has allowed the company to build a knowhow base and organization that is tailor-made for turbine installation.

Van Oord has gained a position in the market as being an integrated operator. For the wind farm developer it is convenient if an operator takes the risk to construct the foundation and WTGs of a wind farm, such as Van Oord did with the Gemini Offshore Wind Park. By executing both transportation as installation in a project they can innovate in logistics and installation concepts. This year, the upgraded wind turbine installation vessel the Aeolus will be operational, having the biggest heavy-lift crane in its class (Fig. 2.8).

Saipem is a direct competitor to Heerema for the installation of wind turbines as they also own semi-submersible crane vessels. In the Hywind Pilot Park, they demonstrated that inshore installation of fully pre-assembled wind turbines is possible with a floating vessel, the Saipem 7000 (Fig. 2.9).

The last type of competition is a heavy lift floating installation vessel with DP3, called the Orion built by GeoSea (Fig. 2.10). Due to the large deck space ( $8,000 \text{ m}^2$ ) it has a high transport and load capacity. The loads can be lifted to an unrivaled height of more than  $170 \text{ m}$ . Besides these capacities, the vessel has dual fuel engines and can run on natural gas (LNG). It will have a Green Passport and Clean Design notation. It could be an exceptional advantage in the future if the government puts targets on  $\text{CO}_2$  emissions during constructions.

### 2.3.2. Power of wind farm developers as consumers

Currently there are a few major players on the market with the ownership of offshore wind farms. Ørsted is the largest owner of offshore wind power in Europe with 17% of cumulative installations at the end of 2017. E.ON is the second largest owner with 8% of installed capacity owned, followed by Innogy (7%), Vattenfall (7%), and Macquarie Capital (6%). The top five owners represent 42% of all installed capacity in Europe, a slight decrease compared to the end of 2016 [17].

The customers of installation operators are the public and private energy companies, who operate the wind farms. Wind power is purchased by energy companies, that distribute the electricity further on to other industries and private households. Energy companies are not only engaged in the generation and transmission of electricity, but they may act as a developer as well when they manage the construction of a wind farm. Therefore, their level of involvement significantly influences the development of the OWE industry. Ørsted is for example a majority shareholder in the market leading offshore wind turbine installation company A2SEA [11]. Since wind farm developers are the main customers of wind technology designed for offshore installation, their bargaining power affects the profit potentials of all their subcontractors; from turbine manufacturers to installation and O&M operators.

The dependency on energy companies and the level of (public) investments in offshore wind farms mean that the installation companies are very reliant on the policy making of the states. Even if the customers are large companies with considerable bargaining power, the ability of installation operators to move into other sectors reduce the customer dependency of the installation companies.

For the wind farm developer, there is a wide variety of vessels available for the installation of small to average sized wind turbines. On the other hand, installation vessels for larger turbines with a capacity of 8 MW and more in deeper waters, the supply and demand ratio changes. Simply because there are only a handful installation vessels capable of installing 8 MW wind turbines in deeper waters yet, the supply side is limited. Therefore, bargaining power of developers of wind farms in waters deeper than 50 meters and with wind turbines larger than 8 MW, is relatively low. This makes the market for an installation operator of larger wind turbines more attractive.

### 2.3.3. Power of wind turbine manufacturers as suppliers

Turbine manufacturers are the ones supplying wind technology that is to be installed by the installation operator. According to the current market share, turbine manufacturers are very concentrated offering similar turbine types and designs. Even though only a few turbine manufacturers are dominating the industry, it is not in their interest to increase the price of its product and services. Turbine manufactures currently active on the offshore wind market compete for every project initiated in the North Sea. Siemens Gamesa Renewable Energy has the most offshore wind turbines in Europe with 64% of the total installed capacity. MHI Vestas Offshore Wind (18%) is the second biggest turbine supplier, followed by Senvion (8%) and Adwen (6%) [17].

As mentioned before, the most occurring wind turbine is a three bladed wind turbine positioned on a monopile foundation. One can assume it is the reason most installation vessels are designed for installing this type of wind turbine and that it is difficult for an installation operator to differentiate. However, market trends of turbines increasing in size and installation in deeper waters creates opportunities for installation operators. It allows new players in the market, like Heerema, to demonstrate their technologies are suitable for larger turbine and for deeper waters.

Furthermore, enormous potential for innovation and development of technology itself opens opportunity for new market entrants. There are numerous alternative turbine concepts, but

they have not gained a significant position in the market yet. Still, only being capable of competing on scales of economy through industrialization of its manufacturing activities, reducing costs through optimization of logistics and new installation concepts will allow new players to raise their cost competitiveness and increase their bargaining power. All in all, the bargaining power of today's turbine manufacturers are relatively low.

### 2.3.4. Threat of substitutes

The share of offshore wind energy in the electricity market can be reduced, when the oil and gas industry is picking up speed again. The North Sea has always been known as the oldest field for offshore gas and oil industry, therefore convincing many participants of that particular sector that their business in that region is not yet over. Significant developments in other parts of the energy sector, such as breakthroughs in  $CO_2$  storage technologies, can have an influence on the prolonged utilization of coal and gas-powered generation utilities. Thereby it could increase the competition to the offshore wind sector [39].

The emphasis of the offshore wind and decommissioning markets on cost reduction, results in the requirement for cost-effective heavy-lift vessel solutions. As such, in a market where day rates are often driven by tonnage requirements, super heavy-lift vessels may have a somewhat limited market reach, and vessels that are over-specified will risk lower day rates.

The third type of threat is that heavy-lift installation vessels become financially less attractive for operation because wind turbines with a floating substructure gain a market share. Besides the potential for standardization of foundation designs it is possible to tow out floating substructures including the turbine with a tug boat, resulting in lower costs. For installing the catenaries, it is indicated that the technology can be borrowed from offshore oil and gas industry that already possesses extensive experience operating in rough and hostile environment of the North Sea through decades. It is assumed that 80% of all the offshore wind resource is located in waters 60 m and deeper in European seas, where traditional bottom-fixed offshore wind (BFOW) is not economically attractive. Even though there is a large potential, R&D within offshore floating wind requires high capital investment in order to compete with BFOW or other clean energy generators, such as such as onshore wind power, solar technology, and nuclear power for potential investments. At the moment there are four substructure designs for floating offshore wind: barge, semi-submersible, spar buoy and tension leg platform (Fig. 2.11). The first three are loosely moored to the seabed, allowing for easier installation, while the tension leg platform is more firmly connected to the seabed. This allows for a more stable structure.

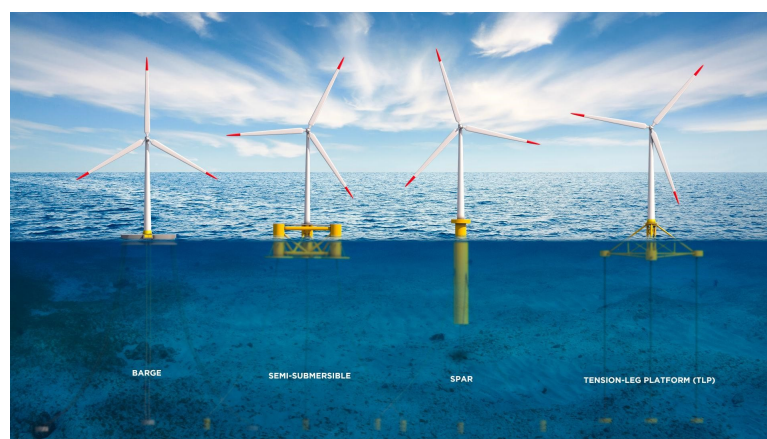


Figure 2.11: Floating substructures: barge, semi-submersible, spar buoy and tension leg platform *f.l.t.r.*

### 2.3.5. Barriers to entry

From 2008 to 2010 the market was booming and several new companies entered the market. This happened despite the high entry barriers. First, new entrants must invest in equipment to execute efficient and reliable installations operations. It can be assumed that jack-up vessels were low-priced at that time due to the decline of the oil and gas market. Second, new players need to invest in building an adequate knowhow base and organization. Because of the complexity of the wind turbine technique and the installation operation a lack of experience and qualified people can become a major obstacle for new entrants. Most entrants were large companies with activities in offshore oil and gas.

## 2.4. Conclusion

With the use of the 'PESTLE' framework, the offshore wind market in the North Sea is evaluated to be attractive as a business environment. There is a large potential for building new OWFs in the North Sea. It is expected another 54 GW of new installations is build in an average scenario according to WindEurope. The trends in deeper waters, further offshore and increasing size of turbines are positive for floating installation vessels with larger crane capacity, as JUV's have reached their maximum capacities. It is recommended to list the announced tenders in deeper waters (where jack-up vessels cannot operate), that can be potential OWFs for HMC to install. The governmental support is significant and is assumed to be stable in the future.

With the use of the 'Porter's Five Forces' framework, the competition for HMC as an installation operator is assessed. The barriers to enter the OWE industry are high, due to large capital requirements for initial manufacturing costs, a competition from well-established brand names and a need for experienced and qualified people. The power of the OWF developers is high, because it seems to be difficult to convince the developer to take risk of using a new method. Although, there power of OWF developers diminishes for installations in deeper waters, since the supply and demand ratio changes. Due to the many operating jack-up vessels, the price competition among installation operators is still fierce. On the other hand, the threat of alternative WTGs becoming mainstream is small due to economies of scale and the potential of new OWF development is enormous. As competitors succeeded through specialization, there is an opportunity for Heerema to enter the market with their SSCVs and focus on the installation of extra large WTGs ( $\geq 10$  MW).



# 3

## Installation phase in the development of an offshore wind farm

This chapter will give background information on the supply chain of the installation phase of an offshore wind farm. Also the advantages and disadvantages per installation vessel, pre-assembly and re-supply strategy are given. This will help the reader to understand the current challenges for determining the installation strategy.

### 3.1. Focus of the supply chain

The purpose of operating a wind farm is getting as much power out of the wind energy, and hence electricity, as possible. Therefore selected offshore sites have high wind speeds, and consequently higher sea states, which affect the transport and installation process in a negative manner. The challenge is to minimize offshore installation time due to the dependency on weather. Because restricting weather windows are the main cause of delays, the logistics should be such that turbines and vessels are in the right place at the right time. If the upstream stages of supply chain manufacturers produce their parts on schedule, the installation phase may be interrupted by weather resulting in formation of stock backups within the supply chain. Therefore, a pre-assembly strategy is preferred to comprise a minimum number of components for installation onsite and a maximum number of components on vessel per load out [43].

The installation phase can be divided into the following sub phases [44]:

- Site preparation for offshore substation
- Installation of offshore substation
- Site preparation for export cables
- Installation of export cable(s)
- Site preparation for foundations
- Foundation installation
- Site preparation for inter-array cables
- Installation of inter-array cables
- Installation of wind turbines

This study will focus on the last phase: installation of wind turbines. The supply of the turbine components at the harbor is not included in the scope, as it is likely to change in the

future with the upscaling of components, and therefore the supply chain of the installation will change. Turbine supply involves the manufacture, assembly and functional tests of all electrical and mechanical components and systems at the factory. Most of the installed wind turbines originate from two factories of the largest turbine suppliers, MHI Vestas and Siemens Gamesa, which are located in Esbjerg, Denmark and Hull Plant, United Kingdom. Afterwards the components are transported over land or over sea. With the increased size of the components, such as the blades, it will be problematic to transport over land, crossing roundabouts and tunnels. Therefore, factories could be placed at the port in the future to avoid onshore transportation of components. These ports also need the infrastructure to accommodate novel large foundations and bigger installation vessels. Depending on the speed of the installation vessel, sailing time from port to site location will be significantly increased [45].

The logistic operations in the installation phase involve: preparations at the port to mobilize utilities such as the cranes on land and onboard, pre-assembly of components if planned and loading onto the vessel, transportation to the site, installation at the site location.



Figure 3.1: Logistical operations involved during installation phase offshore wind turbines

### 3.2. Capacities of installation vessels

Also in the installation phase, the increase in the scale of the turbines requires adaptation; the carrying and lifting capacities of installation vessels have to be upgraded. As the offshore wind industry is developing, OWFs are constructed further offshore and in deeper waters. The increase in water depth has an effect on the jacking time of the jack-up vessel. It is possible to upscale the vessel for deeper waters with leg lengths around 70 m, but there will be a trade-off where duration of this step is too long compared to the relatively lower day rate of the vessel. A more important drawback is that the sea bed conditions need to be analyzed before jacking, and that they can be restricting if stability of the jack-up unit cannot be guaranteed. Semi-submersible crane vessels are not restricted by deep water but by shallow waters at around 15 m, when the under keel clearance limit is reached it becomes unable for the vessel to maneuver on those locations. As mentioned before, an increase in distance to the port calls for higher sailing speed and larger available deck space on the vessel to be able to carry more sets of turbine each trip. Huisman developed a vessel especially dedicated to installing fully assembled wind turbines offshore, called 'The Shuttle' (Fig. 3.2). Each vessel has its own advantages and disadvantages, shown in table 3.1.

Table 3.1: Pros and cons per type of installation vessel

	<b>Pros</b>	<b>Cons</b>
Jack-up vessel	Stable working platform Attractive price (good availability in industry)	Jacking up- & down takes time Limiting crane capacity
Purpose-built installation vessel	High transit speed Active motion compensation	Max. number of transporting turbines: 2 No feeder system possible
Semi-submersible	Fast turbine installation Heavy lift capacities Capable installing large water depths Large deck space Larger weather window (than other floating WTIV)	Limited hook height Expensive Low transit speed



Figure 3.2: Conceptual purpose-built installation vessel 'The Shuttle', Huisman

### 3.3. Pre-assembly and re-supply strategies

Besides the distance to port and vessel storage capacity, pre-assembly is a major factor that influences the installation time of an offshore wind farm. The purpose of pre-assembly is to partly overcome challenges from dependency on weather conditions. Increasing the number of pre-assembled components per load out reduces the total offshore installation time. On the other hand, the increased volume of the assembled structures can lead to less efficient use of storage capacity on vessel. Another disadvantage is the need of calm sea during the transportation since the wind turbines are not designed for resisting the dynamic loads when their components are attached to each other, making it another factor that increases the weather dependency of the travel that can affect the project flow. As depicted in Figure 3.3 there are various concepts through which wind turbines can be assembled:

- Five Pieces separately
- Bunny Ear
- Pre-assembled Rotor
- Completely pre-assembled

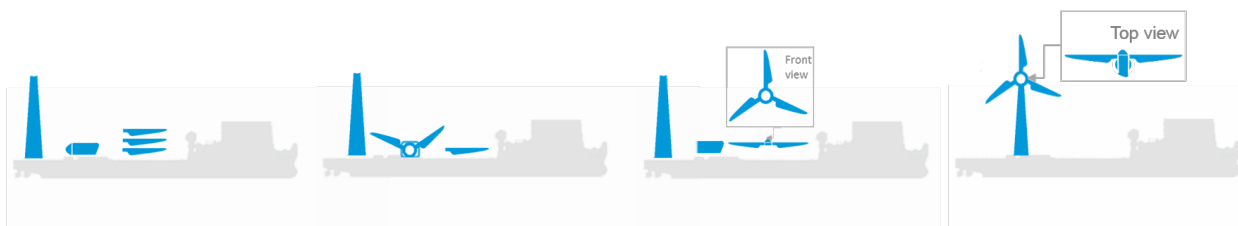


Figure 3.3: Pre-assembly configuration: 5 Pieces separately, Bunny Ear, Pre-assembled Rotor, Complete WTG *f.l.t.r.*

The most common method is to install the tower, nacelle with hub and 3 blades separately. A Bunny Ear configuration consist of 3 parts: the tower, the nacelle with hub and 2 blades attached, and 1 last blade. When the rotor is pre-assembled, the 3 blades are already connected to the hub onshore. Depending on the size of the tower or the crane capacity of the installation vessel, the tower can be installed in 1 or 2 pieces. An overview of the advantages and disadvantages are given in table 3.2.

After the choice of pre-assembly, the project developer or the installation sub-contractor needs to decide on a logistical method to transport the components from port to the wind farm location. According to literature there are two possibilities to get the components to the site; using an all-in-one or a feeder system [43]. With the all-in-one system the installation vessel also transports the components, and hence there is no unloading process needed.

Table 3.2: Pros and cons per pre-assembly strategy [46]

Strategy	Pros	Cons
Separate parts	Both vertical and horizontal blade fits possible (Although depend. on facilitator)	Time consuming: longest offshore time
Bunny Ear Method	Efficient with limited harbor facilities Narrow port entrances possible Known and proven methodology	Fatigue during transit
Complete pre-assembly	Time saving: shortest offshore time	Very dependent on wind conditions at site Large deck space required Large harbor cranes required

When the feeder system is applied, the installation unit stays at the wind farm. The 'feeder' vessels or barges bring the necessary components to the site. In Fig. 3.4 the supply chain of an all-in-one system is depicted. Depending on the pre-assembly strategy, components are prepared and assembled before the loading starts. As soon as the weather window allows, the components can be loaded to the vessel. The high lifting of large components is restricted by wind speeds. When the maximum amount of turbines are loaded on the vessel it can sail to the site. Before the installation starts, the vessel needs to be positioned; jacked down or by dynamic positioning (DP). When assembling the five separately, the tower is installed first, followed by the nacelle and the hub. Afterwards the 3 blades are connected to the hub. The installation vessel sails to the next site and repeats the loop until the all the loaded turbine components on deck are installed. The next step, the vessel sails back to the port and collects new components. This loop is repeated and stops when the last turbine of the wind farm is installed.

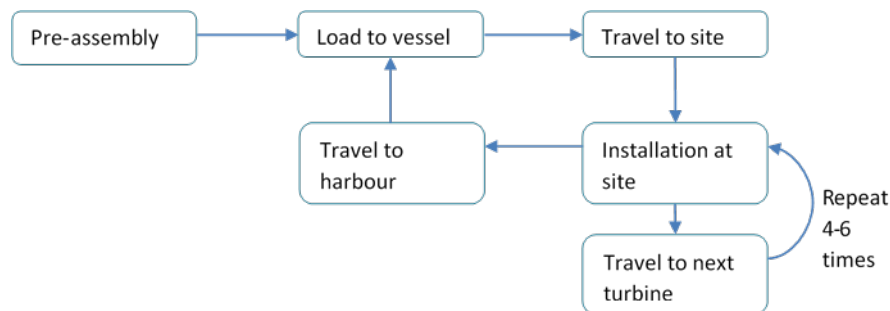


Figure 3.4: All-in-one system: WTG installation in which components supplied by installation vessel

The feeder system uses one or multiple barges to deliver the components at the site. In Fig. 3.4 vessel can be replaced with 'barge'. Also the 'installation at site' is not done with the barge but with another vessel, the installation unit. To complete the supply chain of the feeder system the installation vessel is to be seen parallel to the supply chain of the barge (Fig. 3.5).

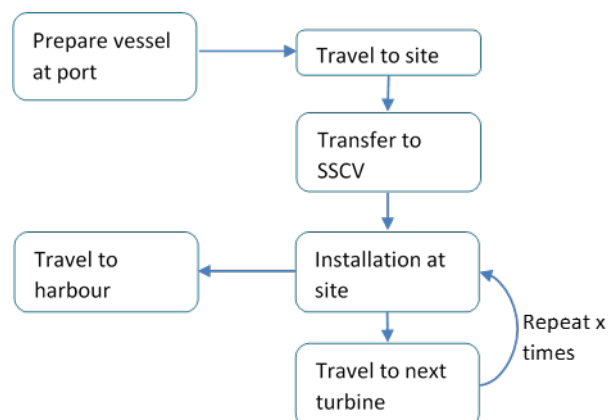
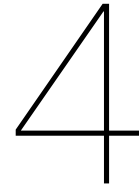


Figure 3.5: Feeder vessel logistics: WTG installation in which components supplied by feeder vessel



# Comparison of installation costs depending on pre-assembly and re-supply strategies

The goal of this comparison study is to increase the transparency in logistical methods for installing offshore wind turbines in terms of installation time and installation costs, as a function of site particularities.

## 4.1. Set-up of analysis

### 4.1.1. Relevance to the existing literature

As the offshore wind industry is evolving at a high speed, research from five years ago can be outdated today when innovations changed the technical layout of the turbine, the supply chain or the highly complex planning of an entire project. Past research on the offshore wind industry has been mainly focused on the technical challenges in the design, manufacturing, installation and operation of the facilities in the port. In comparison to the operation and maintenance phase, relatively little research has focused on the logistics involved in the installation phase of the offshore wind industry. However, Uraz has created an approach for time-wise modeling of the transportation and installation process of offshore wind turbines in order to figure out the effect of different parameters on the overall duration [46]. Existing literature consider only current operating installation vessels and do not offer insight in the parameters influencing installation time and installation costs of conceptual wind turbine installation vessels that should be capable of installing large wind turbines of 10 MW. This part of the thesis adds to the existing literature by comparing installation strategies, some of which are conceptual, and taking the disturbances due to weather conditions into account.

### 4.1.2. Scope of the analysis

For this study a standard jack-up vessel, a dedicated wind turbine installation vessel (WTIV) and a heavy-lift Semi-Submersible crane vessel (SSCV) are considered. It is assumed that a 10 MW turbine can be installed by all three vessels. Trends of installation costs per vessel are analyzed depending on:

- the distance to port
- size of wind farm
- pre-assembly strategy

Excluded in this study:

- Installation of foundations
- Floating wind turbines
- Uncertainty and disruptions in the supply chain

#### **4.1.3. ECN Install Tool**

To perform the analyses an external tool, called ECN Install, was used. As the name implies the tool is developed by ECN, which is the national institute of the Netherlands for energy research. ECN Install is a time based program with which the expected commissioning date and the cost of installation can be estimated. As input, all relevant parameters- vessels, equipment, harbors, components, weather conditions and permits are specified. Additionally, the entire installation plan is defined in the form of 'steps'. The assumptions in the input values are the biggest uncertainties in the calculation. These assumptions were checked with an industry expert, who has experience with the planning of the Gemini offshore wind farm. Some of the assumptions are were checked by performing an sensitivity study.

#### **4.1.4. Scenarios based on installation vessel, pre-assembly and re-supply strategy**

With the use of ECN Install, 6 scenarios were compared. A scenario was based upon the vessel choice, pre-assembly choice and the choice whether a barge or a vessel supplied the components or turbines.

The 6 scenarios, depicted in Fig. 4.1, are:

1. Jack-up vessel with separate parts
2. Jack-up vessel with Bunny Ear configurations
3. Dedicated WTIV with fully pre-assembled turbines
4. SSCV supplied by barge with components
5. SSCV with fully pre-assembled turbines
6. SSCV supplied by barge with fully pre-assembled turbines

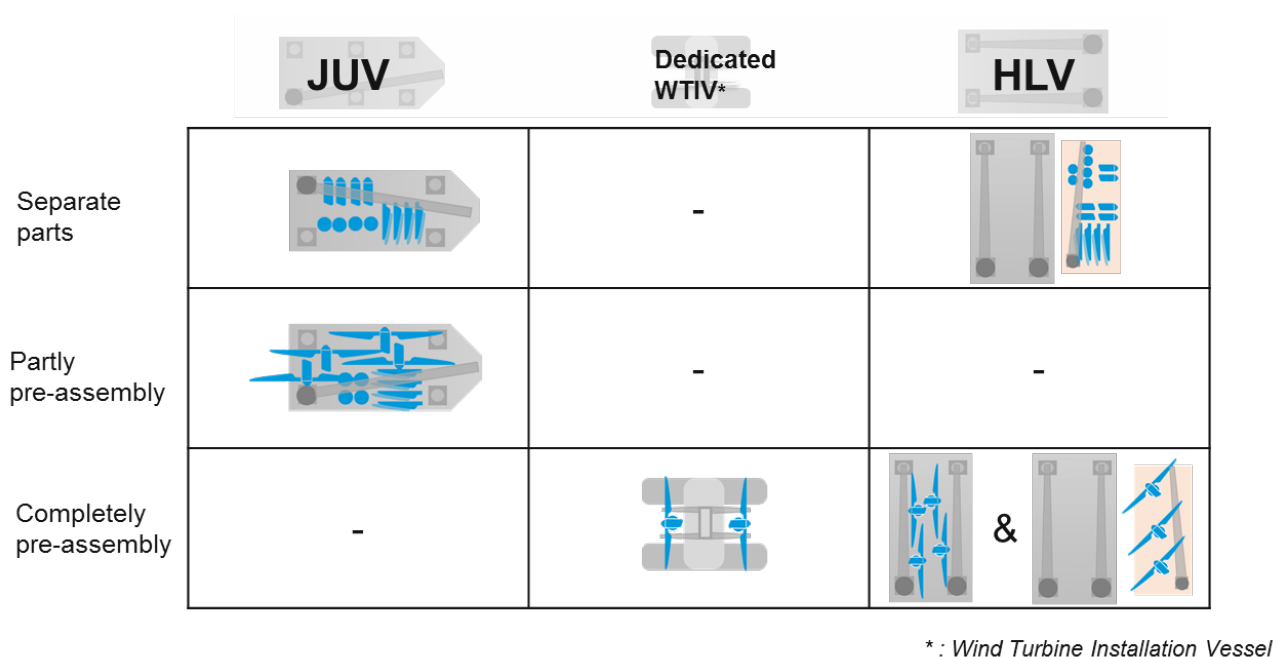


Figure 4.1: Top view of WTG components on installation vessels or feeder barges

#### 4.1.5. Model characteristics for the ECN Install Tool

The following input data was used in the ECN Install Tool:

- *Climate data*: Weather information of 3 locations in North Sea is used. Specifically, the data is corresponding to Borselle I & II, Ijmuiden Ver (K13) and Doggersbank (satellite data) for offshore locations. The weather data are available with 3 hours of resolution.
- *Operation bases*: For the entire installation process, Vlissingen Port was used for Borselle and Esjberg Port is used for Ijmuiden Ver and Doggersbank. The wind farm was the other operation base for the installation process.
- *Distance to port*: For Borselle, Doggersbank and Ijmuiden Ver the distance between the base port and the farm is 70 km, 350 km and 450 km respectively. The distances were established by using 'Google Earth' software (Appendix A.1.5). The coordinates of the wind farms were inserted in order to determine the exact location. Locations of the ports were found manually by using the 'search tool' of the same software. Distance between ports and corresponding wind farms were achieved by drawing the path (that a vessel can take on the sea) by using the 'path tool', where new shipping routes of the Dutch Rijkswaterstaat were taken into account.
- *Wind Turbine*: A conceptual 3 bladed turbine design of 10 MW was considered for installation. This is a reference turbine designed by the DTU, university of Copenhagen, Denmark. Rotor diameter and hub height are 178 m and 119 m respectively.
- *Components*: Five components were considered to be installed for each turbine. They are – Tower, Nacelle and three Blades.
- *Size of wind farm*: 3 Different sizes of wind farms are considered: 750 MW, 1500 MW and 3000 MW. Because the total installation time in the tool could not exceed 2 years, and parallel use of vessels was too complicated to insert in the tool, a limitation of wind farm size was set at 3000 MW.
- *Pre-assembly*: 3 Different methods of pre-assembly strategies are used: 5 pieces separately, Bunny Ear method and fully pre-assembled turbines. Appendix A.1.1 shows possible deck configurations per pre-assembly strategy.

- *Vessel*: Technical specifications of the installation vessels have been collected from the technical sheets that were accessed via the websites of the owner and/or the designer companies. Based on the deck space, the amount of total turbines per load out is estimated. The day rate of each vessel is estimated, listed in Appendix A.1.3.
- *Installation steps*: In Appendix A.1.4 the steps, the duration of each step and the weather restrictions are listed per scenario. Because the WTIV and the SSCV are not used yet for further offshore wind farm installation, the step durations are assumed based on industry standards from the jack-up vessel.

## 4.2. Trends installation costs per vessel

### 4.2.1. Installation costs for varying offshore wind farm size and distance to port

The following can be concluded from the simulations. As fixed costs have a relatively lower impact on the overall price when upscaling the wind farm size, the installation costs per turbine decrease. Furthermore, the installation costs when using the SSCV both as a transportation and installation vessel rank as the highest compared to the other vessels. Because the day rate of the SSCV is assumed to be more than circa 3 times the day rate of a jack-up vessel, it is preferable to use another vessel for the transportation of the turbine components or the fully pre-assembled turbine.

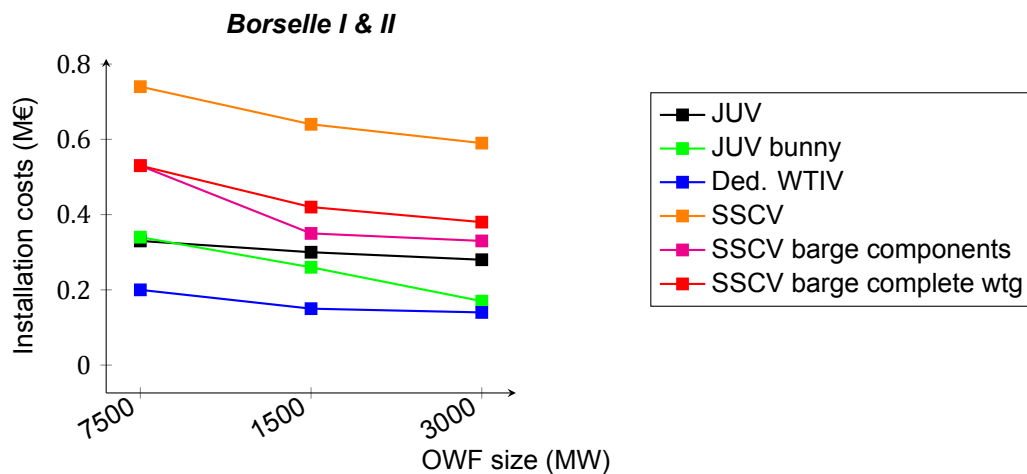


Figure 4.2: Installation costs per WTG (M€) 10 MW

A second conclusion that can be drawn is that the distance to port is not crucial in most scenarios, which can be seen in Fig. 4.3 as most lines are horizontal. For short distances to port (70 km) the scenario with a dedicated WTIV is favorable for all 3 sizes of wind farms. Even though the vessel can transport merely 2 wind turbines per trip, the sensitivity to distance can be explained due to the relatively high sailing speed of 12 knots and the claim of the company of the fast installation time of 2 hours for the turbine. The reason for insensitivity to the site location, and hence the distance, of the jack-up vessel can be caused because the jacking time (45 min) is taken the same for the 3 wind farm locations. The water depth range is overlapping but not entirely the same: Borselle I & II: 16 – 38 m, Doggersbank: 18 – 25 m, Ijmuiden Ver: 16 – 44 m.

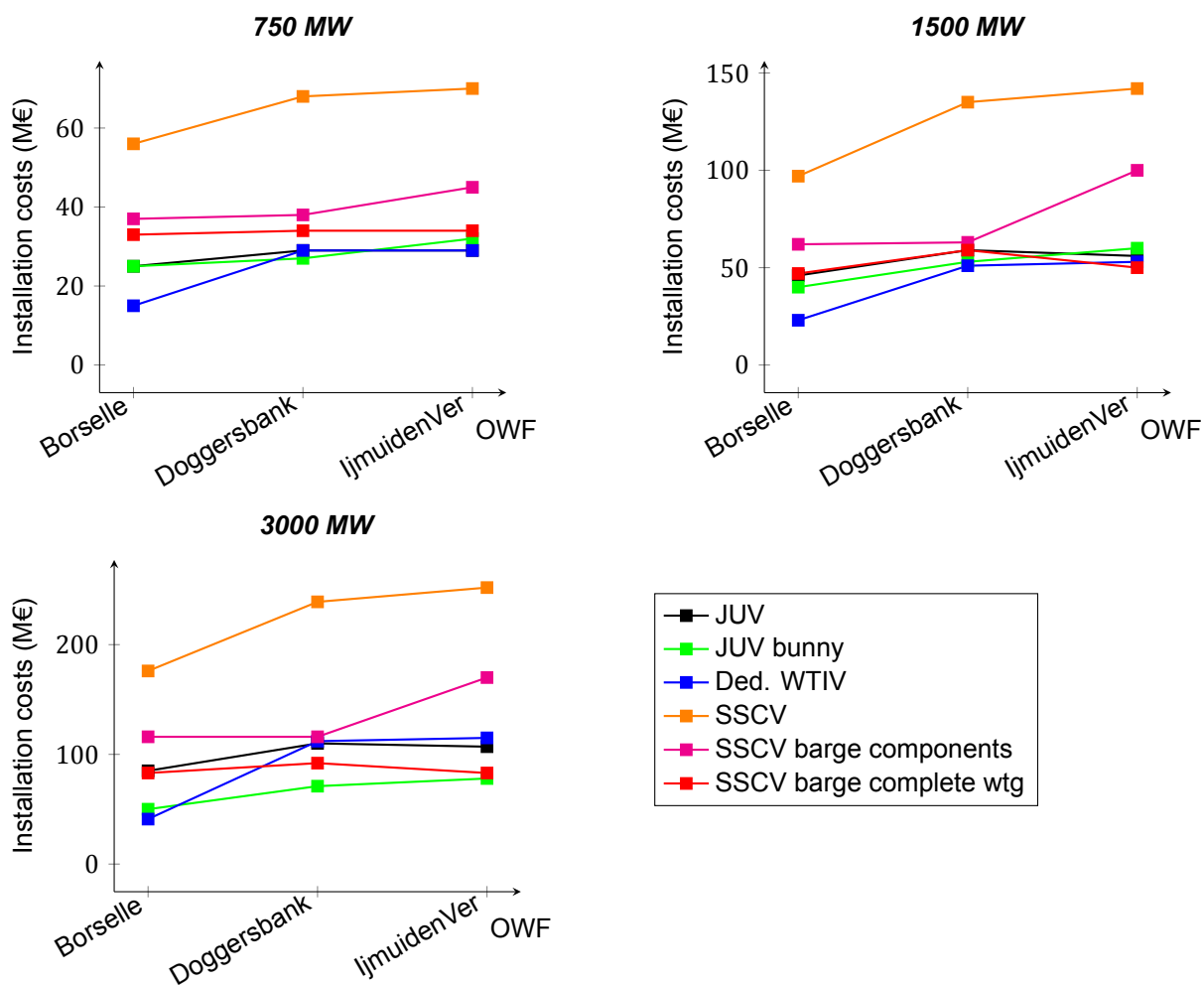


Figure 4.3: Installation costs (M€) 10 MW WTG, depending on OWF size

When looking at the installations costs per wind farm size (Fig. 4.4), the range of results is too small to draw extra conclusions. To understand the sensitivity of an assumption, the step durations of installing a turbine with the dedicated WTIV and the SSCV, and the costs of the JUV and the SSCV were changed (Fig. 4.5).

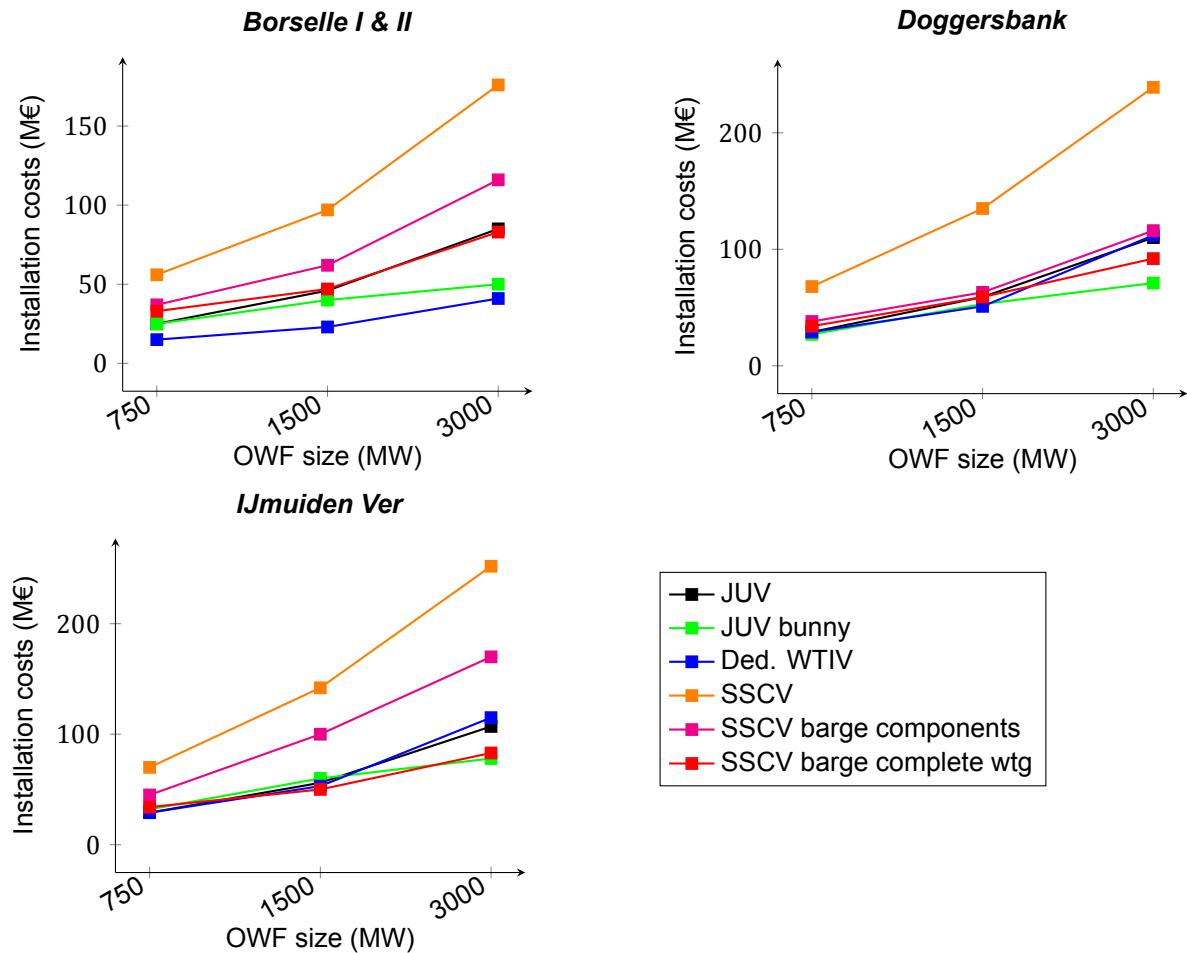


Figure 4.4: Installation costs (M€) 10 MW WTG, depending on distance to port

#### 4.2.2. Sensitivities on step duration and day-rate vessel

Change 1: Decrease installation time of complete turbine from 8 hours to 6 hours using a SSCV (Fig. 4.5, upper left). The abbreviation 'FIT' stands for Faster Installation Time. When comparing the costs one scenario becomes remarkable favorable for large wind farms of 3000 MW: the SSCV supplied with fully pre-assembled wind turbine by barge. When assuming positioning the vessel and sailing on to the next turbine takes 2 hours, it takes 8 hours in total for installing a turbine offshore. One can state if the SSCV can install 3 wind turbines per day, it is financially optimal to use the SSCV supplied with fully pre-assembled wind turbine by barge when constructing a 3000 MW wind farm.

Change 2: Increased installation time of complete turbine from 2 hours to 6 hours when using a dedicated WTIV (Fig. 4.5, upper right). The abbreviation 'SIT' stands for Slower Installation Time. In the brochure of the conceptual vessel the installation time is stated to be 2 hours, but according to experts, this seemed to be fairly underestimated. The change in installation time makes this scenario an average performer.

Change 3: Increased day rate of a jack-up vessel with 25% (Fig. 4.5, lower left). The two scenarios with a jack-up vessel end up higher in the graph, directly competing with the SSCV.

Change 4: Increased day rate of a SSCV with 25% (Fig. 4.5, lower right). All three scenarios with a SSCV are most unfavourable in terms of installation costs. The division in installation time is different, where the scenario with SSCV supplied with fully pre-assembled wind turbine by barge is most favorable.

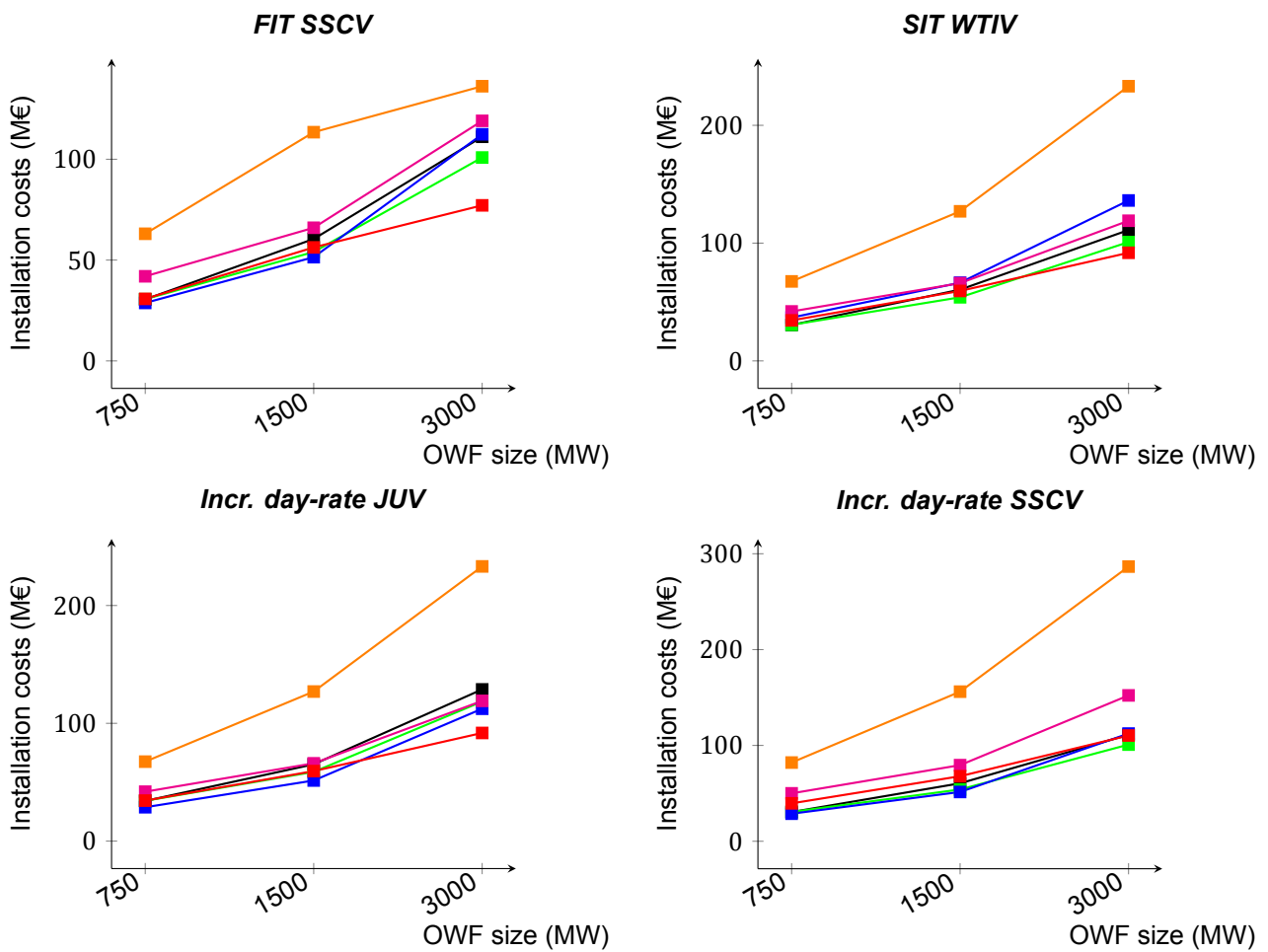


Figure 4.5: Installation costs (M€) 10 MW WTG for Doggersbank, changing installation time and day-rate

Because the range of installation cost per scenario is small, changing the day rate, directly affects the order of financially preferable installation vessel. Therefore, it is advisable to revise the costs per vessel. Especially, the assumption on the cost per grillage have a large influence on the costs of supplier barges. If one assumes the grillage costs can be shared over more than one wind farm project, the feeder supply method could become more financially attractive. When developing wind farms of 3 GW and larger using an SSCV is economically optimal to install complete pre-assembled wind turbines supplied by barge.

### 4.3. Challenges for the single-lift installation with a floating vessel

After the assessment of installation methods the focus for the second section is on the single-lift installation with a semi-submersible crane vessel, where components are supplied per barge. The advantages of using a SSCV and installing a completely pre-assembled turbine are mentioned in Chapter 3. To install next generation offshore wind turbines (>10 MW) with a SSCV there are multiple challenges occurring:

- Connections blade to nacelle
- Location of pre-assembly
- Transportation of components
- Soft landing on transition piece

First, the connection technique of the blade to the nacelle is copied from onshore turbines and is not optimal when transporting a fully pre-assembled turbine offshore. Secondly, the location of pre-assembly can be optimized per wind farm, which can be done either onshore or offshore on deck of a barge using DP, a jack-up vessel or the semi-submersible crane vessel itself. Thirdly, the transportation of the large components or the pre-assembled wind turbines is restricted due to weather conditions. The turbine design or the supporting construction can be optimized to meet the stress, impact load and stability requirements. The last challenge is a potential bottleneck for installation with floating installation vessels if not secured (Fig. 4.6). As the size of the components increase, both landing a fully pre-assembled wind turbine before it gets bolted on the transition piece as well as landing only the tower on the transition piece, is a crucial operation that should meet the impact load criteria. If this part of the installation phase fails, the whole installation method cannot be used. Therefore, the second section of this thesis focuses particularly on the soft landing of the wind turbine on the transition piece.

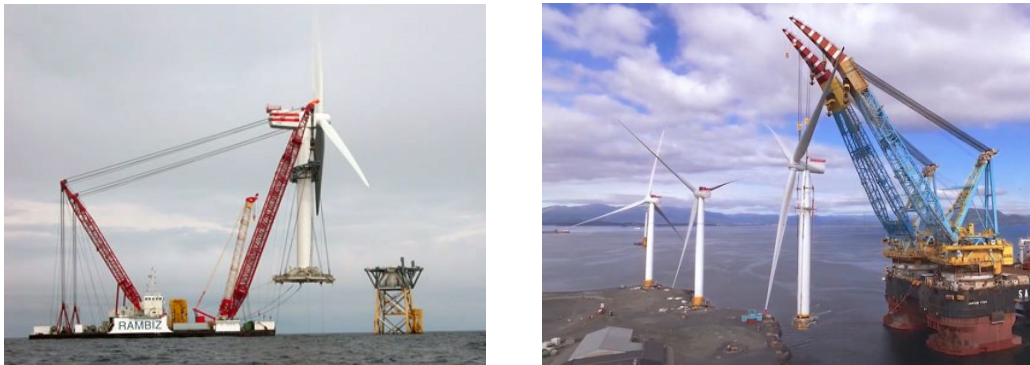


Figure 4.6: Single-lift installation with floating vessel

# 5

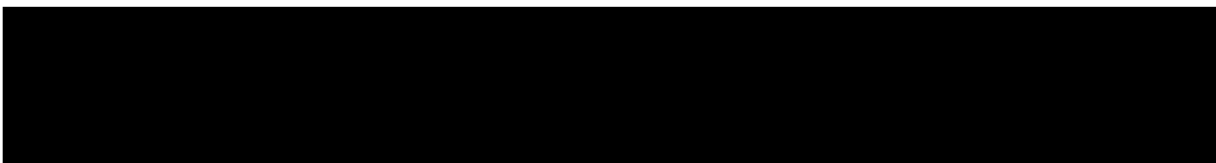
## Analysis on resonance risk and impact loads on the offshore wind turbine

The goal of chapter 5 is to make a realistic model of an WTG in the free-hanging and set-down phase. The first two sections of this chapter explain the operational limits, the installation sequence and the crane rigging of the Thialf, that determine the WTG model characteristics which are used for further calculations. Section 5.3 analyzes the risk on resonance during the free-hanging phase. The impact loads on the bottom of the wind turbine tower are analyzed in section 5.4 during the set-down moment. Finally, section 5.4.6 confirms the reduction in impact loads, for lowering the WTG in an optimal moment with the least hydrodynamic loading.

### 5.1. Operational limits and weather restrictions during the installation phase

When calculating the workability of an installation (Chapter 6) a single or multiple operational limit(s) can be set for each step. RAOs are generated from a specific point of the WTG with LiftDyn (section 5.3), and operational limits can be applied to these specific points. For a WTG in the free-hanging phase, it is for example possible to state a most limiting criteria of an acceleration in horizontal direction of the COG of the WTG that should not exceed  $0.1 \text{ m/s}^2$ . Beside operational limits, it is possible to put weather restriction on a certain installation step. The wind speed and significant wave height limits are based on guidelines in the industry [47]. For an optimal selection of limiting criteria, a comparison study can be made of multiple simulations to determine what is most limiting in a certain scenario. In addition, operations should be measured in real life under which conditions the crane operator still can perform the tasks. In the model of this thesis no tugger wires are added to constrain horizontal or vertical motions because the system is stable enough (section 5.3.3). Neither a damper is added between the transition piece on the bottom of the tower to lower the impact force during the set-down moment. This resulted in the following operational and weather restrictions (table 5.1):

Table 5.1: Operational limits and weather restrictions per step for one WTG installation



**Note:** The motion restrictions are defined as Significant Double Amplitude (SDA). For example, a SDA of 1 m means that the nacelle can move 0.5 m from equilibrium in horizontal direction during the lift of the bunny on the tower. The vertical velocity limit is defined as Significant Single Amplitude (SSA), as it only applies in a downward direction.

The barge load-out implies loading the components of 4 WTGs on deck of the Thialf. The components should be organized on deck in such an order, so that the WTG can be constructed with 'easy logistics'. The WTG is limited by a vertical velocity during the lift. In table 5.1 the velocity limit is stated that is imposed by hydrodynamic loading. When calculating the impact load on the bottom of the tower, the lowering velocity is taken into account as well. This velocity is the speed of lowering the hoist wires. The maximum vertical velocity of the bottom of the tower, during the set-down is:

$$V_{max,set-down} = V_{dynamic} + V_{lowering} \quad (5.1)$$

Where  $V_{max,set-down}$  is 0.1 m/s [48],  $V_{dynamic}$  is 0.04 m/s and  $V_{lowering}$  is 0.06 m/s.

In subsection 5.4.2 the mating technique is explained. At the start of the mating operation the clearance between the TP and the bottom of the tower is 3 m. A clearance between the pin and bucket of 1.5 m is taken, which is estimated by the Renewables Department at Heerema that performed similar WTG installations in the Simulation Center. Given the clearance and set-down velocity, the duration of the set-down is 30 s at minimum and 50 s at maximum. When looking at the total time required for the set-down, an extra 10 s can be added for 'thinking time' of the crane operator to decide to lower and an extra 5 s can be added for the delay of hoist wires. The moment a crane operator pushes a button to lower the hoist wires, it takes around 10 s to roll out the cable. Therefore, a time-frame of 65 s without exceeding the operational limits is required to start the operation.

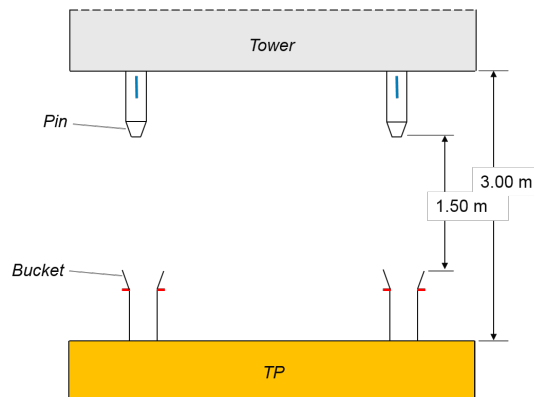


Figure 5.1: Clearance between tower and transition piece

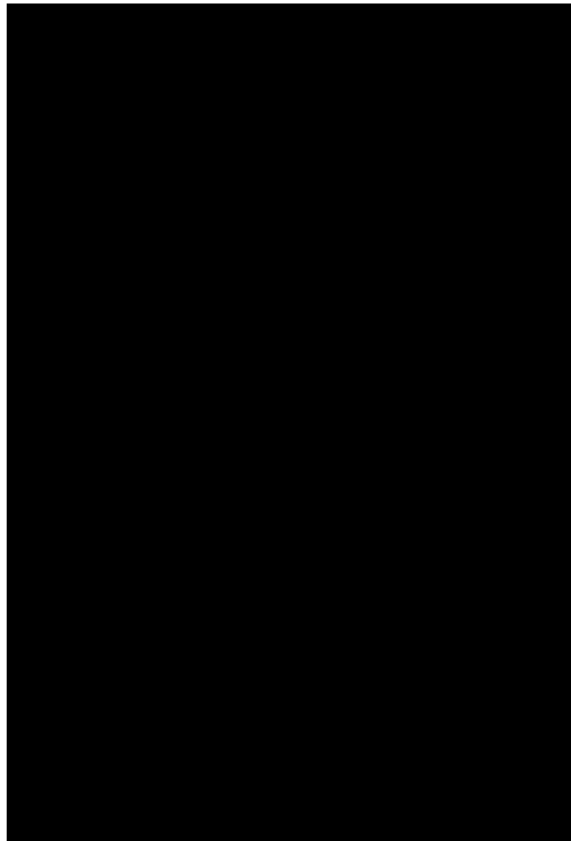
## 5.2. Constructing the offshore wind turbine

### 5.2.1. Sequence of critical path

As mentioned before the scenario where a barge supplies the components to the SSCV was chosen for the second section of this thesis. Currently, Heerema is investigating the options to construct the WTG on a frame connected to the aft of the vessel. In the following calculations it is assumed it is possible to load out the components from the barge to the deck, and consequently to construct a complete WTG on the aft of the vessel. In one barge it is assumed components of four 10 MW WTGs can be transported. Due to the large deck space of the Thialf it is assumed components of four WTGs can be stored on deck in such an order they can be picked up for construction. In table 5.2 steps of the critical path are stated when using one crane for the assembly and two cranes for the WTG lift. This means that during

the assembly of the first bunny of one barge, the tower can already be constructed on the aft with the second crane. When the bolts of the first WTG of one barge are being tightened to the transition piece, the bunny of the second WTG can be assembled meanwhile. All the steps need to be executed without interruption, except the loading the WTG components out of the barge (step 1) can be done in several occasions, which requires a weather window of 3 hours to start or continue this step. The critical path changes if two cranes are used for the assembly of the WTG.

Table 5.2: Critical path of steps for installation of 4 WTGs



In chapter 6 the waiting on weather was calculated for the installation of an entire wind farm. It is assumed the wind farm consists of 80 WTGs with a capacity of 10 MW. This means that for the installation of 80 WTGs it takes 1600 hrs (67 days) without waiting on weather. With a decrease of 2 hours in the critical path mentioned above, a reduction in total installation time without WoW of almost 2 days can be realized.

The step 'WTG lift' is assumed to consist of the following sub-steps:

- WTG lift from frame
- Crane reposition
- WTG set-down by lowering hoist wires

The step 'WTG torque bolts' is assumed to consist of the following sub-steps:

- WTG torque bolts
- SSCV sail to next TP

### 5.2.2. Crane position

In Figure 5.2 the load curve of the cranes of the Thialf is depicted, and shows the maximum hookload and the maximum lifting height at a certain crane radius per type of crane block

(Main hoist, Aux or Whip). The crane positions for lifting the tower, the bunny and the third blade to the bunny for construction and the WTG lift with two cranes are defined as followed (table 5.3):

Table 5.3: Thialf crane specifications per lift operation



Where the hookload consists of the weight of the WTG ( $\approx 1174 t$ ), the crane block and lift-frame. The hookload is stated in short tonnes (1 *Sh.t.*  $\approx 907 kg$ ). The Auxiliary block has a weight of  $29.2 t$ , the Whip block  $10.2 t$ , the lift-frame for the bunny  $30 t$ , the lift-frame for the third blade  $46 t$  and the lift-frame for the complete WTG has a weight of  $136 t$ . The hook height is measured from the keel of the Thialf (with an average draft of  $26.6 m$ ) to the crane block. The dimensions of the WTG and the lift-frame are listed in Appendix A.2.

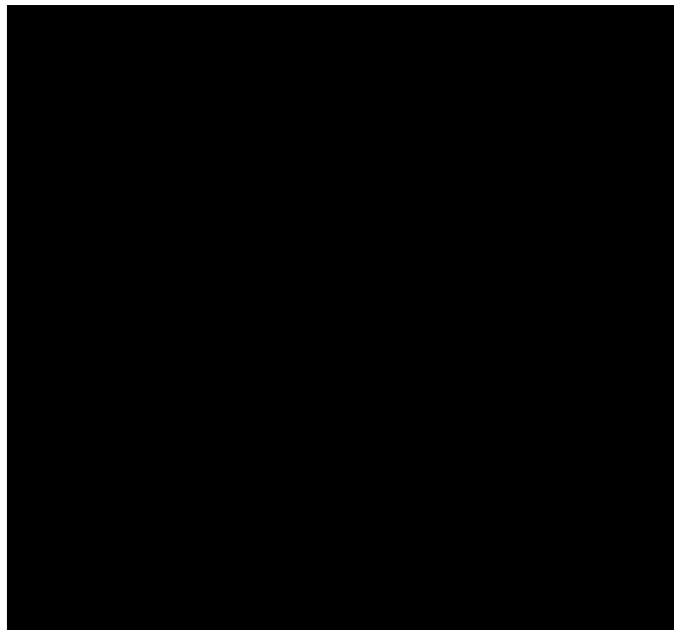


Figure 5.2: Hookload curve and maximum lifting heights Thialf

**Note:** Is not possible to reach the required hook height for the lift of the Bunny with the Aux block. In this model the whip block is chosen for its height capacity, but it does not have the load capacity. Therefore in reality, this operation is not possible. The cranes should be upgraded or another vessel should be used, like the Sleipnir. Second, it is assumed the cranes can operate simultaneously during the WTG lift. In reality this is difficult, and a small misalignment can cause the WTG rotate (e.g. roll motions can occur).

### 5.3. Free-hanging wind turbine in the installation phase

After the lift-off of the WTG from the frame at the aft of the vessel, the wind turbine is in its so called 'free-hanging phase'. During the free-hanging phase of the wind turbine there is a risk that resonance occurs, due to hydrodynamic wave loading on the vessel. In section 5.3.1 - 5.3.2 the theory is explained, that is used to perform calculations in the in-house software tool 'LiftDyn'. In section 5.3.3 the mode shapes, of the free-hanging WTG, are computed in order to understand how the system behaves and for which frequencies it is

sensible. It concludes if there is a risk of resonance of the free-hanging WTG, due to wave loading.

### 5.3.1. Frequency domain analysis

For the motion forecast of a vessel with a module hanging in its cranes, it is most practical to use an frequency domain approach. The calculation is easy to understand and much less time consuming than a time domain calculation, which is convenient when performing multiple calculations to analyze the systems behavior.

Within the linear wave theory, any irregular sea-state can be described by a superposition of sinusoidal (harmonic) waves as a Fourier series (equation 5.2). For the vessel response, the superposition principle states that the total response of a linear system equals the sum of multiple individual responses of linear subsystems. In other words, the equations of motions are solved for each harmonic wave. For small motions, the response of a vessel to waves can be linearized and can also be described as a Fourier series (equation 5.3):

$$\zeta(t) = \sum_{n=1}^N \zeta_{a,n} \cos(\omega_n t + \phi_{\zeta,n}) \quad (5.2)$$

$$Z(t) = \sum_{n=1}^N Z_{a,n} \cos(\omega_{\zeta,n} t + \phi_{Z\zeta,n}) \quad (5.3)$$

Where  $\zeta_a [m]$  is the wave amplitude,  $Z_a [m]$  the motion amplitude (heave),  $\omega$  [rad/s] the angular frequency,  $t$  [s] the time,  $\phi$  [rad] the phase angle,  $N$  the number of samples and  $n$  the sequence number.

This linearization is no longer valid when vessel motions become larger, as damping and hydrostatic terms in the Equation of Motion (EOM) become non-linear, second order wave forces occur or when calculating impact loads (or other discontinuous phenomena). Even though it is more time consuming, a time domain analysis would allow to solve such dynamic problems. When calculating the impact loads on the docking system between the transition piece and the tower a time domain approach is required.

### Response Amplitude Operator

The frequency characteristics of a system consists out of amplitude and phase characteristics. The amplitude characteristics are also referred as the 'Response Amplitude Operator' (RAO), a ratio of motion amplitude per unit wave amplitude ( $\frac{Z_a}{\zeta_a}$ ). The RAO is thus a transfer function of translations, and is often denoted as  $H_{ij}$ , where  $i, j = 1 \dots m$  represent the motion components. The phase characteristics are expressed as the phase difference between motion and wave ' $\phi_{\zeta}$ '. The vessel response can be calculated by multiplying the wave amplitude by a linear transfer function, the RAO. This is possible due to the fact the wave elevation (equation 5.2) and vessel response (equation 5.3) are linear proportional in linear wave theory. This means that the ratio (the RAO) of the force and response amplitude and phase is constant. The heave response motions of a vessel are noted as follows:

$$Z(t) = \sum_{n=1}^N RAO_z(\omega_n, \mu_n) \cdot \zeta_{a,n} \cos(\omega_n t + \phi_{\zeta,n}) \quad (5.4)$$

The response spectrum of a motion can be found by using the squared value of the transfer

function of that motion  $H_{ij}$  and the wave spectrum  $S_{\zeta}(\omega)$ :

$$S_{R_{ij}}(\omega) = |H_{ij}|^2 \cdot S_{\zeta}(\omega) \quad (5.5)$$

Where  $ij = 1 \dots m$  represent the motion components (e.g.  $H_{33} = RAO_z$ ).

## Liftdyn

To solve the linear hydrodynamic problem in the frequency domain, 'LiftDyn' was used. LiftDyn is an in-house software package of HMC that is designed to solve linear hydrodynamic problems in the frequency domain. The equations of motions are constructed for the global motions of the COG of each rigid body. So with  $n$  bodies in the model, there are  $6n$  unknowns and  $6n$  equations of motion. The  $6n$  equations of motions can be written in a single matrix equation:

$$(M + A(\omega)) \cdot \overline{X''(\omega, \mu_n)} + B(\omega, \mu_n) \cdot \overline{X'(\omega, \mu_n)} + C \cdot \overline{X(\omega, \mu_n)} = \overline{F(\omega, \mu_n)} \quad (5.6)$$

Where  $M$ ,  $A$ ,  $B$  and  $C$  respectively the mass, added mass, damping and stiffness matrices are square matrices of size  $6n \times 6n$ . The Force vector  $F$  contains the forces on the COG of the rigid bodies. The unknown motion vector  $X$ , consists of the 6 motions of the COG of each rigid body. The RAO is depending on frequency ( $\omega$ ) and wave direction ( $\mu$ ) and can be post-processed to a motion, velocity or acceleration RAO at any desired point relative to any other point.

### 5.3.2. Radii of gyration of offshore wind turbine

In order to analyze the dynamic behavior of the completely pre-assembled wind turbine hanging in the cranes, also referred to as 'the module', it is required to know the radii of gyration. Several simplifications and assumptions were made to use Liftdyn in an fast manner. First, it is assumed the module with its components acts as a rigid body. Second, the radii of gyration of the nacelle and three blades were combined. The construction of these components connected is called a 'star'. Third, COG of the star is known from an internal source in Heerema. Fourth, the tower is assumed to be a cylinder with an equal diameter instead of having one tapered side.

The mass moment of inertia about the centroidal  $x_c$ -,  $y_c$ -, or  $z_c$ -axis of the tower was calculated with the general formula of a hollow cylinder [49]:

$$I_{x_c x_c} = I_{y_c y_c} = \frac{m(3 \cdot a^2 + 3 \cdot b^2 + l^2)}{12}; \quad I_{z_c z_c} = \frac{m(a^2 + b^2)}{2} \quad (5.7)$$

Where  $m$  is the mass,  $a$  is the inner diameter and  $b$  is the outer diameter, and  $l$  the length of the tower. It is assumed the mass is distributed equally.

The mass moment of inertia about the centroidal  $x_c$ -,  $y_c$ -, or  $z_c$ -axis of the nacelle was calculated with the general formula of a rectangular prism [50]:

$$I_{x_c x_c} = \frac{m(l^2 + h^2)}{12}; \quad I_{y_c y_c} = \frac{m(l^2 + w^2)}{12}; \quad I_{z_c z_c} = \frac{m(h^2 + w^2)}{12} \quad (5.8)$$

Where  $l$  is the length,  $h$  is the height and  $w$  is the width of the nacelle. It is assumed the mass is distributed equally.

The mass moment of inertia about the  $x$ -,  $y$ -, or  $z$ -axis of the blade was calculated with the general formula of a rectangular prism [50]:

$$I_{xx} = \frac{m(w^2)}{12} + \frac{m(0.25 \cdot l^2)}{3}; \quad I_{yy} = \frac{m(h^2)}{12} + \frac{m(0.25 \cdot l^2)}{3}; \quad I_{zz} = \frac{m(h^2 + w^2)}{12} \quad (5.9)$$

Where  $l$  is the length,  $h$  is the height and  $w$  is the width of the blade. It is assumed the COG of the blade is positioned at 25% of its total length.

The radius of gyration of the tower was subsequently calculated with the following formula [51]:

$$R_{xx,yy,zz} = \sqrt{\frac{I_{xx,yy,zz}}{m}} \quad (5.10)$$

To calculate the combined mass moment of inertia about the  $x$ -,  $y$ -, or  $z$ -axis of the star the 'parallel axis theorem' was used, given the body's moment of inertia about a parallel axis through the object's center of gravity and the perpendicular distance between the axes [52].

$$I = I_{cm} + m \cdot d^2 \quad (5.11)$$

Where  $I_{cm}$  is the moment of inertia of the body with respect to the  $z$ -axis passing through the body's center of gravity,  $d$  is the perpendicular distance between the axis  $z$  and the parallel axis  $z'$  and  $m$  is the mass of the body.

About each axis, the  $x$ -,  $y$ -, or  $z$ -axis of the star, the sum of the mass moment of inertia per component was calculated. The distance  $d$  from the COG of the nacelle and of each blade to the (known) COG of the star was calculated by using Pythagoras' theorem. Finally, the radii of gyration of the star was calculated using equation 5.10.

### 5.3.3. Resonance risk

The behavior of the RAO can be separated in three sections of frequencies, which is presented in Figure 5.3. The natural frequency of the system determine the boundaries of the sections. Input frequencies significantly lower than the natural frequency result in motions that are dominated by the spring terms. Input frequencies close to the natural frequency are dominated by the damping terms and input frequencies significantly higher than the natural frequency are dominated by the mass terms. The natural frequency is dependent on the ratio between the mass, stiffness and some extended damping of the system. Resonance can appear, depending on the magnitude of the damping, somewhere in the neighborhood of the natural frequencies; the ratio  $r = \frac{\omega}{\omega_n}$  is close to 1. Resonances are usually marked in the RAO diagram by a local maximum. The magnitude of resonance can be reduced if the natural frequency can be shifted away from the forcing frequency, by changing the stiffness or mass of the system, or the magnitude can be reduced by adding damping to the system.

According to Huygens law for a swinging pendulum suspended from one pivot [54], the first natural period of the module is calculated with equation 5.12. In reality the WTG is more constrained due to two hanging points, which will influence the sway modulus. Therefore, the value of  $T_n$  is just indicative.

$$T_n = 2\pi \sqrt{\frac{L}{g}} = 2\pi \sqrt{\frac{49.22}{9.81}} \cong 14 \text{ s}, \quad \text{Natural period pendulum} \quad (5.12)$$

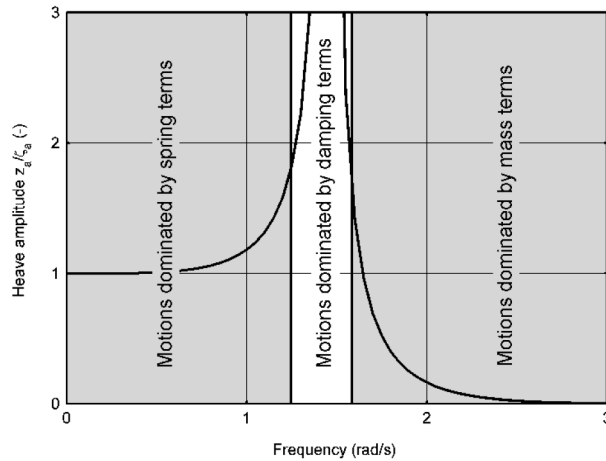


Figure 5.3: Frequency areas with respect to motional behavior [53]

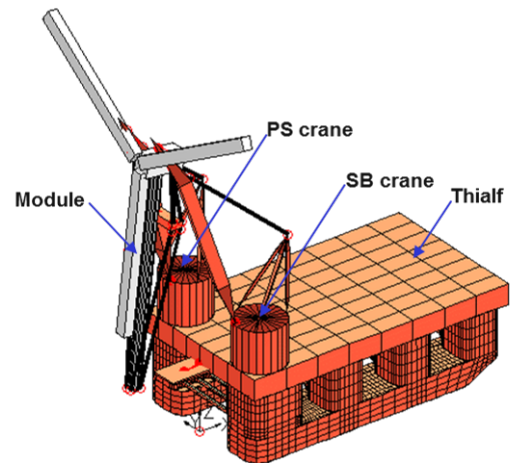


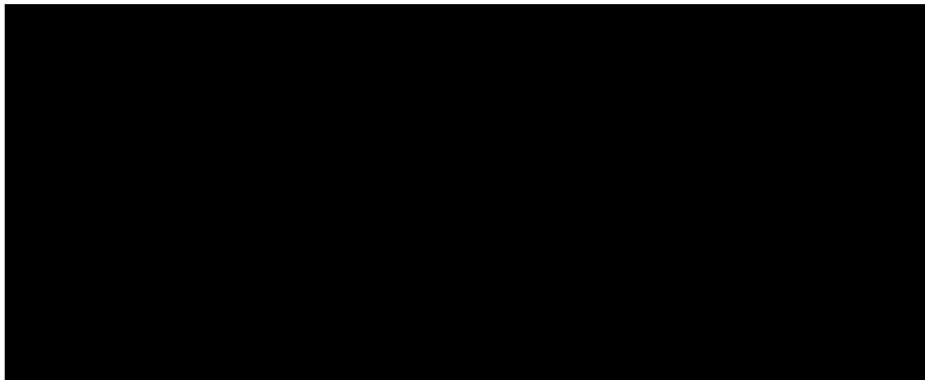
Figure 5.4: LiftDyn Model

Where  $T$  [s] is the natural period,  $L$  [m] the length of pendulum to the overall effective CoG and  $g$  [ $m/s^2$ ] the gravitational constant.

## Mode shapes

LiftDyn is used to compute the mode shapes of the systems, to give an idea of how the system behaves and for which frequencies it is sensible. A graphical representation of the amplitude of a mode shape (i.e. 9<sup>th</sup>) in figure 5.4 is magnified for a better understanding, and therefore is not representing reality. In total 20 mode shapes were found, however mode shape 10 until 20 will have an insignificantly influence on the system. In table A.4 the relevant mode shapes are listed.

Table 5.4: Mode shapes of free-hanging WTG computed by LiftDyn



The significance of a mode is indicated by Mass Participation, where a factor indicates the amount of the total structural mass that is activated by a single mode. If all modes of a structure are considered, the cumulative Mass Participation will be 100%. An example of an output file of LiftDyn for mode shapes 7,8 and 9 is listed in Appendix A.3. It shows that the Thialf responds very little to mode shapes  $\geq 7$ . The Thialf is mainly moved by eigenperiods and maximum wave forces. Mode shapes 1 to 3 are controlled by the DP-system of the Thialf, which typically have a damping of  $> 70\%$ , hence no significant response is observed in these mode shapes. The pendulum responds to mode 7 up to and including mode 9.

The frequency of input (waves) is the same as the frequency of output (motions). Typical periods of wind waves are dependent per project location. For example, the North sea spectral peak period ( $T_p$ ) can range between 3-16 seconds. In Doggersbank (Central North Sea) more than 80% of wind waves range between 5-12 seconds, which is 1.26 rad/s to 0.52 rad/s

respectively. For wave periods of 12 seconds and longer, there is a possibility of occurring of around 3% on a yearly basis. Considering installation will not take place in the winter months, the percentage will be even lower for the months of interest (in spring and summer). Therefore, it can be concluded the module has an inertia dominated response to mode shape 8, where the load frequency of the wave is higher than the eigenfrequency of the pendulum. In other words, the wave period is lower than the natural period of mode 8.

More interesting, in terms of resonance risk, is mode shape 9. Waves with periods of 4-5 s and  $H_s$  of 0-2 m are very likely to occur (around 13% on a yearly basis measured in a period of 50 years). Figure 5.5 shows that the operability is not limited at waves of 4-5 s ( $T_p$ ) and  $\geq 6m$  ( $H_s$ ). Waves of 4 s and  $\geq 6m$  do not occur; due to the steepness, waves of 4 s already break at  $H > 3.57 m$ . In deep water the theoretical limit for wave steepness is given in the following formula of Michell [55]:

$$\frac{H}{\lambda} < \frac{1}{7}, \quad \text{where } \lambda = \frac{g}{2\pi} \cdot T_p^2 \quad (5.13)$$

Where  $H$  [m] is the wave height and  $\lambda$  [m] the wave length. The wave length is 25 m (for  $T_p=4s$ ) and can be calculated with the dispersion relation (presented in second part in equation 5.13).

It can be concluded that the module does not give a resonance response to mode shape 9. The Thialf does not transport the small load frequencies of waves to the module, which is mainly due to the heavy weight of the Thialf (around 170,00 mT). Overall, the system is stable and it is unnecessary to add tugger wires, adjust the mass of the module or adjust the stiffness of the wires from the lifframe.

### 5.3.4. Influence mass and wires on operability

Even though in section 5.3.3 it is concluded the system is stable, it is interesting to analyze if the influence of mass and stiffness of liftframe wires can increase the operability. In section 5.3.1 it is explained how a response spectrum of a motion can be found. LiftDyn is used to generate multiple JONSWAP spectrum's with a peak range from 4 to 10 seconds and for multiple directions. All waves have a significant wave height of 1 meter,  $\gamma$  is set on 2 and no spreading is applied. After applying an operation limit of a vertical velocity at the bottom of the tower of 0.04 m/s, the operability can be generated given a certain sea state.

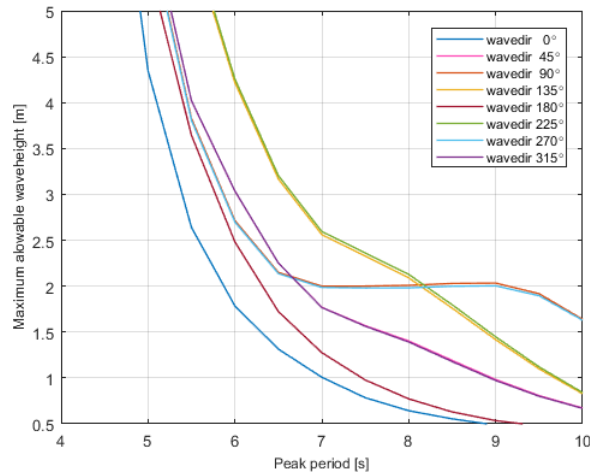


Figure 5.5: Operability Curve

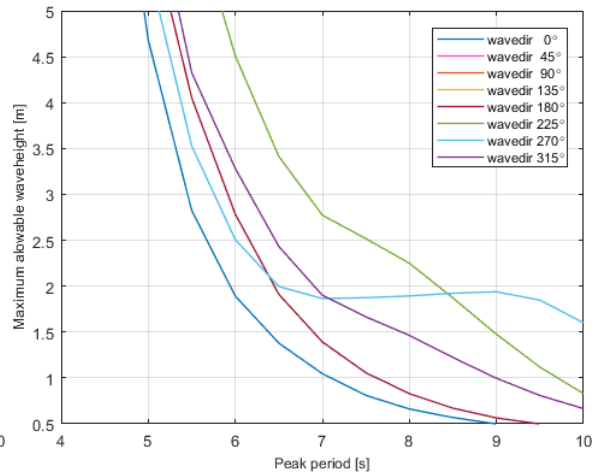


Figure 5.6: Operability Curve with WTG mass increase (factor 2)

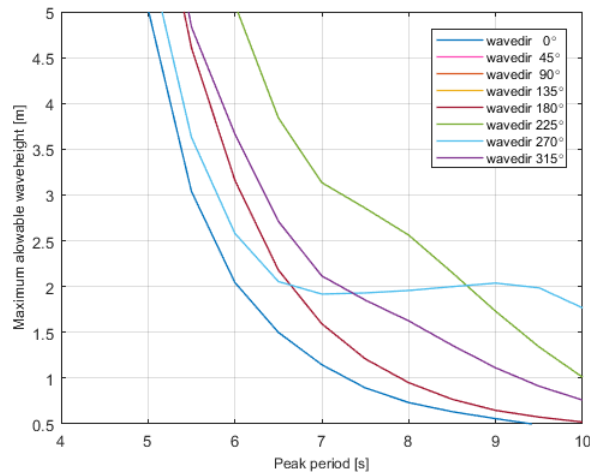


Figure 5.7: Operability Curve with sling stiffness increase (factor 100)

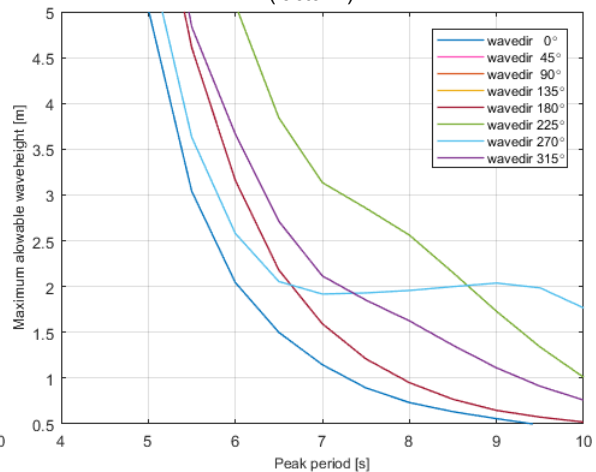


Figure 5.8: Operability Curve with sling stiffness increase (factor 10000)

Increasing the mass of the WTG will not influence the mode shapes of the system. Only the change in COG will result in a smaller  $L$  in equation 5.12, and a smaller natural period. With the WTG lift of 10 MW the maximum crane height capacity of the Thialf is almost used. Therefore, only a small change in COG, due to a increase in mass, can be assumed.

## 5.4. Set-down moment of the wind turbine in the installation phase

During the set-down phase, impact loads act on the docking system and between the bottom of the tower and the flange of the TP. In this paragraph impact loads are obtained with OrcaFlex (section 5.4.3), which is a common engineering tool to analyze dynamic offshore marine systems. The behavior of the impact load is analyzed for one sea state in section 5.4.4. In section 5.4.5 the impact loads are computed in OrcaFlex for multiple sea states. Subsequently, in section 5.4.6, the maximum impact load is compared to the maximum impact load when the set-down is performed at an optimal moment (i.e. with the least hydrodynamic loading).

### 5.4.1. Time domain analysis

When calculating impact loads, it is more adequate to use a time domain approach due to non-linear responses. The set-down is a dynamic phase with a transient phenomena. The result is a simulation of the behavior as we experience it in the real world. A disadvantage of a time domain analysis is that it is very time consuming: the analysis itself is time consuming and multiple simulation are required to obtain statistical reliable results.

### 5.4.2. Mating technique

In Appendix A three mating techniques for the connection of the tower to the transition piece are depicted: a grouted or a flanged connection, bolted connection or a bolted connection with a docking system. Considering the resemblance with the Hywind Project [12], the same mating technique is chosen: a bolted connection with a docking system. The docking system consists of two pins mounted on the tower, and two stabbing buckets mounted on the transition piece (Fig. 5.9). The bucket guides the motion of the tower and absorbs the shock with a spring/ damper unit at the bottom of the bucket. The system shall ensure a smooth vertical load transfer to limit the hard contact forces in the flange and limit the global transient dynamic motions resulting from the impact forces when the tower is set down on the substructure. The docking system is mounted on the inside of the tower and transition piece, therefore it will not need to be removed after installation [48].

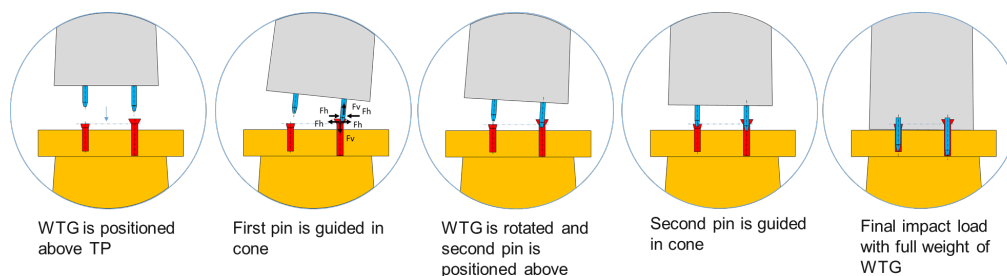


Figure 5.9: Mating procedure of connection tower to transition piece

### 5.4.3. OrcaFlex model

The dynamic impact force of the flange on the buckets and the TP is considered in the OrcaFlex model. The impact force is absorbed by elastic deformation of the TP, a change of kinetic (velocity) energy of the WTG and a change in potential energy of the WTG and the vessel due to an upwards displacement of the WTG, and consequently a hydrostatic displacement of the vessel.

The transition piece and the buckets are modeled as elastic solids in OrcaFlex. The upper part of the bucket, the cone, must be strong enough to resist the first impact, which has a

horizontal component. When both pins are guided through the cones, the pins encounter a vertical resistance from the spring/ damper unit at the bottom of the bucket (Fig. 5.10).

The general model of the Thialf, crane, rigging and WTG is prepared in LiftDyn, and imported in OrcaFlex. Here the weights, attachment points and stiffness, hydrostatics and hydrodynamics are defined.

### Damping

The damping value of the spring/ damper unit is set to  $400 \text{ kN}/(m/s)$ , 35% of the critical damping [48]. Steel-to-steel friction is set to 0. Recent internal studies of Heerema showed that steel-to-steel normal impact energy absorption is around 0.5% of the critical damping, which is applied in the model.

### Stiffness

The axial stiffness of the TP is calculated with the following formula:

$$k = \frac{EA}{L} \quad (5.14)$$

Where  $A$  is the cross-sectional area of the flange,  $E$  is the elastic modulus of steel ( $E = 210 \text{ GPa}$ ), and  $L$  is the (partial) length of the TP.

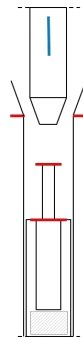


Figure 5.10: Representation of docking pin and bucket

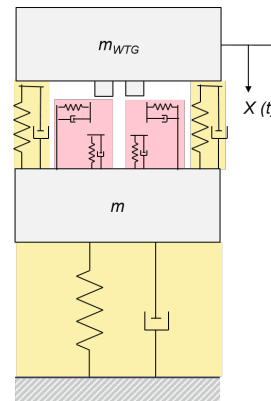


Figure 5.11: Representation of spring and dampers in TP (yellow) and buckets (red)

### Environmental sea state

The operability curve in Figure 5.5 shows that a wave headings of 0 degrees is the most limiting. This is due to the asymmetrical design of the Thialf. A Jonswap wave spectrum is used without spreading, similar as was used for LiftDyn.

Table 5.5: Environment used in OrcaFlex

Parameter	Variation
Hs	0.5m, 1.0m, 1.5m, 2.0m, 2.5m, 3.0m, 3.5m, 4.0m, 4.5m, 5.0m
Tp	4s, 5s, 6s, 7s, 8s, 9s, 10s

#### 5.4.4. Impact loads during set-down moment in one sea state

The impact force on the flange of the TP and the two buckets is analyzed of 50 simulations per sea state. Impact forces of interest are listed in table 5.6:

Table 5.6: Measured impact loads during set-down

Value impact load	Component	Moment i.r.t. first flange contact between tower & TP
Max.	Bucket (left & right)	During
Avg.	Bucket (left & right)	100 s after
Max.	Flange TP	During
Max.	Flange TP	After
Avg.	Flange TP	100 s after

The maximum stroke of the spring/ damper unit in the bucket is 0.3 m. The expected maximum contact force is around 115 kN with  $V_{max,set-down}$  ( $\dot{x} = 0.1$  m/s in  $F = x \cdot k + \dot{x} \cdot c$ ), or 100 kN with  $V_{lowering}$  (0.06 m/s) when there is little hydrodynamic loading. The expected natural period is calculated with the following formula:

$$T_n = 2\pi \cdot \sqrt{\frac{m}{k}} \quad (5.15)$$

Where  $k_{buckets}$  before flange contact results in  $T_n = 10.17$  s (with a heave motion), and  $k_{buckets+flange}$  after first flange contact results in  $T_n = 0.024$  s. The natural period of the TP, including the length of the monopile (76 m), is  $T_n = 0.105$  s.

In Appendix A.4 the horizontal impact loads on the buckets are depicted and analyzed.

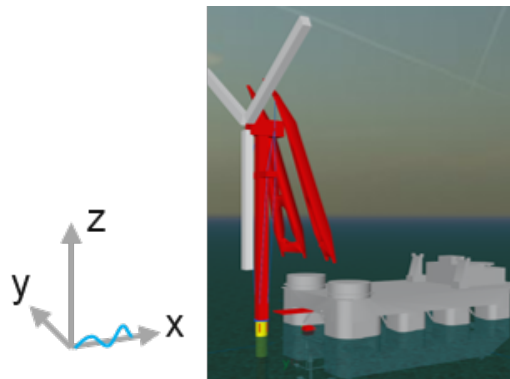
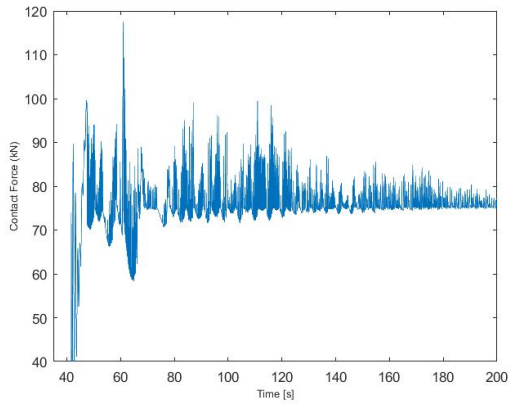
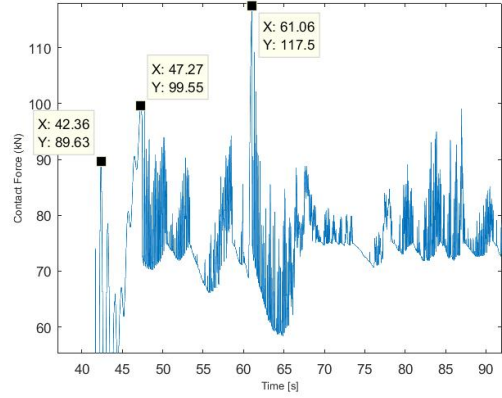


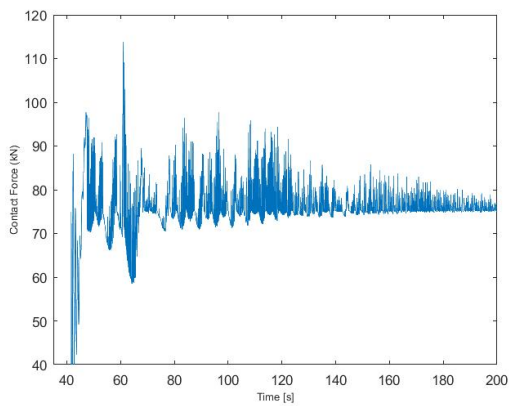
Figure 5.12: Sign convention OrcaFlex model



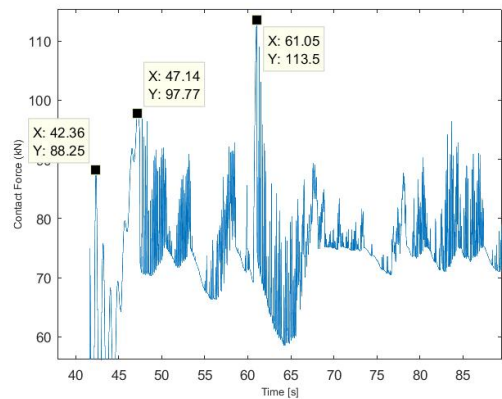
(a) Time-trace of vertical impact load bucket left



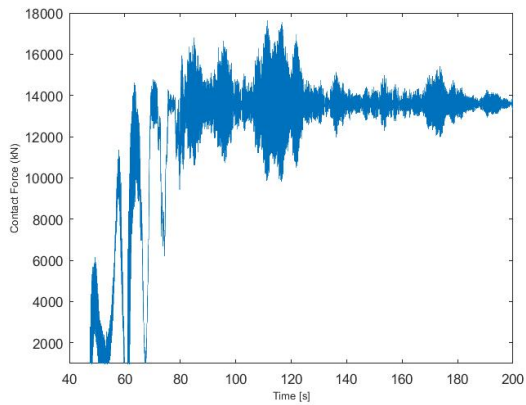
(b) Zoomed-in time-trace of vertical impact load bucket left



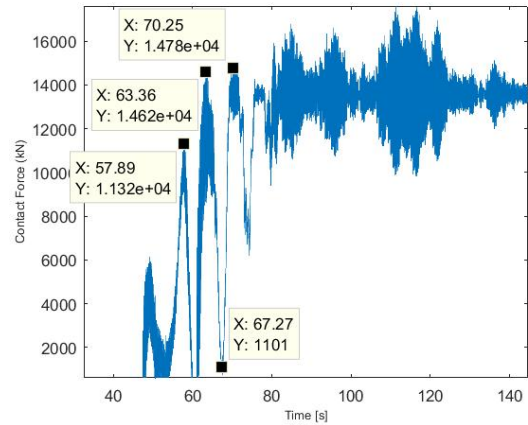
(c) Time-trace of vertical impact load bucket right



(d) Zoomed-in time-trace of vertical impact load bucket right



(e) Time-trace of vertical impact load TP



(f) Zoomed-in time-trace of vertical impact load TP

Figure 5.13: Impact load on buckets & TP [kN], sea state  $H_s : 2.5m, T_p : 6s$

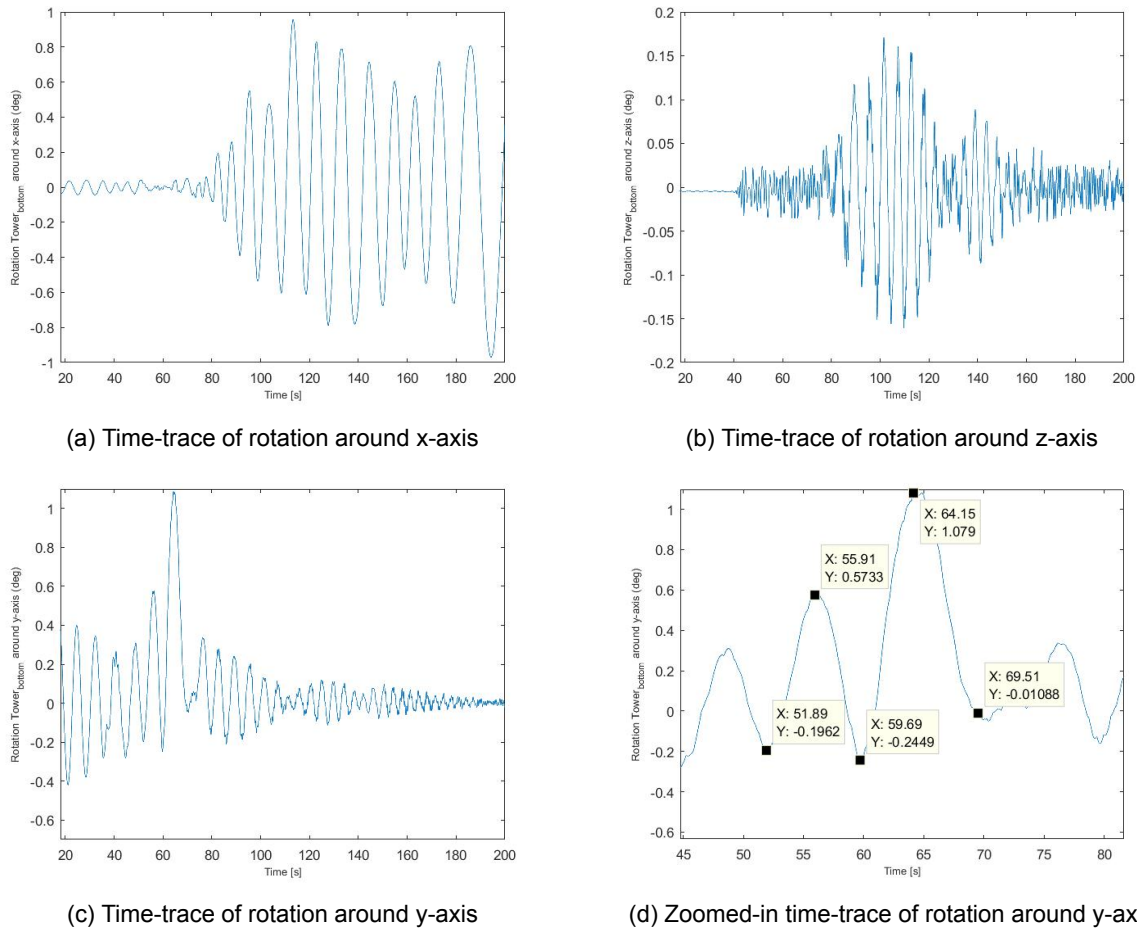


Figure 5.14: Rotations of Tower bottom [deg], sea state  $H_s : 2.5m$ ,  $T_p : 6s$

The following can be noted when looking at the time series of the impact loads (Figure 5.13) and rotations (Figure 5.14):

1. 100 s after the first contact of the tower on the flange of the TP, it can be assumed the system is relative stable and the average of the load represent the static load. The sum of these loads is 13,750 kN, which is close to the total weight of the WTG and the lift frame (12,851 kN).
2. However, due to only 0.5% of the critical damping on steel-to-steel, the system is not completely stable after 100 s. This can be observed in the rotations around the x-axis as well. The bandwidth of the fluctuation of the dynamic impact load (Figure 5.13f) will be smaller if damping or any steel-to-steel friction is added.
3. The maximum impact load in the buckets confirm the expectations based on the sum of spring and damper forces, for sea states with  $H_s : 2.5m$   $T_p : 6s$  the maximum is 117.5 kN (left) and 113.5 kN (right) (Figure 5.13b, 5.13d).
4. The buckets experience more peaks of impact loads after the first contact. In most cases the first contact is the maximum peak. The smaller peaks after the first maximum are correlating to rotations of the WTG around the y-axis (relative to the length of the Thialf).
5. Rotations of the WTG around the y-axis (relative to the pitch motions of the Thialf) are significantly larger than rotations around the x-axis (relative to the roll motions of the Thialf) and rotations around the z-axis (relative to the yaw motions of the Thialf). See Figure 5.12 for sign conventions.

6. The first contact load on the flange of the TP is damped by the buckets. The difference between  $TP_{avg}$  and  $TP_{first,max}$  is bigger for sea states with with 2.5  $H_s$  6  $T_p$  than for sea states 0.75  $H_s$  9  $T_p$ ; the latter sea state has a bigger influence on the first maximum impact load on the TP.
7. Damping of the buckets can only be modeled OrcaFlex in downward direction. This means there is no damping term when the WTG is moving upwards. In Figure 5.13b, 5.13d the effect of asymmetrical damping can be seen; the impact force is increasing until it suddenly drops to 75 kN (force with spring term only). Afterwards the impact load quickly increases and decreases several times in succession, with an overall decrease due to damping.
8. The maximum impact load on the flange of the TP mostly occurs after the first maximum impact. Rotations of the WTG around the y-axis are correlated to the moment of occurrence of impact loads on the TP.
9. The natural period of the TP, 100 s after first contact, is around 0.125-0.142 s. This is in the order of magnitude of the expected value (0.105 s).
10. The 'group' vibration of the TP after 100 s can be explained with the way the TP is modeled (Figure 5.11): the extra mass at the top of the TP can cause some inertia.

#### 5.4.5. Impact load during set-down moment in multiple sea states

The environment as stated in section 5.4.3, is used for the analysis of impact loads occurring in multiple sea states. First, the simulations that failed are thrown away. In most failed simulations the pins stabbed outside the buckets, which will not happen in reality due to human interaction. A small part of the failed simulations the pins were guided through the cones, after which pins moved through the cylinder or cone. This latter effect shows a modeling flaw, which should be corrected if more analyses were to be done. It is observed that when a operation is succeeded, the Tower is relatively stable after 100 s from the lowering start. The average static load on each bucket is  $\approx 75$  kN. Therefore, simulations are thrown away were the average static load of the bucket is less than 40 kN. In Figure 5.15 the number of successful and failed simulations are depicted, with 43 % succeeded simulations of the total 3187 performed simulations for all sea states. The figure shows that the threshold of 40 kN is correct. The distribution of failed simulations are illustrated in Figure 5.16.

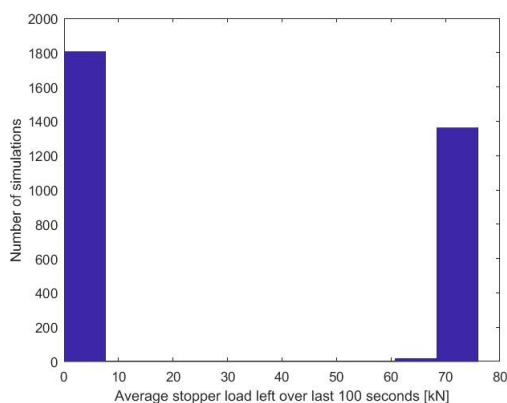


Figure 5.15: Total number of failed simulations (left bar) and successful simulations (right bar)

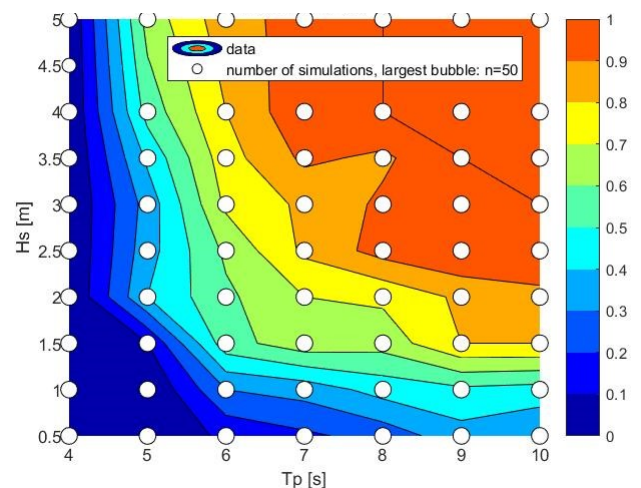


Figure 5.16: Distribution of failed simulations per sea state (mean)

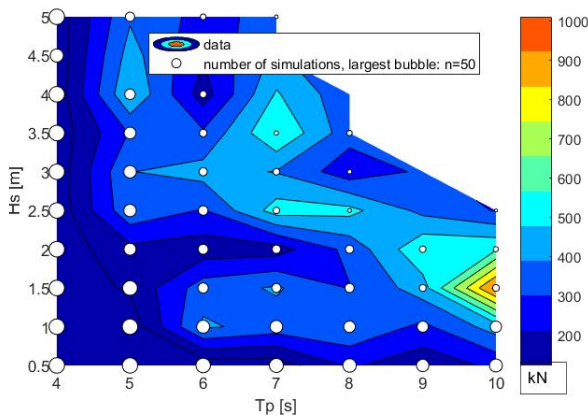


Figure 5.17: Maximum impact load on left bucket [kN] (P90)

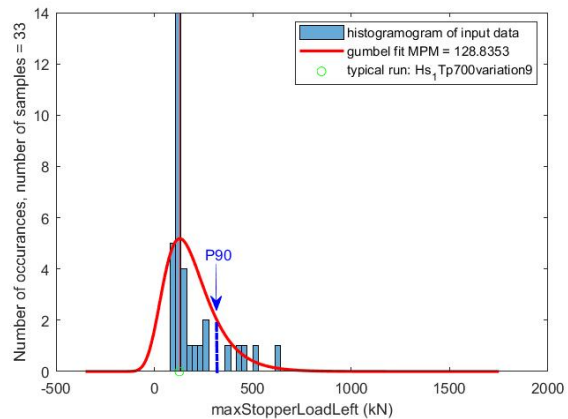


Figure 5.18: Distribution of maximum impact load on left bucket,  $H_s : 1m, T_p : 7s$

The maximum impact load on the left bucket is depicted per sea state in Figure 5.17. Keeping in mind the (average) operability curve, the maximum impact load on the left bucket is lower than 400 kN in most sea states. Note that the size of the white circle implies the number of successful simulations. Therefore, conclusions cannot be drawn from the sea state with  $H_s : 1.5m, T_p : 10s$ . This can be the result of not having statistically sound data. Moreover, note that the upper right corner is lacking information due zero successful simulations. Finally, note that a P90 is taken from the data as this provides information for engineering purposes for the ultimate limit state, instead of using a Gumbel distribution. Figure 5.18 shows the distribution of maximum impact loads on the left bucket for one sea state with  $H_s : 1m, T_p : 7s$ . It illustrates that there are some outliers in maximum impact loads, which occurs in most sea states.

As can be seen from Figure 5.19 and 5.20 the maximum load on the TP after the first contact with the Tower, is in most cases lower than the maximum load occurring in the entire time of the simulation. This means the set-down of the wind turbine is successfully guided

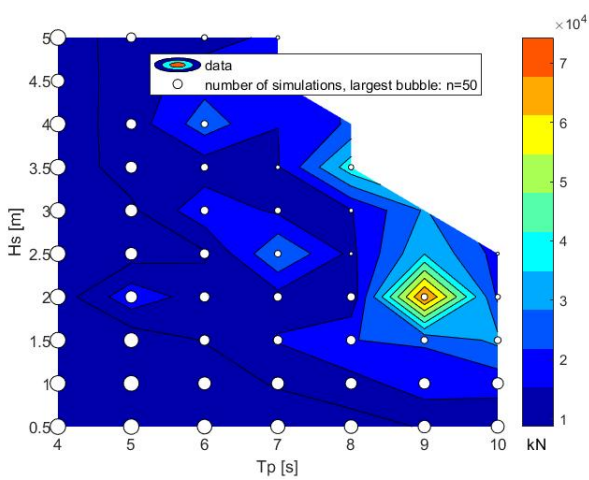


Figure 5.19: First maximum impact load on TP [kN] (P90)

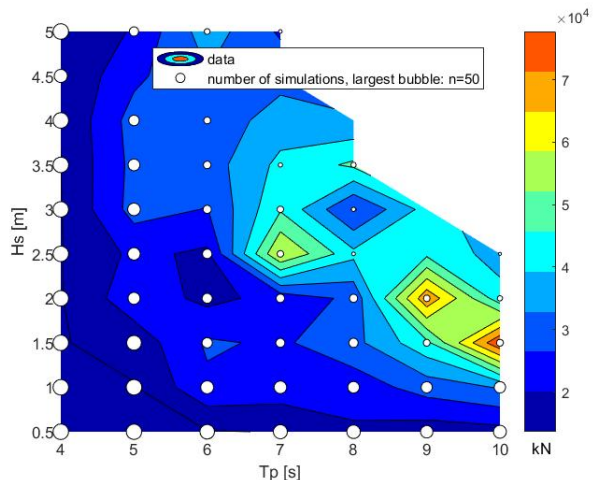


Figure 5.20: Maximum impact load on TP [kN] (P90)

It is interesting to analyze the relation of the impact load on the TP with the velocity of the bottom of the WTG Tower. As mentioned before, this velocity is the result of the lowering velocity of the hoist wires and the velocity induced by the hydrodynamic loading. In this case, the maximum impact load after the first contact is considered. Of course, the impact loads of later impact moments could be analyzed as well.

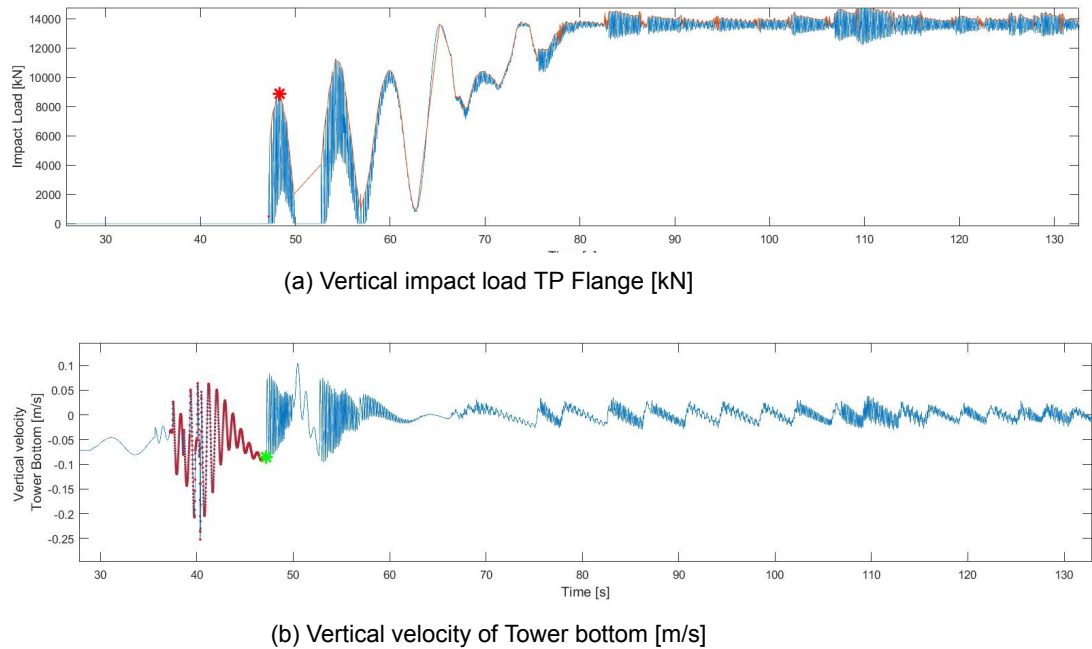


Figure 5.21: Zoomed-in time-series of impact load TP (a) and velocity Tower (b), sea state:  $H_s = 1.5m$ ,  $T_p = 6s$

In Figure 5.21a the red line is 'smoothed' out over the maxima of impact loads, and the red star marks the maximum impact load of interest. In Figure 5.21b the vertical velocity of the Tower can be observed, where the green star marks the velocity of the Tower before the first contact with the TP.

Before the Tower hits the TP, the pins make an impact on the buckets, which can explain the sudden change in velocity at  $t = 36s$ . The red line marks 10 seconds before the first contact of the TP and the Tower. It shows high fluctuations in velocity at  $t = 40s$ , this could be due to the low stiffness of the spring at the bottom of the bucket ( $250 \text{ kN/m}$ ). At  $t = 47.2s$ , the first impact on the TP occurs, resulting in a shorter natural period of  $T_n = 0.17s$ . At  $t = 50s$ , the Tower is moving in upward direction again, after which the second impact on the TP occurs at  $t = 53s$ . This measured shorter  $T_n$  should be resembling with the calculated  $T_n$  based on the stiffness of the total TP ( $k_{TP} = 4.66E+06 \text{ kN/m} \rightarrow T_n = 0.105s$ ). It is in the order of magnitude, but apparently the TP is less stiff in the OrcaFlex model than the calculated stiffness.

It is recommended to analyze the relation of the impact load on the TP and the velocity of the crane tip as well. The cause of the difference, between the velocity of the Tower and the crane tip should be investigated, as the WTG will vibrate in its own natural period during the free-hanging phase. This motion behavior is caused directly by wind loading, and indirectly by hydrodynamic loading.

In Figure 5.22 and 5.23 the first maximum impact load on the TP and the vertical velocity of the Tower are plotted for one sea state. The green line marks the limit chosen by the crane operator, in this case the maximum vertical velocity is  $V_z = 0.1m/s$ . Therefore, the impact loads left from the green line are of interest in this case.

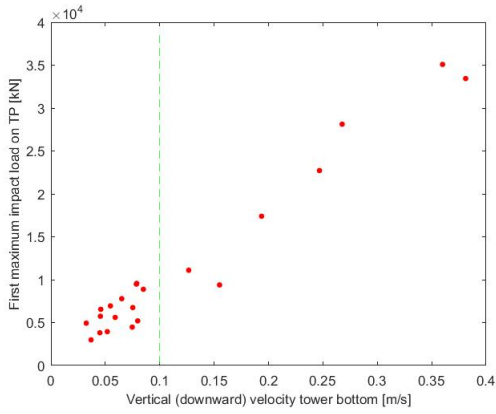


Figure 5.22: First maximum impact load vs. vertical velocity, sea state =  $H_s : 1.5m, T_p : 6s$

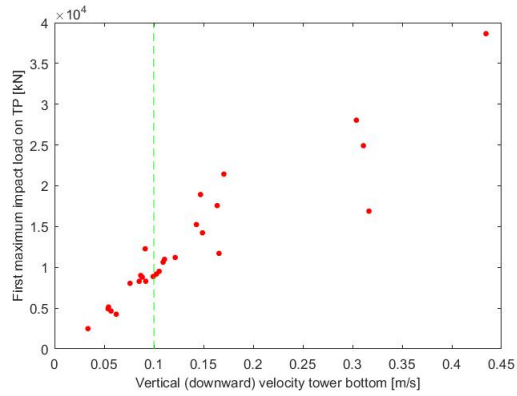


Figure 5.23: First maximum impact load vs. vertical velocity, sea state =  $H_s : 1m, T_p : 10s$

In Figure 5.24 and 5.25 the relation between first maximum impact load on the TP and the vertical velocity of the Tower are plotted for multiple sea state (defined in section 5.4.3). The horizontal green line marks the maximum first impact load (16,200 kN) that can occur when the velocity limit (marked with the vertical green line) is not exceeded. In other words, even though impact loads of 40,000 kN are found with the use of Monte Carlo approach, the expected impact loads are less than 16,200 kN, due to human intervention. It can be observed from Figure 5.25 that more than 95 % of all the successful simulations, the first maximum impact load is lower than the average static load the last 100 s of the simulation. This means that the first impact is successfully damped by the buckets.

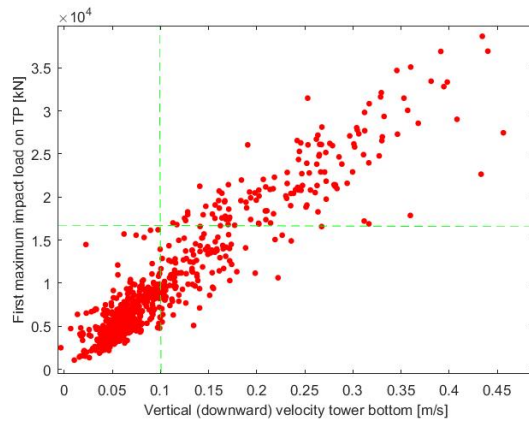


Figure 5.24: First maximum impact load vs. vertical velocity

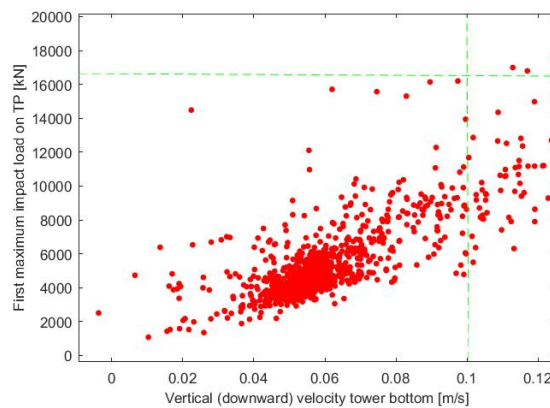


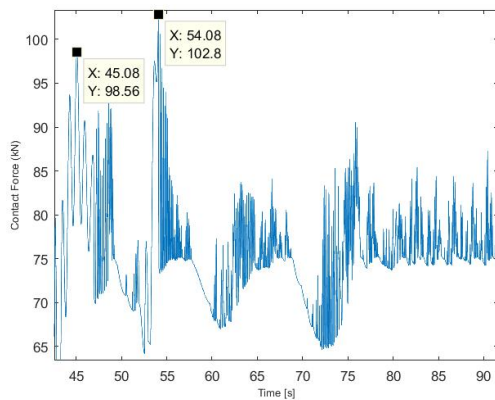
Figure 5.25: Zoomed-in plot of first maximum impact load vs. vertical velocity

### 5.4.6. Impact load during optimal set-down moment

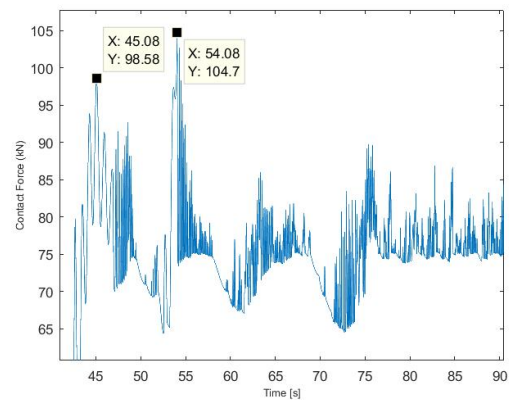
The impact loads on the bucket, the first maximum and the maximum, are relatively low if the velocity of the sea elevation is small during the moment of set-down. In table 5.7 the impact loads of an example (1 simulation with sea state 2.5  $H_s$  6  $T_p$ ) is given.

Table 5.7: Impact loads for optimal set-down moment

JONSWAP 2.5 $H_s$ 6 $T_p$	Average static load (kN)	First Maximum load (kN)	Maximum load (kN)
Bucket_left	75.4	98.6	102.8
Bucket_right	75.4	98.6	104.7
TP	13598.0	7828.0	15197.2



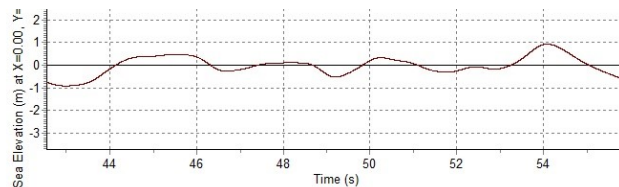
(a) Zoomed-in time-trace of vertical contact force bucket left



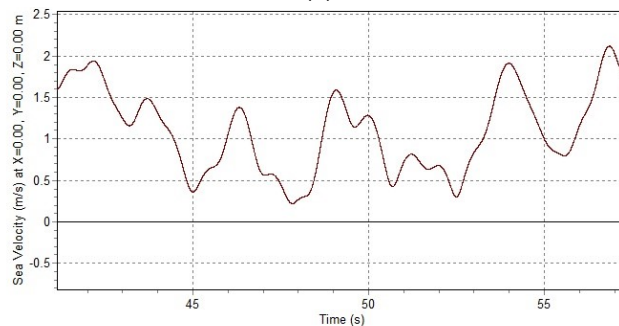
(b) Zoomed-in time-trace of vertical contact force bucket right

Figure 5.26: Contact forces on buckets with sea state 2.5  $H_s$  6  $T_p$

At 45.08 s the velocity of the sea elevation is smaller than 0.6 m/s, and in a 'valley' (Figure 5.27b).



(a)



(b)

Figure 5.27: (a) Sea elevation, (b) Sea velocity

## 5.5. Impact load reduction with a docking system of 3 units

A third pin and bucket is added to the docking system, to analyze the effect on the impact loads and the rotations (Figure 5.28). Table 5.8 shows the reduction in impact loads on the buckets and the transition piece. For the given sea state only 8 successful simulations were taken into account. It is recommended to perform more simulations and for different sea state, in order to validate the result. The reduction in maximum rotations is minimal, as can be seen from Table 5.9 (see Figure 5.12 for sign conventions). This can be the effect of 0.5 % of the critical damping on steel-to-steel, like is stated in point two on page 45.

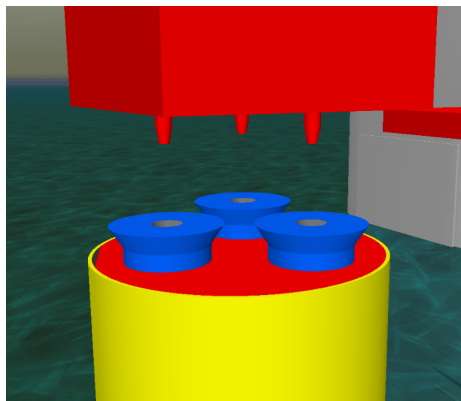


Figure 5.28: Docking system with 3 units

Table 5.8: Reduction in impact loads with 3 pins (average values of 8 simulations)

<b>JONSWAP 0.75 Hs 9 Tp</b>	<b>First maximum load (kN)</b>	<b>Maximum load (kN)</b>	<b>Average static load (kN)</b>
Bucket (left)		137.8	75.2
TP	11463.4	18150.0	13598.6
Bucket (left) - 3 pins		112.0	75.6
TP - 3 pins	8149.6	15958.4	13532.0

Table 5.9: Reduction in maximum rotations of wind turbine tower

<b>JONSWAP 0.75 Hs 9 Tp</b>	<b>Maximum rotations around x-axis (deg)</b>	<b>Maximum rotations around y-axis (deg)</b>	<b>Maximum rotations around z-axis (deg)</b>
Tower	-0.72	0.85	-0.24
Tower - 3 pins	0.68	0.62	-0.11



# Optimization of workability by reducing required time-frame for set-down

## 6.1. Sequence tool

In order to estimate the amount of Waiting on Weather (WoW) for the installation of an OWF, the sequence tool is used. The sequence tool is an in-house software program of Heerema, that bases the WoW estimations on historical time series of wave measurements that are considered indicative for the project location. In section 5.2.1 the different steps (called operations) that will be carried out after each other are listed. For each operation criteria are specified, that determine whether work can be carried out or not (section 5.1). Multiple criteria can be given per operation. The sequence is then used to calculate how much waiting on weather time would have occurred when the project had started at a certain date in the past. This computation is repeated for a large number of dates starting in a particular season (e.g. month) resulting in a probability distribution function of total waiting on weather. Finally, for each month the expected mean duration to finish a operation as well as to finish the whole project are computed. It should be noted that the outcome of the sequence tool is only statistical, and that no (hydrodynamic) loading calculations are made.

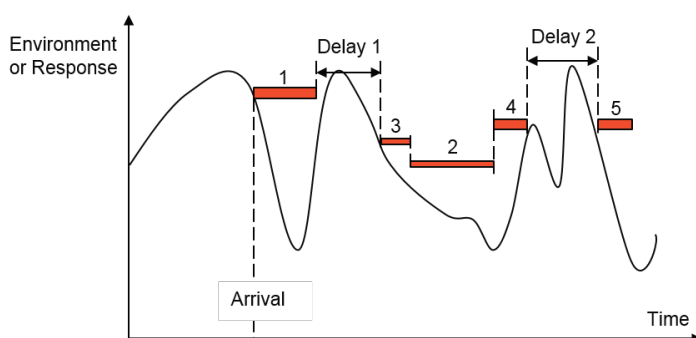


Figure 6.1: Delay determined in sequence tool

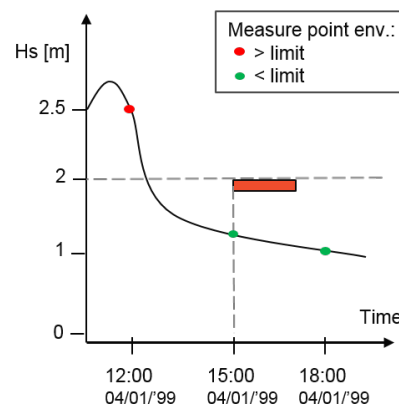


Figure 6.2: Datapoints in environment

In figure 6.1 the way delay is determined in the sequence tool is depicted. If the environmental value (e.g. significant wave height or wind speed) or the response (e.g. motion, velocity or acceleration) is above the limit for the duration of the operation, the delay starts. The length of the red box in figure 6.1 represents the duration of an operation, and the position of the red box relative to the y-axis represents the stated limit.

In figure 6.2 the consequence for the delay of a resolution of 3 hours of wave measurements is depicted. For example, if the duration of an operation is 2 hours and the limit is 2 m of significant wave height, a delay of 3 hours can be estimated which will not occur in reality. Sequence tool determines if the wave measurement is above the limit (red dot in figure 6.2), and continues to evaluate the next measurement. In reality the sea state could be as represented with the black line, and the operation can already be commenced at 13:00 o'clock. In order to take a short step duration of one minute into account, an alternative approach was used, which is explained in section 6.3.

## 6.2. Waiting on weather for installation of entire wind farm

To demonstrate the effect of weather downtime for the installation of an entire OWF, a test case is performed. One of the three project locations, used in section 4.2, is chosen: IJmuiden Ver. The OWF is located at 80 km from the Dutch coastline, and consists of 80 WTGs with a capacity of 10 MW. For the installation of 4 turbines 22 consecutive operations are required (section 5.2.1), and 440 operations in total for 80 turbines. The average waiting on weather time is calculated per step, starting in a specific month. It can be observed from figure ?? that the operation 'WTG lift' has a significantly larger WoW time. Considering this operation is strongly restricted (with a downward velocity of  $Tower_{bottom} = 0.04 \text{ m/s}$ ), it can be expected.

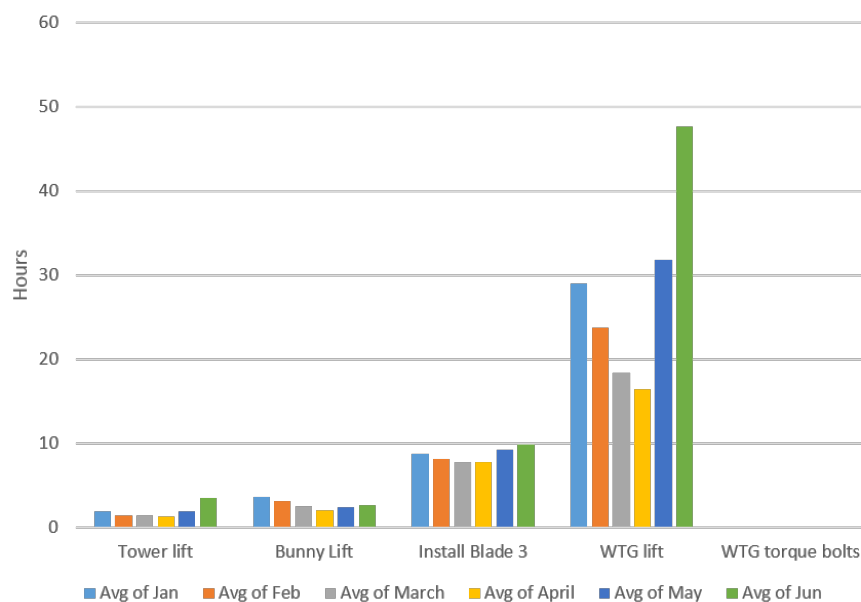


Figure 6.3: Average waiting on weather per installation step

## 6.3. Uptime analysis

### 6.3.1. Wave radar forecast

An internal study at Heerema investigated if the use of deterministic motion forecasting, wave radar particularly, can increase the operability of offshore lifting operations [56]. When vessel motion exceed prescribed limits, an operation will be postponed. The wave radar is able to forecast a quiescent period within a period of limit exceeding vessel motions, and consequently the limits for the module can be broadened. It is assumed it is possible to predict the incoming waves with a forecasted time span of two minutes, using wave radar [56].

With the implementation of wave radar technology in the Thialf, the crane operator can see the wave forecast on a display in the cabin. When a weather window occurs on the display, the crane operator can push a button to start lowering the hoist wires for the set-down. It is assumed software can calculate the motions of the WTG based on the wave forecast. Furthermore, it is assumed software can analyze an optimal moment for set-down with the least hydrodynamic loading. At last, it is assumed software can insert a delay between the moment the crane operator pushes the button and the moment the tower will have a first contact with the TP.

If the 2 minute wave and motion forecast can ensure the moment of set-down, the assumed duration of the step 'WTG lift' can be reduced drastically. The influence of a shorter step duration is concluded in section 6.4.

### 6.3.2. Semi-deterministic Matlab model

For eight incoming wave directions, the motion-, velocity- and acceleration-RAO of  $Tower_{bottom}$ , generated in LiftDyn, are used to produce a response spectrum. The RAO in z-direction for one wave direction is selected, with the accompanying RAO-phase. A wave spectrum is made with varying significant wave heights and wave peak periods. The peak enhancement factor gamma is set to 2. Afterwards a response spectrum is made with equation 5.5. A check on the RAOs is performed, by deriving the velocity- and acceleration-RAO from the z-motion-RAO.

A time-series response is made for the duration of 9000 s, with  $dt = 0.1$  s. Because an aliasing effect is ought to be prevented, a new omega is made based on the maximum duration of the time series. A new response spectrum can be created, and the RAO-phases should be interpolated accordingly based on the new omega. A random phase is generated for the wave spectrum, which is uniformly distributed for deep water. For a given sea state, the time series of a motion response of the WTG is generated using the Inverse Fourier Transformation. Similarly, the time-series of a velocity and acceleration response is generated. In Appendix  the Matlab code can be found for further explanation.

### 6.3.3. Increase in uptime percentage by reducing time-frame for set-down moment

A generated vertical motion response for a given sea state is depicted in figure 6.4. The time-series of the downward velocity of the WTG (Fig. 6.5) is highlighted in pink if it is below the threshold (i.e.  $-0.05 \text{ m/s}$ ). If this limit is not exceeded for a specified short time frame, a weather window is detected (highlighted in green in Fig. 6.5). The influence of the size of the time frame is shown in figure (verwijst naar scatterplots). The percentage of uptime is calculated by the total time of weather windows divided by the total time of the time-series. In figure 6.5 a time-frame of 90 s with a sea state of 1.5 m and 6 s, resulted in an uptime of 22 %.

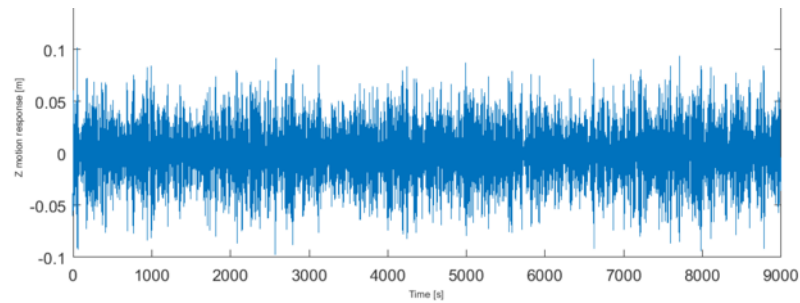


Figure 6.4: Time-series of Z-motion of  $Tower_{bottom}$  (based on  $H_s = 1.5 \text{ m}$ ,  $T_p = 6 \text{ s}$ ,  $wavedir = 0 \text{ deg}$ )

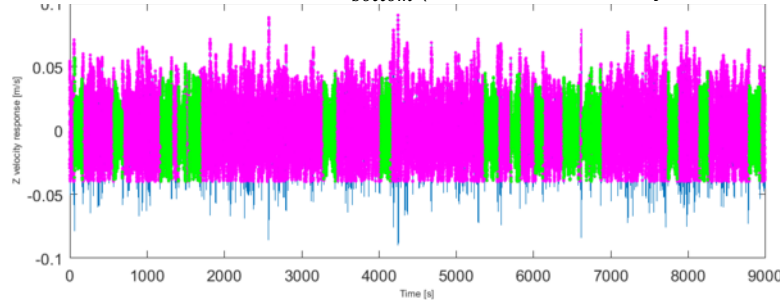


Figure 6.5: Time-series of Z-velocity of  $Tower_{bottom}$  (with 22% uptime, time-frame = 90 s)

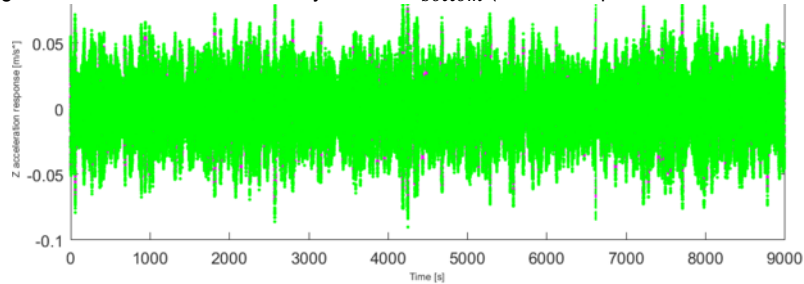


Figure 6.6: Time-series of Z-acceleration of  $Tower_{bottom}$  (with 100% uptime, time-frame = 90 s)

Likewise, the uptime is calculated for the downward acceleration of the WTG (Fig. 6.6). For each sea state, the velocity threshold was more limiting than the acceleration threshold. Therefore, the acceleration threshold is not considered in the following calculations.

When performing the uptime analysis for more sea states, a scatter diagram can be produced. In figure 6.7 the uptime is presented in a scatter diagram, with an incoming wave direction of 0 degrees. As the time-frame increases the transition area from a high to a low uptime decreases.

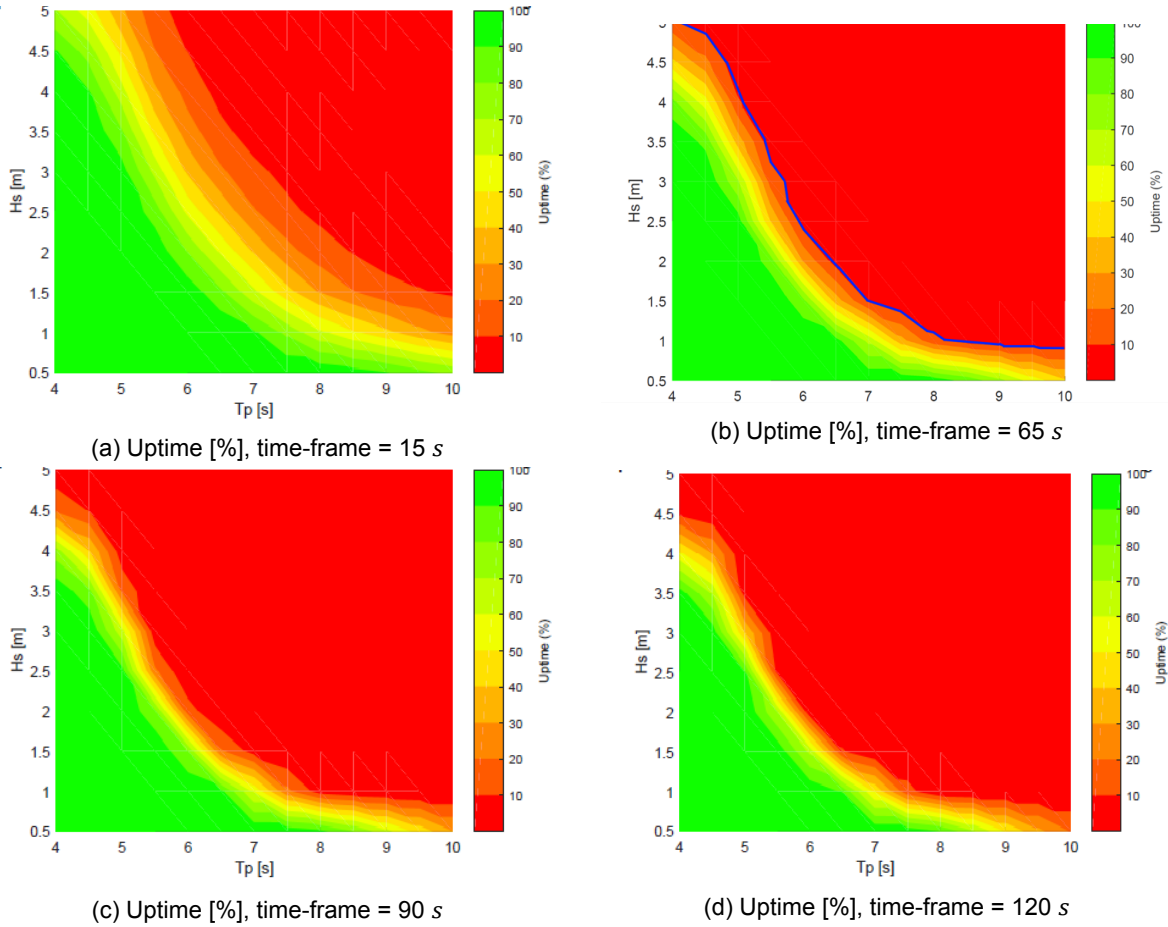


Figure 6.7: Scatter diagrams of uptime [%], with varying time-frame

As mentioned before (section 5.1), the required time-frame for the set-down operation is 65 s. The scatter diagrams for different incoming wave directions with a time-frame of 65 s can be found in Appendix A. The area below the blue line (Fig. 6.7b) marks the sea state for which the uptime is larger than 10 %. The average waiting time before a weather window occurs is 576 s. In figure 6.8 it can be observed that the average waiting time decreases when stating a higher threshold of uptime percentage.

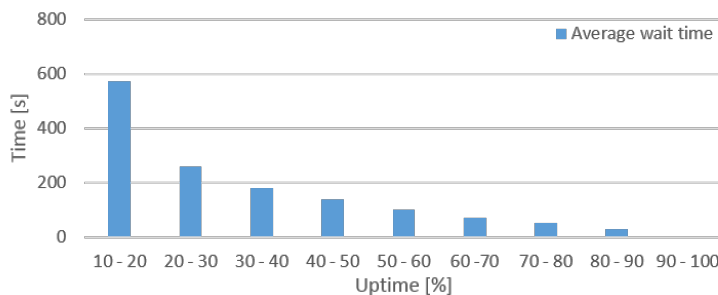


Figure 6.8: Average waiting time before a time-frame occurs depending on uptime percentage

## 6.4. Average waiting on weather with new time-frame

Now the WTG lift with a duration of 4 hours is replaced with a duration of 1 hour, combined with a WTG set-down of 65 s plus 576 s (the average waiting time a window occurs). Unfortunately, with the way the sequence tool is modeled it will not see a difference between a step duration of three hours and 65 s (Fig. 6.2). Therefore, inserting a step duration of 65 s will not affect the calculated WoW time.

An alternative way to include the velocity limit for the set-down with a duration of 65 s, is to modify the inserted environment in the sequence tool. An extra criteria is added in the environment document called 'unity check'. This unity check is the value of the Hs of the environment document divided by (the vector of) the blue line of figure 6.7b. If the value of the unity check is below one, it means the condition of staying below the velocity threshold is met (Appendix A.6). It also means that the uptime is larger than 10 % and the average waiting time before this operation can be started is 576 s. Finally, the operational limit for the set-down moment is that the unity check should be below 1.

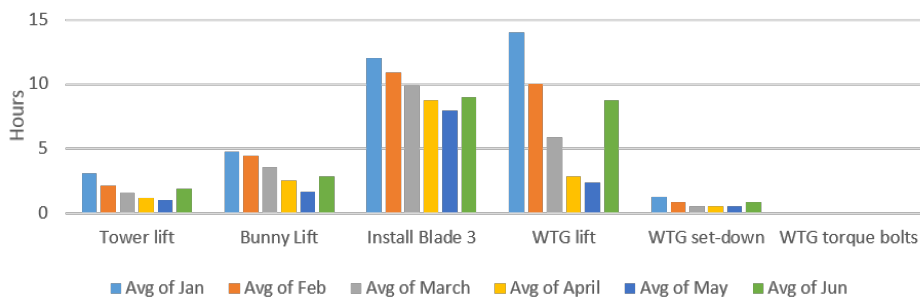


Figure 6.9: Average WoW per installation step, WTG set-down = 65 s

It can be observed that the average WoW of the 'WTG set-down' operation is drastically reduced. The average waiting time before a time frame of 65 s is included in the calculation. Furthermore, the average WoW of the 'WTG lift' is partly increased. Perhaps, the operational limits of this step are on the conservative side.

## 6.5. Total installation time for installation entire wind farm

The output file of the sequence tool states the average total operation time including WoW per each of the 440 steps, for starting in every month of the year. The start date of each step can be calculated if the average operation time including WoW is added to the step before. This resulted in figure 6.10. It can be noted that a whole day of waiting of weather for installing one turbine is very significant. The total installation time with the new time-frame of 'WTG set-down', is depicted in figure 6.11. Here 'WTG lift' is split up in 1 hour combined with WTG set-down (duration = 65 s).

Table 6.1: Total WoW days, OWF size = 80 WTGs

Month Start Installation	WoW Standard [days]	WoW New [days]	Difference WoW Stand. - New [days]
Jan	136	125	11
Feb	112	100	12
Mar	90	76	14
Apr	75	55	20
May	105	49	56
Jun	107	82	25

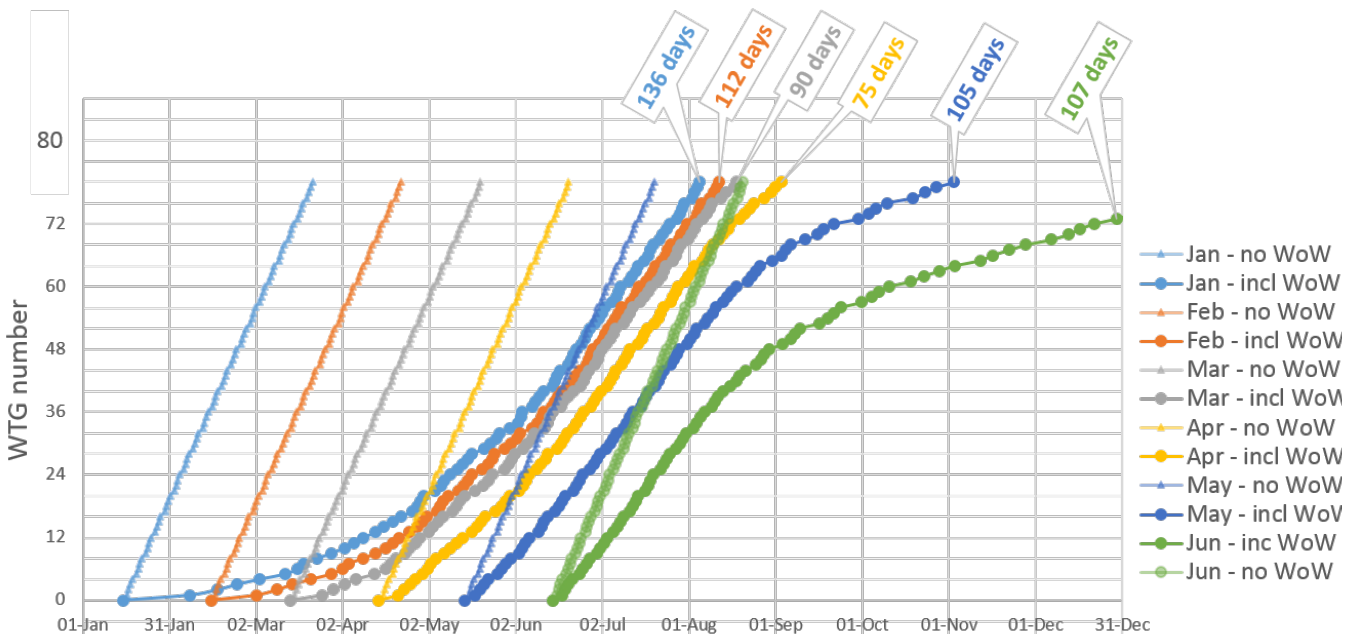


Figure 6.10: Total installation time incl. WoW

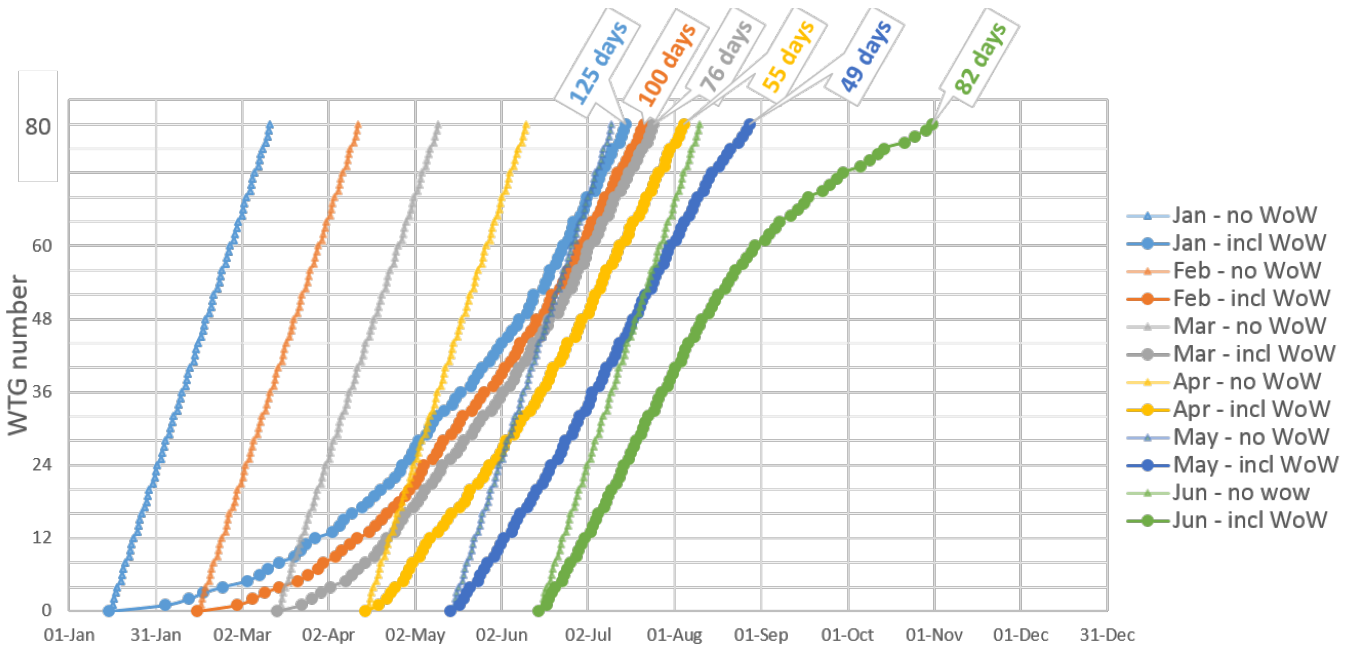


Figure 6.11: Total installation time incl. WoW, shorter time-frame



# 7

## Conclusions and recommendations

In section 1.4 the main research objective for this thesis is formulated as: 'Determine the economic and technical feasibility for Heerema to enter the offshore wind industry'. In this chapter conclusions and recommendations regarding the research question are formulated. The conclusions are split up in three sections, of which each section answers a sub-objective. The first section is on the attractiveness of the offshore wind market (section 7.1.1), the second section is on the installation costs related to logistical methods (section 7.1.2) and the third section is on the influence of wave forecast on the workability of installing a fully-assembled 10 MW WTG with a SSCV (section 7.1.3). The recommendations are given in section 7.2.

### 7.1. Conclusions

For the analysis of the offshore wind market as a business environment (Chapter 2), the theoretical framework 'PESTLE' is applied. Through the application of the 'Porter's Five Forces' model, the competitive position of Heerema as an potential entrant to the offshore wind market is analyzed. In Chapter 4 the installation costs are calculated using the current version of the ECN Install Tool. With LiftDyn the modeshapes the free-hanging WTG are computed, in order to review the risk on resonance (Chapter 5). In Chapter 5 OrcaFlex is used to simulate impact loads during the set-down moment. In order to analyze the influence of the required time-frame for the WTG set-down, a model was build in Matlab (Chapter 6). With the Sequence Tool, the installation time including the waiting on weather was calculated (Chapter 6).

#### 7.1.1. Offshore wind market

As the offshore wind market in the North Sea is rapidly evolving, it is important to comprehend the factors influencing the industry's further development and internal competition. The following conclusions can be drawn:

- The offshore wind market in the North Sea as a business environment is evaluated to be attractive. Additionally, there is a large potential for building new OWFs in the North Sea and the governmental support is significant and assumed to be stable in the future. The trends that OWF development moves into deeper waters and further offshore, as well as the increase in size of wind turbines are all positive for floating installation vessels with larger crane capacity, as many JUVs have reached their maximum capacities.

- Although the barriers to enter the OWE industry are high, the power of the OWF developers is significant and the price competition among installation operators is fierce, the threat of alternative WTGs becoming mainstream is small due to economies of scale and the enormous potential of new OWF development. There is an opportunity for Heerema to enter the market with their SSCVs and focus on the installation of extra large WTGs ( $\geq 10$  MW).

### 7.1.2. Economic feasibility

The following can be concluded, after comparing different installation strategies for installing offshore wind turbines:

- Based on the current ECN Tool (version 2.1) and the assumptions made in section 4.1, it is economically feasible to use an SSCV for the installation of completely pre-assembled wind turbines in a large OWF ( $>1500$  MW). In the scenario used in the ECN Tool, the duration of the WTG lift, installation and the SSCV sailing to the next TP should be less than six hours.

### 7.1.3. Technical feasibility

The lifting of the WTG and the soft landing on the transition piece are crucial operations with high operational limits, when utilizing a floating installation vessel. In order to optimize the workability, the effects of a 2 minute wave and motion forecast are analyzed. The following conclusions can be drawn:

- With the use of a 2 minute wave and motion forecast, the waiting on weather for the 'WTG lift' and 'WTG set-down' on the TP can be reduced from 28 hours per turbine to 7 hours for the 'WTG lift' and 48 minutes for the 'WTG set-down' (on average of 5 months).
- With the use of a 2 minute wave and motion forecast, the impact load on the bottom of the tower and the TP can be reduced by 13 % by choosing an optimal sea elevation for the set-down moment.

## 7.2. Recommendations

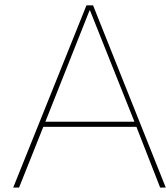
In this study the attractiveness of the offshore wind market and the economic feasibility for installing WTGs with a SSCV are analysed. Furthermore, the potential benefits of using a 2 minute wave and motion forecast are shown. Assumptions can be verified, implementation should be investigated and other areas can be explored in order to optimize the wind turbine installation. Therefore, some recommendations are given:

- As the offshore wind market is evaluated to be attractive for the coming years, it is recommended to enter this industry as an installation operator, on the condition that new developments in the market are watched closely.
- It is important to maintain close contact with the supplier of the WTGs, in order to understand in which areas innovation is possible and to cooperatively develop an installation method feasible with floating vessels.
- The estimation of step durations and operational limits, has a large influence on the analysis of installation time and accompanying costs (section 4.2). Therefore, a closer

and more detailed cooperation with industry experts is required to estimate new durations more accurately.

- As the average waiting on weather time is relative high for the steps 'Install Blade 3' and 'WTG lift', it is recommended to investigate the influence on wave radar forecast on these steps.
- In order to improve the accuracy of the RAO of the bottom of the tower, generated by LiftDyn, wind loading should be implemented. Also the influence of wind loading on WTG components during transportation and construction on the aft of the vessel should be analyzed.
- Different options of a critical path for the installation of a wind farm can be explored, such as combining two installation vessels or two cranes of one vessel for the construction of the WTG.
- It can be interesting to perform more research on the guidance of the tower to the TP, because the OrcaFlex model showed that the pins could stab outside the buckets due to hydrodynamic loading.
- Finally, in order to realize a reduction in the duration of 'WTG set-down', the implementation of wave radar technology should be investigated.





# Appendix A

## A.1. Vessel characteristics

### A.1.1. Deck configuration of pre-assembly strategies



Figure A.1: 5 Pieces Separately with Tower in 1 Piece, SealInstaller – SeaJacks



Figure A.2: Bunny Ear, Haliade - Alstom



Figure A.3: Rotor Star with Tower in 2 Pieces, Senvion

### A.1.2. Bolted connections



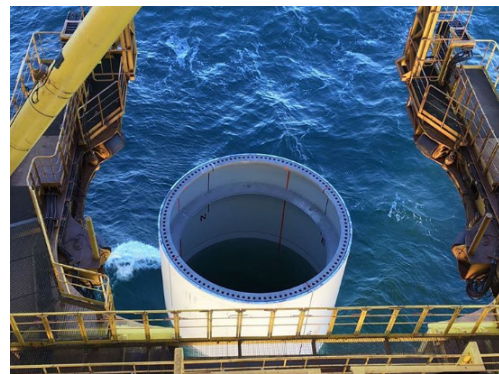
(a) Connection rotor-star assembly to nacelle



(b) Connection blade to rotor



(c) Connection inside tower



(d) Openings for bolt connections of tower

Figure A.4: Bolted connections between WTG components

### A.1.3. Vessel costs

Vessel type	Assembly	Fixed Costs, MOB/DEMOB not included (€)	Day rate (€/day)	MOB/DEMOB (€/order)	Number of components (WTG) on board	Travel Speed (kt)	Crane Lift Capacity (tonnes)	Transport Capacity (t)	Deck Space (m²)	Vessel names in this class	Turbine Class
Jack-Up Vessel	Separate components	300,000	125,000	3,250,000	5	10	>= 1200	8,000	3,800	DP2 INNOVATION, SeaJacks Scylla, Seafox 5, Pasific Osprey, Pasific Orca, Vole au Vent, Teras Sunrise	10 MW
JUV 25% +	"	375,000	156,250	4,062,500	"	"	"	"	"	"	"
SSCV	Completely pre-ass.	960,000	400,000	7,850,000	6	7	>= 7000	15,000	4,500	Thialf (HMC)	10 MW
SSCV 25% +	"	1,200,000	500,000	9,812,500	"	"	"	"	"	"	"
Dedicated WTIV	Completely pre-ass.	600,000	250,000	1,000,000	2	12	-	-	-	Shuttle (Huisman)	10 MW
Barge (met tug)	Completely pre-ass.	42,480	17,700	1,248,900	3	7			4,000		10 MW
Barge (met tug)	Separate components	42,480	17,700	1,923,900	6	7			4,000		10 MW
SSCV + 3 barge	Completely pre-ass.	1,087,440	453,100	6,546,700	3	7	>= 7000	15,000	4,000	Thialf (HMC)	10 MW
SSCV + 3 barge	Separate components	1,087,440	453,100	8,571,700	6	7	>= 7000	15,000	4,000	Thialf (HMC)	10 MW
SSCV + 3 barge 25%	"	1,327,440	553,100	9,271,700	"	"	"	"	"	"	"
SSCV + 5 barge	Completely pre-ass.	1,172,400	488,500	9,044,500	3	7	>= 7000	15,000	4,000	Thialf (HMC)	10 MW
SSCV + 5 barge 25%	"	1,412,400	588,500	9,744,500	"	"	"	"	"	"	"
SSCV + 5 barge	Separate components	1,172,400	488,500	12,419,500	6	7	>= 7000	15,000	4,000	Thialf (HMC)	10 MW

Figure A.5: Costs per vessel type, based on known JUV day-rate

Assumptions made in costs:

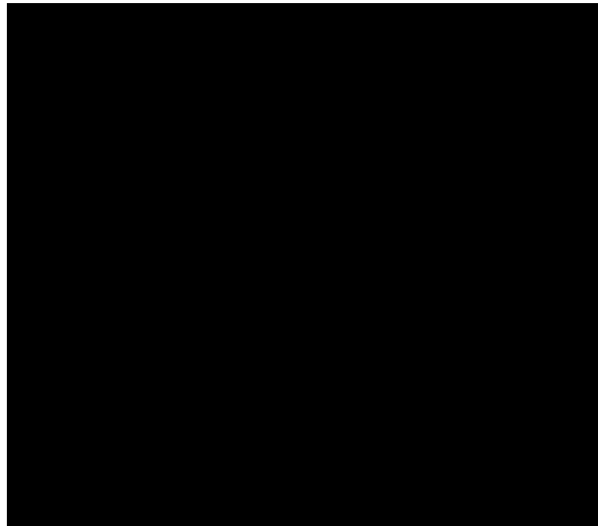
- The costs of a jack-up vessel are derived from an average of 7 vessels in the same class. For the other vessels, the same distribution is taken. The estimations of day rates of other vessels are checked with industry experts from ECN and HMC.
- Fixed costs: The 'booking' costs for reserving the vessel. This is assumed to be 2.4 times the day rate.

- Grillage: 375,000 €. It is assumed that a grillage for components is 80% of the costs of a grillage for a complete pre-assembled wind turbine.
- MOB/ DEMOB: (14 day rate vessel) + (# of WTGs on board grillage cost). These are the costs to prepare the vessel for operation, installing the grillages etc. For a vessel it is assumed that 2 weeks of preparations are necessary, for vessel in combination with a feeder barge 1 week of preparation are considered to be necessary.
- Day rate waiting: It is depending on the contract with the developer. It can be 80%, but for the performed cases it is assumed to be 100%.
- Barge: 17,700 €/ day. It is assumed this price includes 1 tug boat.
- Port: The cost of the operation bases will be assumed to be the same for all 3 ports at a day rate of € 15,000/day. In reality this will be dependent on the quay length and the tonnage per square meter the quay area can handle.
- During the installation is it assumed working shifts can be filled 24/7.
- It is assumed there are no permit constraints for the installation of wind turbines.

#### A.1.4. Step duration for a jack-up vessel

The duration per installation step for installing an offshore wind turbine with a jack-up vessel, is in-house knowledge of ECN.

Table A.1: Duration per installation step of a jack-up vessel



### A.1.5. Sailing route from port to site location

For the estimation of the distance of sailing route from port to site location, 'Google Earth' is used. New shipping routes, published by Rijkswaterstaat, are taken into account.

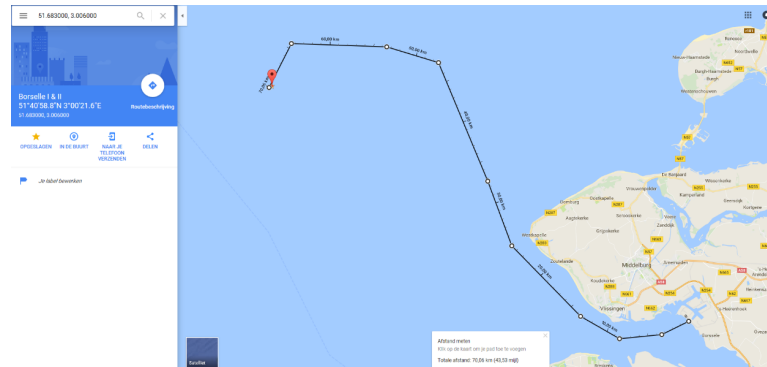
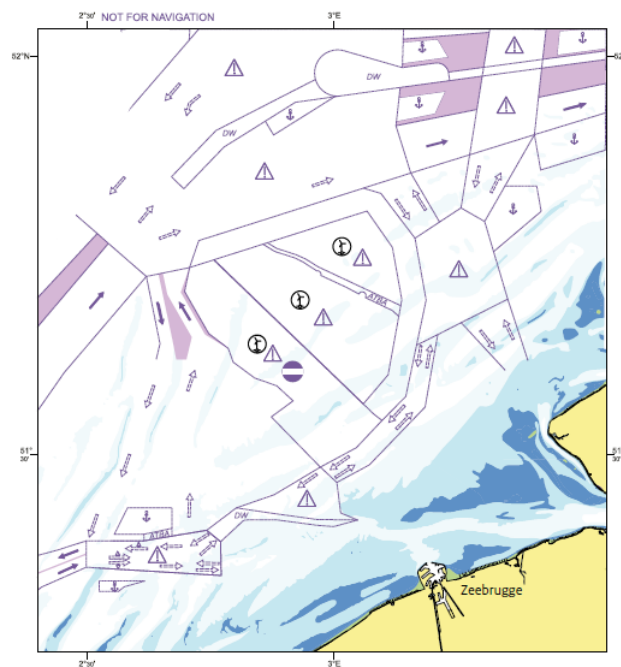


Figure A.6: Example sailing route: from Vlissingen port to Borselle I & II ( $\approx 70$  km)

Situatie vanaf 1 juni 2017



#### Nieuwe regels voor varen in windparken

Naast het vastleggen van de nieuwe routes, hebben België en Nederland afspraken gemaakt over de doorvaart van de (nog aan te leggen) windparken bij Borssele:

- Alle Belgische windparken zijn gesloten voor doorvaart.
- Nadat de windparken bij Borssele zijn opgeleverd, mogen kleine schepen (<24 m) onder voorwaarden door de Nederlandse windparken varen.
- In het Nederlandse windenergiegebied Borssele is een scheepvaartcorridor opgenomen waarin schepen kleiner dan 45 m mogen varen.

Figure A.7: New shipping route for sailing in offshore wind farms

## A.2. Dimensions offshore wind turbine and lift-frame

Currently the largest wind turbine is designed by MHI Vestas and has a capacity of 9.5 MW with a rotor diameter of 164 m [57]. It is an upgraded version of the originally 7 MW turbine introduced in 2011. The originally 7 MW was already designed for at least 8 MW, but an extra 2.5 MW of upscaled capacity was not expected by the industry. It shows that there is an range of possible generators constructed in a wind turbine with the same physical dimensions of tower, nacelle and blades. Because there is only information available on the 8 MW WTG with a rotor diameter of 164 m (known as V164-8.0MW), this was taken as a starting point for upscaling [58]. A study from the Technical University of Denmark (DTU) designed a Reference Wind Turbine (RWT) of 10 MW, stated some of the dimensions: rotor diameter of 178.3 m and hub height of 119 m [59]. Also the mass of the tower, nacelle and blades were stated: 605 t, 446 t and 41 t respectively. The complete 10 MW wind turbine has a mass of 1174 t. The unknown dimensions were linearly upscaled, resulting in dimensions presented in table A.2. As the 10 MW RWT is originally upscaled from 7 MW, of which its dimensions are also applicable for a 9.5 MW WTG, it can be assumed the calculated dimensions are conservative. It can be assumed the dimensions of the 10 MW RWT could be valid with an upgraded generator of 12.5 MW.

Table A.2: Dimensions of 10 MW RWT

Item	Length [m]	Width [m]	Height [m]	Weight [t]
Nacelle & Hub	23.0	9.8	10.4	446
Blade	89.2	5.3	6.7	41
Item	Length [m]	Bottom dia. [m]	Top dia. [m]	Weight [t]
Tower	119	7.6	5.6	605

The locations of the Center of Gravity (COG) per component were also linearly upscaled (table A.3). The COG of the tower and blade are at 40% and 25% of their total length respectively. It is assumed the COG of the blade is centered to simplify the calculations of the radii of gyration, but in reality it is positioned at around 5% of its width.

Table A.3: COG per component of 10 MW RWT

Item	Length [m]	Width [m]
Nacelle & Hub	13	5
Blade	22	0
Tower	48	0

The design of the lift-frame for the single-lift installation of a complete WTG (Fig. A.8) is based upon the rigging arrangement used in the Hywind project [12]. The dimensions are estimated at  $30\text{ m} \times 7\text{ m} \times 4\text{ m}$  (L x W x H). The width of the frame is determined by the minimum allowable distance between the two cranes, to avoid collision of crane tips: the hoist wires from the crane to the frame should be vertical. The vertical position of the lift-frame is above the COG of the WTG to ensure stability. Four wires are connected from the lift-frame to another lift-frame at the bottom of the tower.



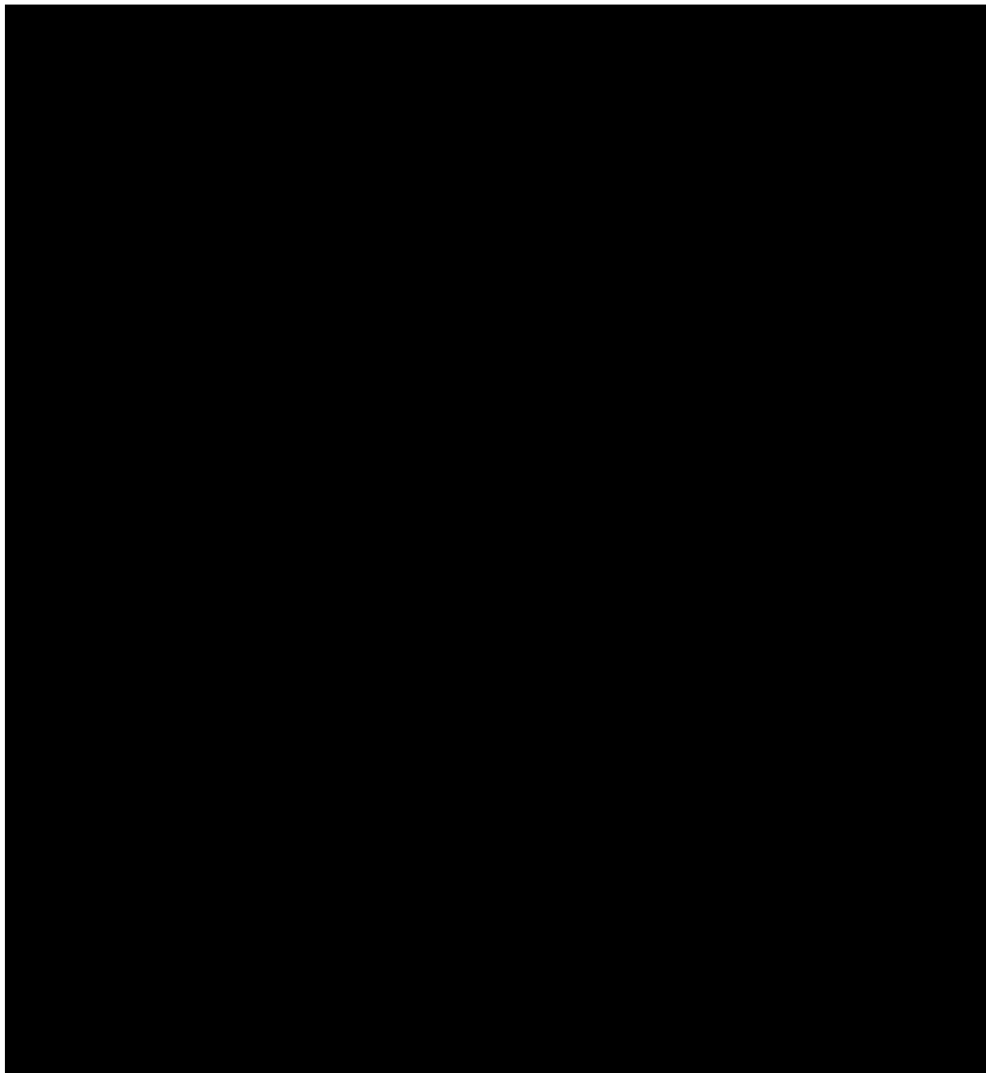
Figure A.8: Conceptual design of lift-frame for single-lift installation of WTG

### A.3. Mode shapes computed with LiftDyn

From table A.4 the following can be noted:

- The mass distribution factors show the dominating motions that are induced by the mode shapes. For example: the dominating motions of the wind turbine for mode 8 are sway and roll and for mode 9 pitch and heave.
- WTG is a rigid body; the dominating motions of mode shapes of the components of the wind turbine resemble.
- Thialf responds very little to mode shapes  $\geq 7$  (Thialf is moved by eigen periods and max. wave forces)
- Natural periods of pendulum are out of range from natural period wave spectrum North Sea (peak: 8 -10 sec) Not for swell waves!

Table A.4: Example of three mode shape mass with distribution factors of the Thialf and three components of WTG



## A.4. Impact loads on buckets during set-down

Impact loads of 1 simulation for sea state  $H_s : 2.5m$ ,  $T_p : 6s$ . The bucket is geometrically divided in 2 pieces, a cone on top to guide the pin and a cylinder below. From Figure A.15 and A.16 it can be observed that the horizontal impact load on the cylinder of the right bucket is significant (25 times larger than the maximum vertical impact load on the spring/ damper unit at the bottom of the bucket). It is recommended to improve the design of the buckets, and investigate how much the steel of the bucket may deform at maximum.

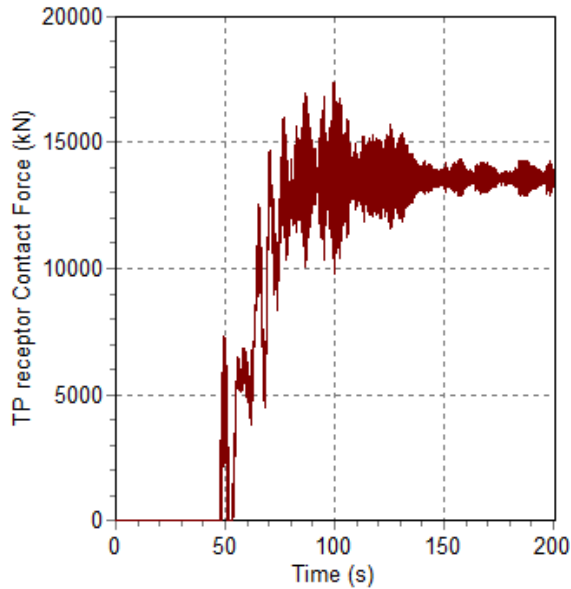


Figure A.9: Time-series of vertical impact load on TP (kN)

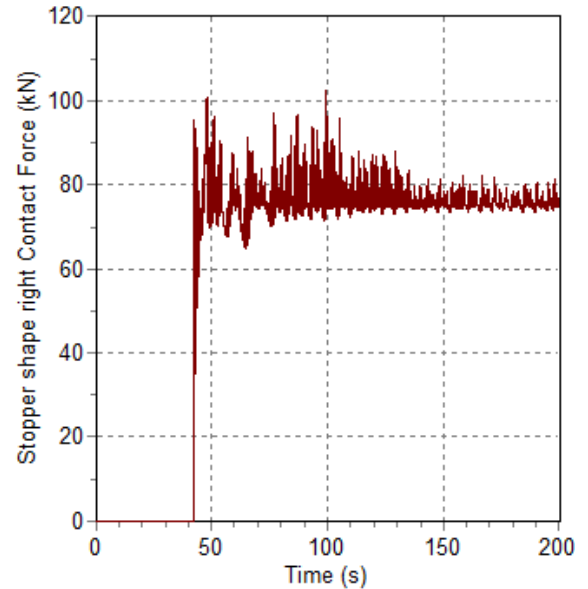


Figure A.10: Time-series of vertical impact load on right bucket (kN)

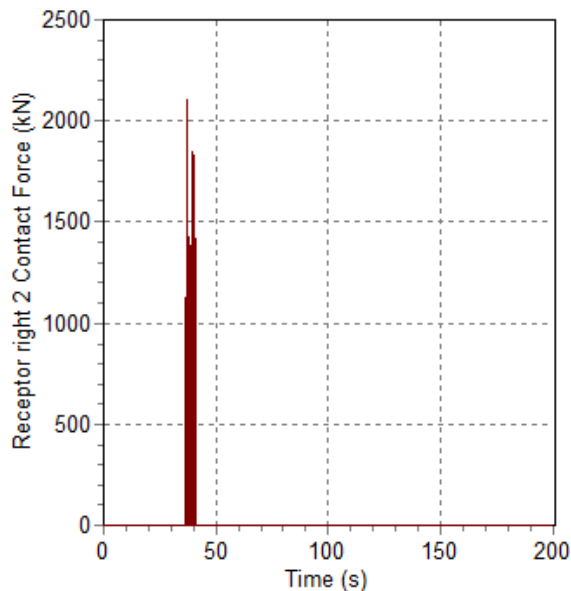


Figure A.11: Time-series of impact load on cone of right bucket (kN)

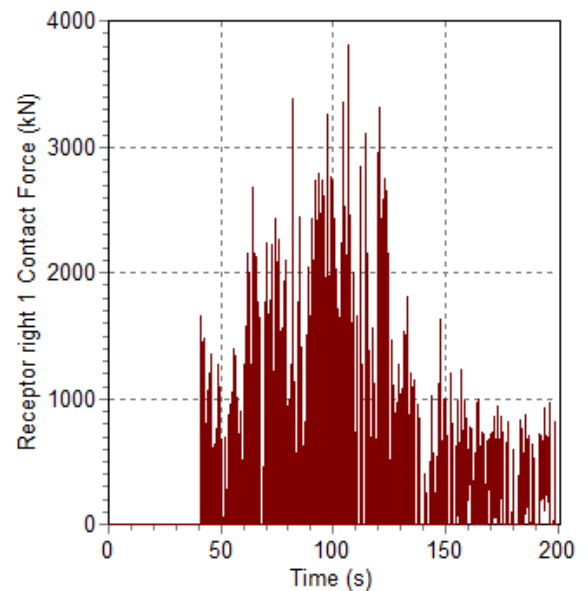


Figure A.12: Time-series of impact load on cylinder of right bucket (kN)

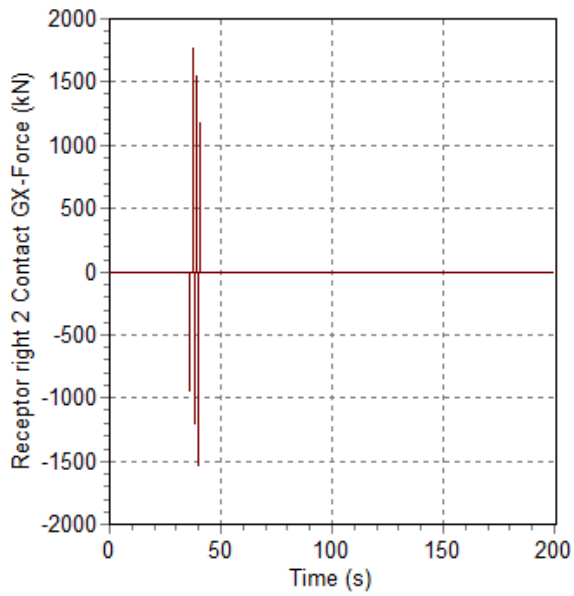


Figure A.13: Time-series of impact load on cone of right bucket in x-direction (kN)

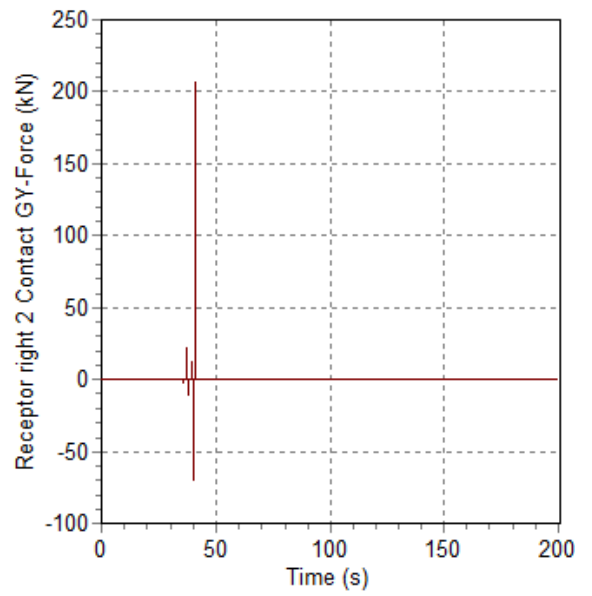


Figure A.14: Time-series of impact load on cone of right bucket in y-direction (kN)

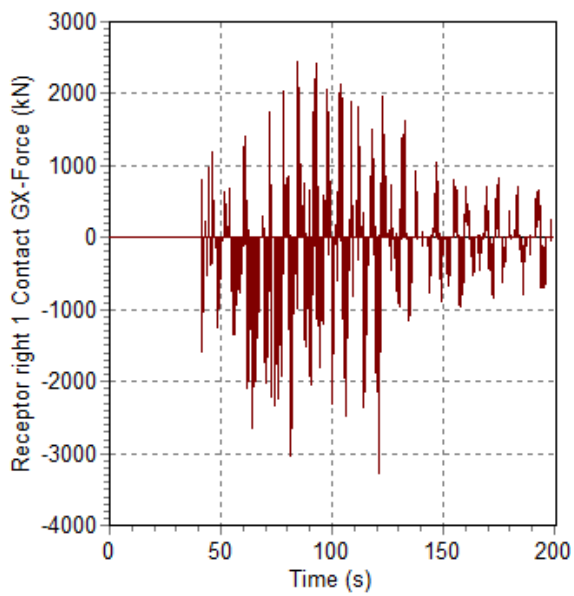


Figure A.15: Time-series of impact load on cylinder of right bucket in x-direction (kN)

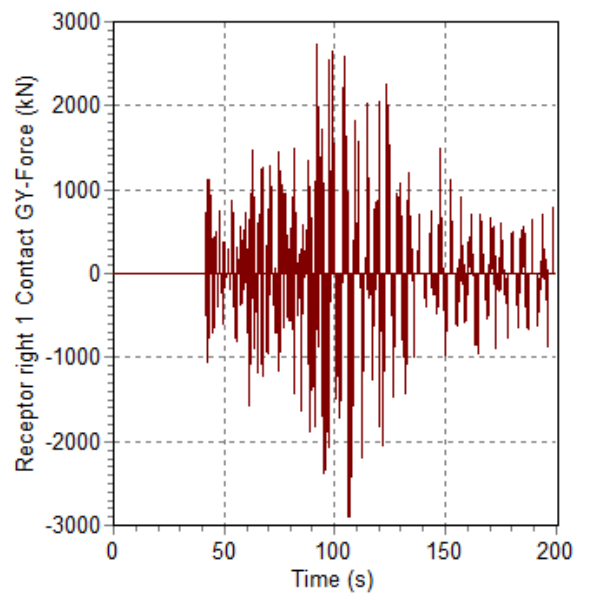


Figure A.16: Time-series of impact load on cylinder of right bucket in y-direction (kN)

## A.5. Tension hoist wires

Tension in Hoist Wires of 1 simulation for sea state  $H_s : 2.5m, T_p : 6s$ . It can be observed that after 80 s, there is no tension in the hoist wires and therefore they hang 'slag'.

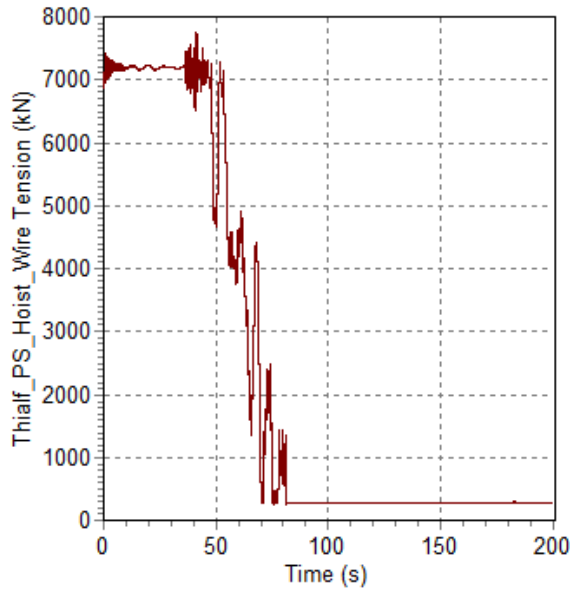


Figure A.17: Time-series of tension in hoist wire on port side crane(kN)

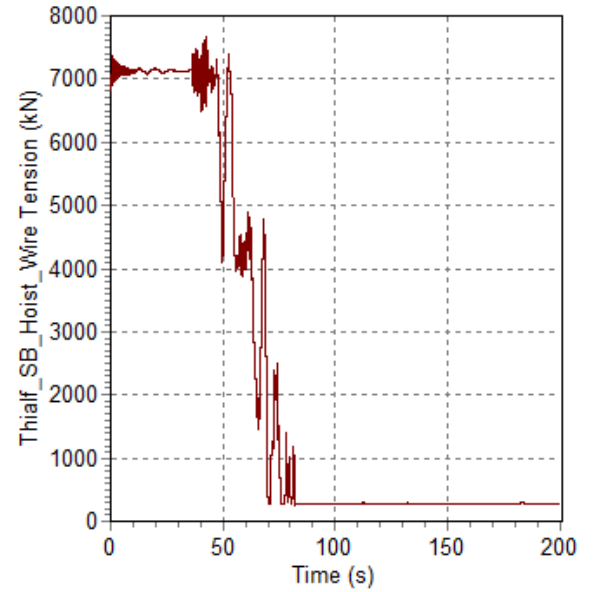


Figure A.18: Time-series of tension in hoist wire on star board crane (kN)

## A.6. Unity check for modified environment

The environment data set is modified by including an extra column, called 'unity check'. A vector, **Hs, limit**, is produced from the sea state limit for which the uptime percentage is larger than 10 % (Fig. 6.7b).

$$\text{Unity check} = \frac{\text{Hs, environment}}{\text{Hs, limit}} \quad (\text{A.1})$$

If  $UC > 1$  = the operation cannot start, and if  $UC < 1$  = the operation can start.

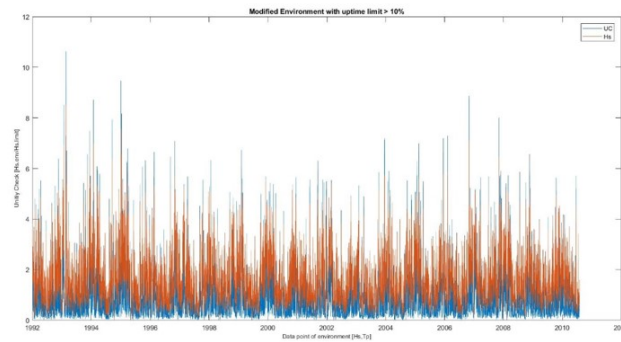


Figure A.19: Time trace of Hs,environment (orange) and Hs,limit (blue)

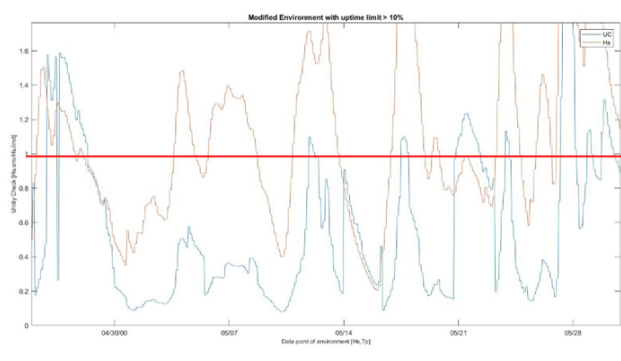


Figure A.20: Zoomed-in time trace of Hs,environment (orange) and Hs,limit (blue)



# B

## Appendix B

### B.1. Matlab codes

#### B.1.1. Matlab code: generate data files as input for OrcaFlex

```
close all; clear all; clc;
addpath('c:\data\merel\matlab\orcaflex\');
OFX_addpath;

% user input
varPath = '\\leinetaapl\condor\Tender Analysis\Student\Merel\Batch
2\runs\';
nRuns = 50;
Hss = 0.5;0.5:5;
Tps = 4:1:10;

m = ofxModel('base_model.dat');

% Loop over the defined states and write variation
mkdir(varPath);
TR = hmcTimeRemaining(length(Hss)*length(Tps));
TR.start;

for Hs = Hss
    for Tp = Tps
        m('Environment').WaveHs = Hs;
        m('Environment').WaveTp = Tp;
        for i=1:nRuns
            OFX_varyEnvironmentSeeds(m);
            filename = [varPath,'Hs_',
num2str(Hs),'Tp',num2str(round(100*Tp)),'variation', num2str(i),'.dat'];
            m.SaveData(filename);
        end
        TR.oneDone;
    end
end

% Copy any additional required files
copyfile('post.py',varPath);
```

Figure B.1: Matlab code: Create OrcaFlex input data files = 50 simulations per defined sea state

## B.1.2. Matlab code: Uptime analysis

```

%% Make a time-series of a response.
% (And get a response from a spectrum and an RAO)
clear, close all, clc
%%

command = 'makedata'; % can be 'makedata' or 'analyzedata'
%command = 'analyzedata'; % can be 'makedata' or 'analyzedata'
switch command

%% generate data
case 'makedata'
    %
    runteller = 0;
    for wavedir = 0 : 45 : 180
        for Hs = 0.5 : 0.5 : 5
            for Tp = 4 : 0.5 : 10
                for Vthresh = 65 : [15,30,45,60,75,90,105,120]
                    for Accthresh = 0.119, tic
                        %% read RAOs from database
                        rao_file = '\\Alecto\innovlei\Dep\DEVs\DEV81130 - Wind\_Workfolder Merel\Thesis\Matlab\RAOs\WTG_dual-lift_10MW_TP-
                        positioned_WTG_Bottom_Tower_Mot.stf_plt';
                        rao_mode = 3; % the 3rd mode = RAO in Z-direction
                        rao_node = 1; % the first poi in the liftdyn file (usually there is only one anyways)

                        rao_z = hmcRAO.createFromLiftdyn(rao_file, rao_mode, rao_node);

                        rao_file = '\\Alecto\innovlei\Dep\DEVs\DEV81130 - Wind\_Workfolder Merel\Thesis\Matlab\RAOs\WTG_dual-lift_10MW_TP-
                        positioned_WTG_Bottom_Tower_Vel.stf_plt';
                        rao_mode = 3; % the 3rd mode = RAO in Z-direction
                        rao_node = 1; % the first poi in the liftdyn file (usually there is only one anyways)

                        rao_vz = hmcRAO.createFromLiftdyn(rao_file, rao_mode, rao_node);

                        rao_file = '\\Alecto\innovlei\Dep\DEVs\DEV81130 - Wind\_Workfolder Merel\Thesis\Matlab\RAOs\WTG_dual-lift_10MW_TP-
                        positioned_WTG_Bottom_Tower_Accz.stf_plt';
                        rao_mode = 3; % the 3rd mode = RAO in Z-direction
                        rao_node = 1; % the first poi in the liftdyn file (usually there is only one anyways)
                        rao_Accz = hmcRAO.createFromLiftdyn(rao_file, rao_mode, rao_node);

                        % select rao for one wavedirection
                        %wavedir
                        irao
                        = find(rao.z.db.headings == wavedir);
                        select_rao_z = rao.z.db.amplitude(irao,:);
                        select_phase_z = rao.z.db.phase(irao,:);
                        select_rao_vz = rao.vz.db.amplitude(irao,:);
                        select_phase_vz = rao.vz.db.phase(irao,:);
                        select_rao_Accz = rao.Accz.db.amplitude(irao,:);
                        select_phase_Accz = rao.Accz.db.phase(irao,:);

```

Figure B.2: Matlab code: Uptime analysis (1/6)

```

%% make wave spectrum
%Fs = 2;
%Tp = 8;
gamma = 2;
omega = rao.z.db_omega;
Swave = wavespectrum(Hs,Tp,gamma,omega);
%% make response spectrum
Sresp_z = Swave.*select_rao_z.^2;
Sresp_vz = Swave.*select_rao_vz.^2;
Sresp_accz = Swave.*(select_rao_z.*omega).^2;
Sresp_accz2 = Swave.*(select_rao_z.*omega.^2).^2;

%% now plot all components
figure(1)
sp1 = subplot(3,1,1); plot(omega,select_rao_z,omega,select_rao_vz, omega,select_rao_accz), title('RAO Tower_{bottom}'),
xlabel('Frequency [rad/s]', 'FontSize', 6), ylabel('Z motion R.A.O [m/m]', 'FontSize', 6)
sp2 = subplot(3,1,2); plot(omega,Swave), title(sprintf('Sea elevation: Hs=%3.1fm, Tp=%2.0fs', Hs,Tp)), xlabel('Frequency [rad/s]',
'FontSize', 6), ylabel('Spectral density [m^2 S]', 'FontSize', 6)
sp3 = subplot(3,1,3); plot(omega,Sresp_z,omega,Sresp_vz,omega,Sresp_accz), title('Response Tower_{bottom}'), xlabel('Frequency
[rad/s]', 'FontSize', 6), ylabel('Z motion response (SDA)[m]', 'FontSize', 6)

%% make time series, based on ifft (based on 'genwave.m')
% define t & dt
dt = 0.1;
t = 0:dt:9000;
% now make new_omega based on t
N = length(t);
dw = 2*pi/max(t);
new_omega = 0:dw:(N-1)*dw;
% create new response spectrum, based on new_omega
Sresp_z_new = interp1(omega,Sresp_z,new_omega,'linear','extrap');
Sresp_vz_new = interp1(omega,Sresp_vz,new_omega,'linear','extrap');
Sresp_accz_new = interp1(omega,Sresp_accz,new_omega,'linear','extrap');
% interpolate phases
Phase_z = interp1(omega,select_phase_z,new_omega,'linear','extrap');
Phase_vz = interp1(omega,select_phase_vz,new_omega,'linear','extrap');
Phase_accz = interp1(omega,select_phase_accz,new_omega,'linear','extrap');
% subplot(3,1,3), hold on, plot(new_omega,Sresp_z_new,'r-'), hold off
SDAz = 4*sqrt(trapz(new_omega,Sresp_z_new));
%% Time series
% time trace Z-motion
rng(12345)
Fwave = 2*pi*rand(N,1); % random phase uniformly distributed (0,1)
[om_DFTz,DFTz] = matfft(new_omega',Sresp_z_new', (Fwave+Phase_z)*180/pi,1); % from
[t,Z_response] = matfft(om_DFTz,DFTz,3);

```

Figure B.3: Matlab code: Uptime analysis (2/6)

```

% time trace Z-velocity
[om_DFTVz,DFTVz] = matfft(new_omega', Sresp_vz_new', (Fwave+Phase_vz)*180/pi,1); % from
[t,Vz_response] = matfft(om_DFTVz,DFTVz,3);
% Velocity based on gradient of Z-motion
Vz2 = gradient(Vz_response,t); % only for checking purposes
% time trace Z-acceleration
[om_DFTAccz,DFTAccz] = matfft(new_omega', Sresp_Accz_new', (Fwave+Phase_vz)*180/pi,1); % from
[t,Accz_response] = matfft(om_DFTAccz,DFTAccz,3);
% final check on spectrum
dom_check = 0.005;
[om_check,Scheck,Sconf] = specdens(t,Z_response,dom_check);
subplot(3,1,3), hold on, plot(om_check,Scheck,'m.',om_check,Scheck+Sconf,'k:'), hold off
xlim([0 1.6]), ylim([0 0.2])
legend(sp1,'Z mot','Z vel','Z acc')
legend(sp3,'Sresp z','Sresp vz','Sresp vz2','Sresp z new')

figure(2)
ax(1) = subplot(3,1,1); plot(t,Z_response), title(sprintf('Time series Z-motion (based on Hs = %3.1f m, Tp = %4.1f sec, wavedir =
%i deg) - SDA_Z = %3.1f m',Hs,Tp,wavedir,SDAZ)), xlabel('Time [s]', 'FontSize', 6), ylabel('% motion response [m]', 'FontSize', 6)
ax(2) = subplot(3,1,2); plot(t,Vz_response), title('Time series'), xlabel('Time [s]', 'FontSize', 6), ylabel('% velocity response
[m/s]', 'FontSize', 6)
ax(3) = subplot(3,1,3); plot(t,Accz_response), title('Time series'), xlabel('Time [s]', 'FontSize', 6), ylabel('%Z acceleration
response [m/s^2]', 'FontSize', 6)
linkaxes(ax,'x')

%% Now look for threshold in velocity
Vthresh = 0.05; % m/s
index = find(Vz_response<Vthresh & Vz_response>-Vthresh); % these are the time points where |Vz| < Vthresh
index = find(Vz_response>-Vthresh); % vertical velocity does not exceed -Vthresh
subplot(3,1,2), hold on, plot(t(index),Vz_response(index),'m. '), hold off
%
Tmin = 30; % minimum required time (sec) needed for installation
iend = find(diff(index)>1); % defines end each section with Vz <= Vthresh
istart = index(1);
teller = 0;
if isempty(iend) % no breaks in time trace
    StartStoptv = [1 index(end)];
else
    StartStoptv = [1 2];
end
%
for icount = 1:length(iend)
    deltaT = t(index(iend(icount)))-t(istart);
    if deltaT>=Tmin
        teller = teller+1;
        StartStoptv(teller,1:2) = [istart,index(iend(icount))];
        subplot(3,1,2), hold on,
        plot([t(StartStoptv(teller,1):StartStoptv(teller,2)), [Vz_response(StartStoptv(teller,1):StartStoptv(teller,2))], 'g. '), hold off
    end
    istart = index(iend(icount)+1);

```

Figure B.4: Matlab code: Uptime analysis (3/6)

```

end
% check last part
deltaT = t(index(end))-t(istart);
if deltaT>=Tmin
    teller = teller+1;
    StartStopv(teller,1:2) = [istart,index(end)];
    subplot(3,1,2), hold on,
    plot([t(StartStopv(teller,1):StartStopv(teller,2))],[Vz_response(StartStopv(teller,1):StartStopv(teller,2))]),'g. '), hold off
end
%
UptimeVz = sum((StartStopv(:,2)-StartStopv(:,1))*dt)/t(end)*100;
waittime = (1-UptimeVz/100)*t(end);
avgwaittime = max(0,waittime/size(StartStopv,1));
title(sprintf('Vertical velocity uptime = %4.1f%% @threshold %4.2f m/s - Tmin = %1.0f sec (Twait_a_v_g = %1.0f s)',UptimeVz,-
Vthresh,Tmin,avgwaittime))

%% Now look for threshold in Acceleration
%Accthresh = 0.119; % m/s^2
%index = find(Accz_response<Accthresh & Accz_response>-Accthresh); % these are the time points where |Accz| < Accthreshhold
index = find(Accz_response>-Accthresh); % vertical acceleration does not exceed AccVthreshold
subplot(3,1,3), hold on, plot(t(index),Accz_response(index),'m. '), hold off

iend = find(diff(index)>1); % defines end each section with Accz <= Accthreshhold
istart = index(1);
teller = 0;
if isempty(iend) % no breaks in time trace
    StartStopa = [1 index(end)];
else
    StartStopa = [1 2];
end
%
for icount = 1:length(iend)
    deltaT = t(index(iend(icount)))-t(istart);
    if deltaT>=Tmin
        teller = teller+1;
        StartStopa(teller,1:2) = [istart,index(iend(icount))];
        subplot(3,1,3), hold on,
        plot([t(StartStopa(teller,1):StartStopa(teller,2))],[Accz_response(StartStopa(teller,1):StartStopa(teller,2))]),'g. '), hold off
    end
    istart = index(iend(icount)+1);
end
% check last part
deltaT = t(index(end))-t(istart);
if deltaT>=Tmin
    teller = teller+1;
    StartStopa(teller,1:2) = [istart,index(end)];
    subplot(3,1,3), hold on,
    plot([t(StartStopa(teller,1):StartStopa(teller,2))],[Vz_response(StartStopa(teller,1):StartStopa(teller,2))]),'g. '), hold off
end

```

Figure B.5: Matlab code: Uptime analysis (4/6)



```

xlabel('Tp [s]')
ylabel('Hs [m]')
map = [ 1.0000      0      0
        1.0000    0.3529    0
        1.0000    0.5294    0
        1.0000    0.7059    0
        1.0000    0.8824    0
        0.9412    1.0000    0
        0.7647    1.0000    0
        0.5882    1.0000    0
        0.4118    1.0000    0
        0.0588    1.0000    0];
colormap(map)
colorbar('Direction','reverse')
c = colorbar;
c.Label.String = 'Uptime (%)';
shading interp
title(sprintf('Uptime based on max Vz = %4.2f m/s and Tmin = %i sec for wavedir = %ideg',Vthresh,Tmin,wavedir))

% now add LiftDyn operability
ope_file = '\\ALECTO\users\merelyb\Thesis\9. LiftDyn\WTG_dual-lift_TP-positioned\WTG_dual-lift_10MW_TP-positioned_Max. vert.
vel. 0.04mps no sprd. _JONSWAP1.ope.plt'; % no spreading
mode = 1; % the 1st mode (there's only 1)
node = 1; % the first poi in the liftDyn file (usually there is only one anyways)

ope_Vz = hmcRAO.createFromLiftDyn(ope_file, mode, node);
wavedir = 0;
iope = find(ope_Vz.db_headings == wavedir);
select_ope_Vz = ope_Vz.db_amplitude(iope,:);
ope_Tp = ope_Vz.db_omega;
hold on, plot3(ope_Tp,select_ope_Vz,100*ones(size(ope_Tp)), 'k', 'linewidth', 2), hold off
axis([4 10 0.5 5])
% PDFname = sprintf('Operability Wdir%ideg_Vlim%4.2fmps_Alim%5.3fmpsc_Tmin%is.PDF',wavedir,Vthresh,Accthresh,Tmin);
print('-dpdf', ['Figures\',PDFname])
pause(1)
%
end
end
%% END SWITCH
end

```

Figure B.7: Matlab code: Uptime analysis (6/6)

### B.1.3. Matlab code: Modify environment as input for Sequence Tool

```

close all; clear all; clc;
db = load_local('\\\\Alecto\apps\Leiden\EnvData\Standard_scatters_timetraces\North Sea\North Sea
South\ARGOSS_SNS_NE_K12_s2d_rev03_plus_2011_currents.env_mat');
Environment = db.Environment;

Tp_lim = [-1, 4, 4.5, 4.8, 5.1, 5.4, 5.5, 5.7, 5.8, 6, 7, 7.6, 7.9, 8.2, 9, 9.5, 10, 9999];
Hs_lim = [5, 5, 4.85, 4.5, 4, 3.55, 3.25, 3, 2.75, 2.4, 1.5, 1.3, 1.1, 1, 0.9, 0.85, 0.8, 0.5];

plot(Tp_lim, Hs_lim), title('Limit uptime larger than 10%');

Hs_limit = interp1(Tp_lim, Hs_lim, Environment.Tp);

% UC is the actual sea-state divided by the allowable sea-state
UC = Environment.Hs ./ Hs_limit;

figure;
plot(Environment.Time, UC, 'displayname', 'UC'); hold on;
plot(Environment.Time, Environment.Hs, 'displayname', 'Hs'), title('Modified Environment with uptime limit > 10%'), xlabel('Data
point of environment [Hs, Tp]', 'FontSize', 9), ylabel('Unity Check [Hs.env/Hs.limit]', 'FontSize', 9);
dynamicDateTicks;
legend show;

% Add UC to the time-trace
Environment.UC = UC;

save('\\\\ALECTO\users\mre1vb\Thesis\10. Sequence Tool\Environment\modified_env_database_65s.env_mat', 'Environment');

```

Figure B.8: Matlab code: Modify environment with unity check inserted, based on uptime (%) limit

## B.1.4. Matlab code: Generate dataset from result of OrcaFlex simulations

```

close all; clear all; clc;
addpath('c:\data\merel\matlab\montecarlo_post\');

Dataset = hmcMCP;
%Dataset.loadDataFromFile('Results_simHs_1.5Tp600.mat')
Dataset.addResults('\leinetappl\condor\Tender Analysis\Student\Merel\Batch 2\runs\Hs_1.5Tp600variation*.mat', @postSingle);
Dataset.saveDataToFile('Results_simHs_1.5Tp600.mat')

% If the average impact load of bucket over the last 100 second is less than 40 kN
% then the simulation is failed

% first check if the threshold is ok
figure;
hist(Dataset.data.avgstatStopperLoadLeft);
xlabel('Average stopper load left over last 100 seconds [kN]');
ylabel('Number of simulations');

Dataset.data.failed = (Dataset.data.avgstatStopperLoadLeft < 40);
figure;
Dataset.plotTitleText = 'WTG installation, failed simulation';
Dataset.plotHsTpContour('failed', @mean);

ok = Dataset.givePartialSet(Dataset.data.avgstatStopperLoadLeft > 40); % ok is now the set
% containing only those simulations that resulted in a successful
% installation

%% Plot successful simulations
figure;
ok.plotTitleText = 'WTG installation';
ok.plotHsTpContour('maxStopperLoadLeft', @P90);

figure;
ok.plotHsTpContour('firstmaxTpPreceptorLoad', @P90);
figure;
ok.plotHsTpContour('maxTpPreceptorLoad', @P90)

figure;
Hs = 1;
Tp = 7;
ok.plotDistribution('maxStopperLoadLeft', 'Hs', 'Tp', Tp);

```

Figure B.9: Matlab code: Create dataset from OrcaFlex simulations

### B.1.5. Matlab code: Function for post-retrieving data of OrcaFlex simulations

```

function R = postSingle(filename)

d = load_local(filename);

% extract the usefull data from d and put it in fields of R

R.Tp = d.Tp;
R.Hs = d.Hs;
R.dir = d.dir;

t = d.time;

R.maxStopperLoadLeft = max(d.Stopper_shape_left.Contact_Force);
R.avgStatStopperLoadLeft = mean(d.Stopper_shape_left.Contact_Force(t>150));
R.maxStopperLoadRight = max(d.Stopper_shape_right.Contact_Force);
R.avgStatStopperLoadRight = mean(d.Stopper_shape_right.Contact_Force(t>150));
R.firstmaxTPreceptorLoad = max(d.TP_receptor.Contact_Force(t<55));
R.maxTPreceptorLoad = max(d.TP_receptor.Contact_Force);
R.avgStatTPreceptorLoad = mean(d.TP_receptor.Contact_Force(t>150));
R.minTPRot1 = min(d.TP_receptor.Rotation_1);
R.maxTPRot1 = max(d.TP_receptor.Rotation_1);
R.minTPRot2 = min(d.TP_receptor.Rotation_2);
R.maxTPRot2 = max(d.TP_receptor.Rotation_2);
R.minTPRot3 = min(d.TP_receptor.Rotation_3);
R.maxTPRot3 = max(d.TP_receptor.Rotation_3);

%% Find first maximum TP impact load
% find the time at which the first impact occurs
ind = find(d.TP_receptor.Contact_Force > 0, 1, 'first');
t_impact = d.time(ind);

% locate the interval that we are interested in
t_duration = 10; %s
t_start = t_impact - t_duration;
ind_d = find((d.time>t_start) & (d.time < t_impact));

% figure;
% subplot(2,1,1);
% plot(d.time, d.TP_receptor.Contact_Force), title('Vertical impact load TP Flange [kN]'), xlabel('Time [s]', 'FontSize',
6), ylabel('Impact Load [kN]', 'FontSize', 6);
% hold on;
% plot(d.time(ind), d.TP_receptor.Contact_Force(ind), 'r. '); hold off;
%
% subplot(2,1,2);
% plot(d.time, d.TP_receptor.GZ_Velocity), title('Vertical velocity of Tower_{bottom} [m/s]'), xlabel('Time [s]',
'FontSize', 6), ylabel('Vertical velocity[m/s]', 'FontSize', 6);
% hold on;
% plot(d.time(ind_d), d.TP_receptor.GZ_Velocity(ind_d), 'r. '); hold off;

```

Figure B.10: Matlab code: Function for retrieving data of OrcaFlex simulations (1/2)

```

%% Find value of maximum impact load on TP after first contact
% 'Smooth' a line over the peaks
[ipks,pks] = findminmax(d.TP_receptor.Contact_Force,'max');
% subplot(2,1,1); hold on;
t_pks = d.time(ipks);
% plot(t_pks,pks);

% Take first peak of the 'smoothed' line
[i,pks] = findminmax(pks,'max');
t_result = t_pks(i(1));
pks_result = pks(1);

% plot(t_result,pks_result,'r*'); hold off;
%% Find Vz value at moment of first impact
% Find the time at which the Vz starts to increase significantly
ind_Vz_result = find(ind_d(end)); hold on;
t_Vz_result = d.time(ind_d(end));

% locate the value of Vz at the moment of first impact
Vz_result = d.TP_receptor.Gz_Velocity(ind_d(end));

% subplot(2,1,2);
% plot(d.time, d.TP_receptor.Gz_Velocity, t_Vz_result, Vz_result,'g*'); hold off;

R.Vz_before_first_impact = Vz_result;
R.time_of_first_impact = t_Vz_result;
R.First_max_impact_load = pks_result;

end

```

Figure B.11: Matlab code: Function for retrieving data of OrcaFlex simulations (2/2)

### B.1.6. Matlab code: Generate scatterplot from OrcaFlex simulations

```

close all; clear all; clc;

addpath('c:\data\merel\matlab\montecarlo_post\');

Dataset = hmcMCP;
%Dataset.loadDataFromFile('Results_all1400sim.mat')
Dataset.addResults('\\\\leinetappl\condor\tender
Analysis\Student\Merel\Batch 2\runs\*.mat',@postSingle);
Dataset.saveDataToFile('Results_all1400sim.mat')

ok = Dataset.givePartialSet(Dataset.data.avgstatStopperLoadLeft > 40);
% ok is now the data set
% containing only those simulations that resulted in a successful
% installation

plot(-ok.data.Vz_before_first_impact,
ok.data.First_max_impact_load,'r','Markersize', 12),title({'Impact
load TP vs. vertical velocity WTG','Sea state: Hs = 1 m, Tp = 10
s'}), xlabel({'Vertical (downward) velocity tower bottom [m/s]'},
'FontSize', 10), ylabel({'First maximum impact load on TP [kN]'},
'FontSize', 10);

```

Figure B.12: Matlab code: Create scatterplot from OrcaFlex simulations

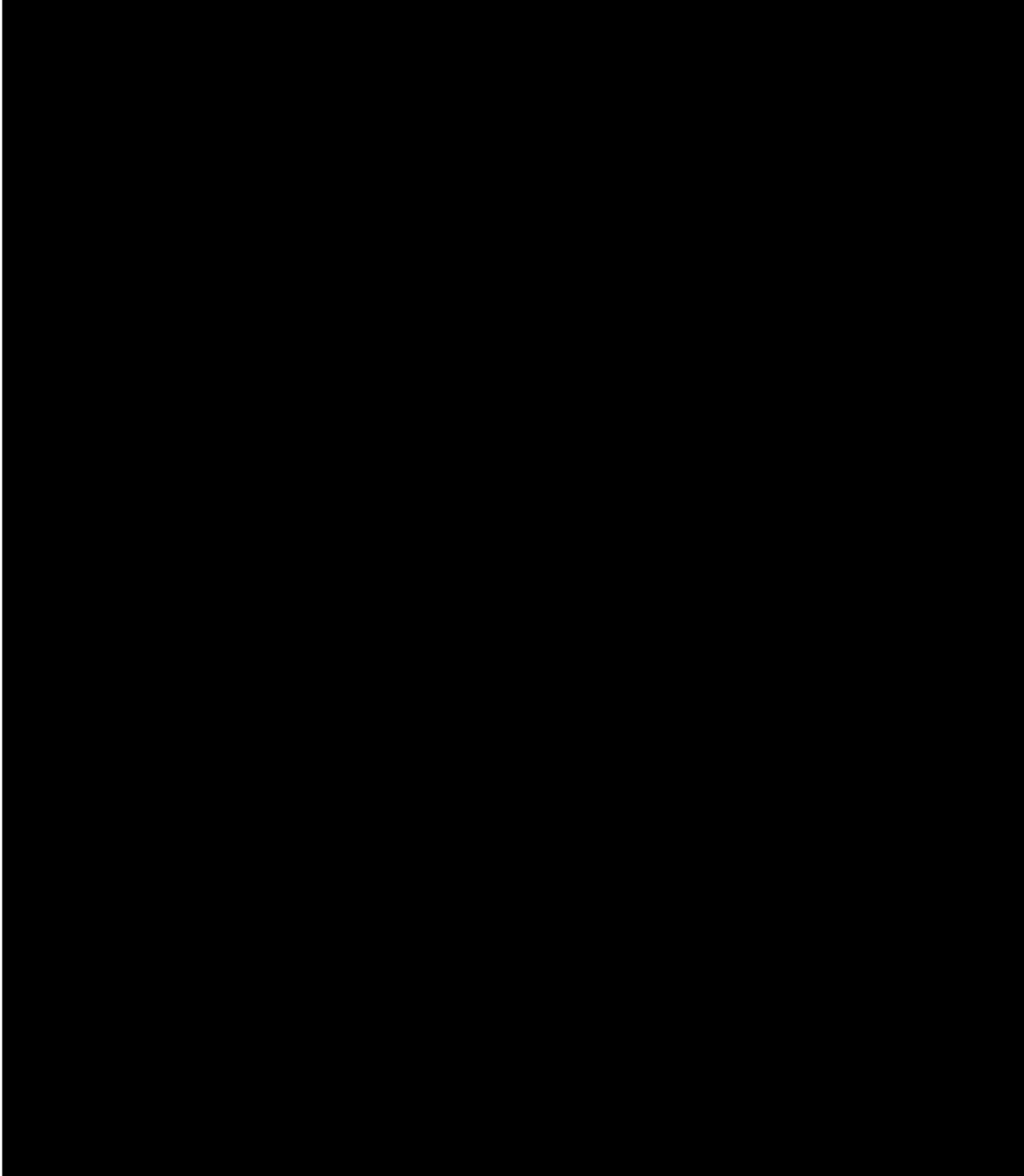
**B.1.7. Matlab code: Used script for IFF**

Figure B.13: Matlab code: Used HMC script for Inverse Fourier Transformation (1/3)

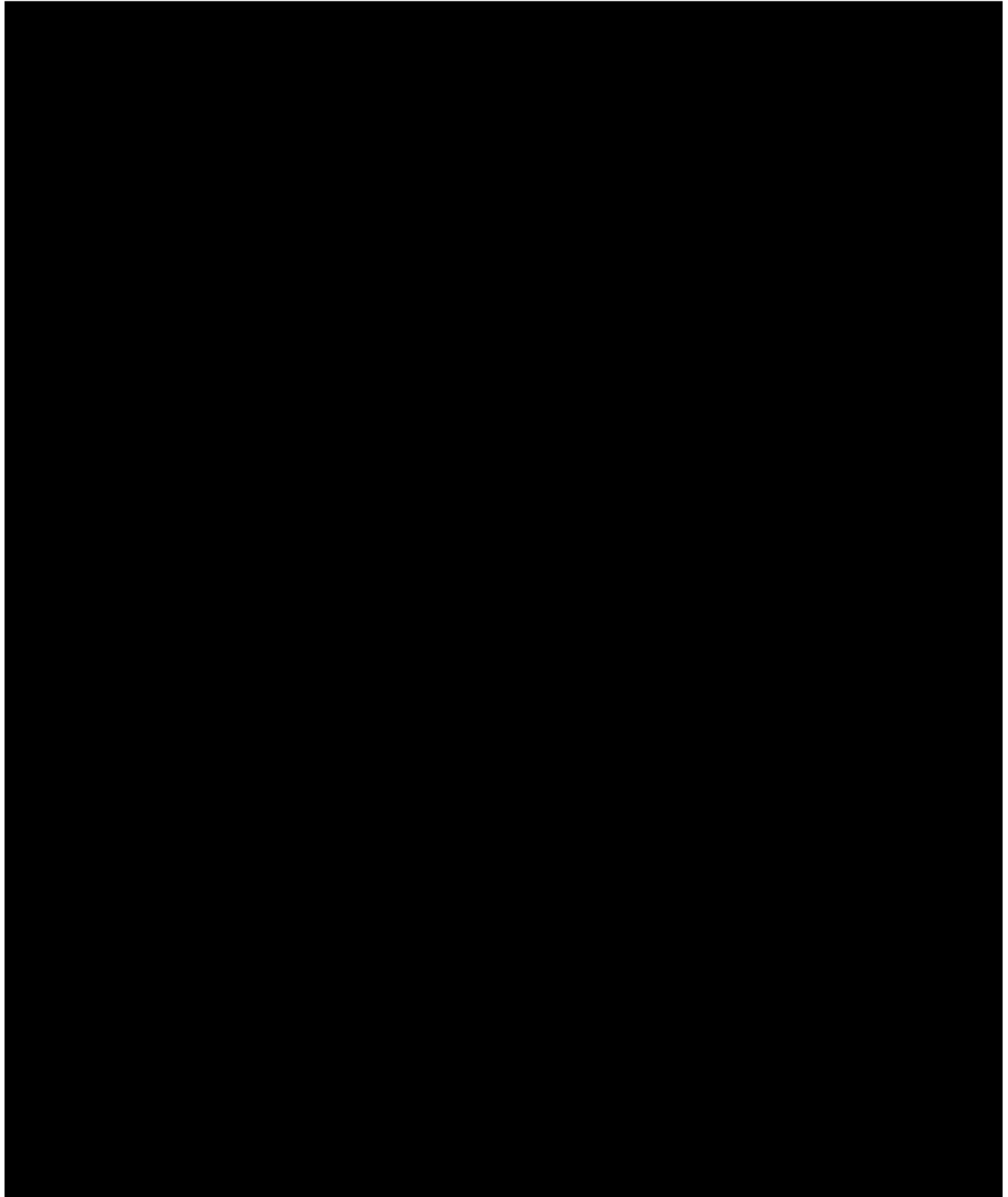


Figure B.14: Matlab code: Used HMC script for Inverse Fourier Transformation (2/3)

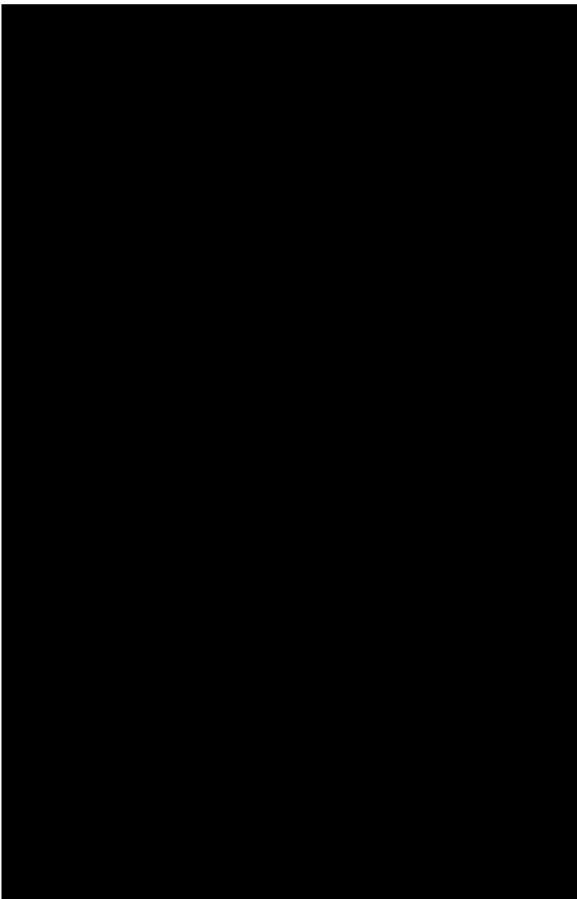


Figure B.15: Matlab code: Used HMC script for Inverse Fourier Transformation (3/3)

### B.1.8. Matlab code: Used script genwave

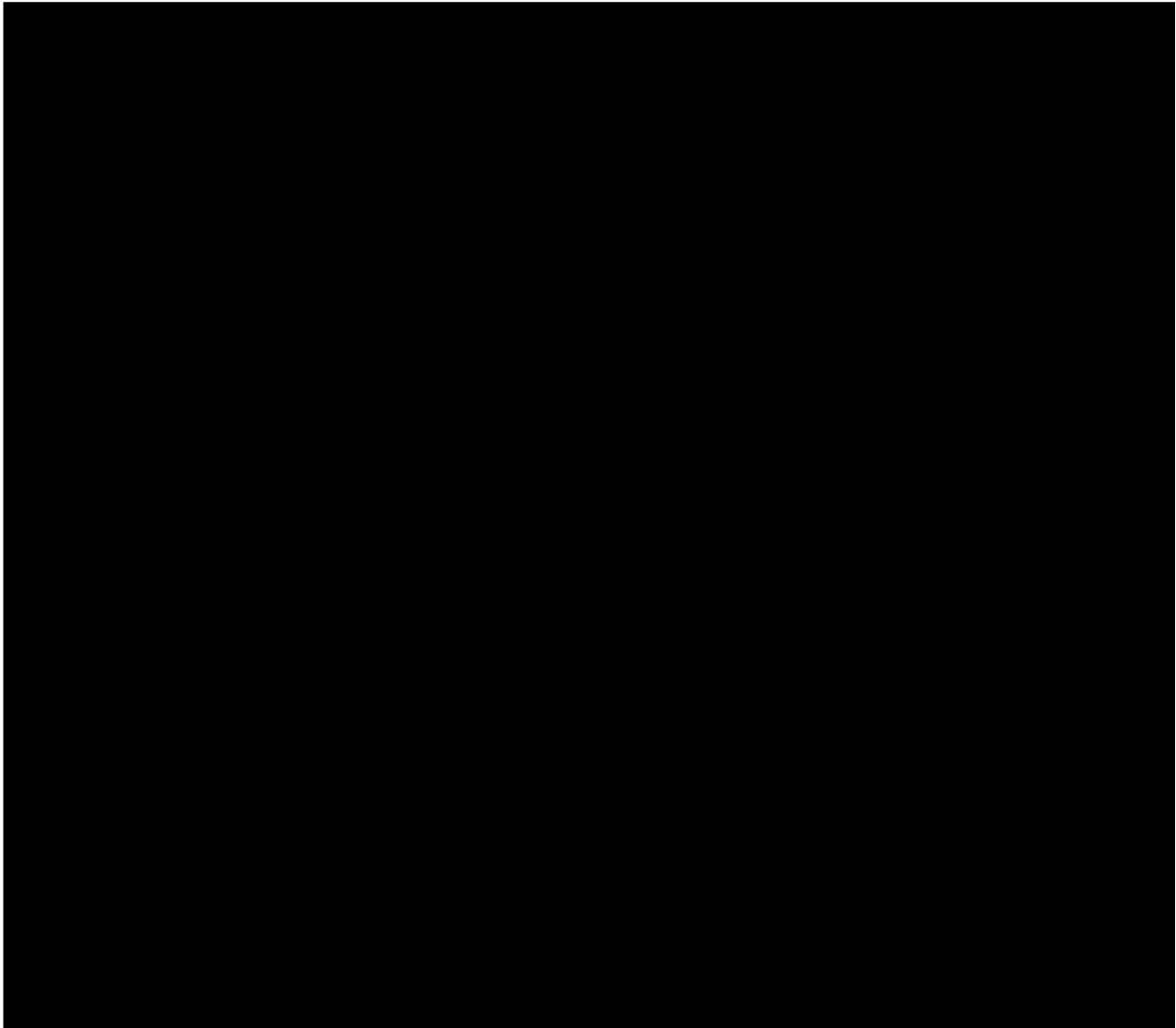


Figure B.16: Matlab code: Used HMC script Function to generate random phase wave train (1/4)



Figure B.17: Matlab code: Used HMC script Function to generate random phase wave train (2/4)

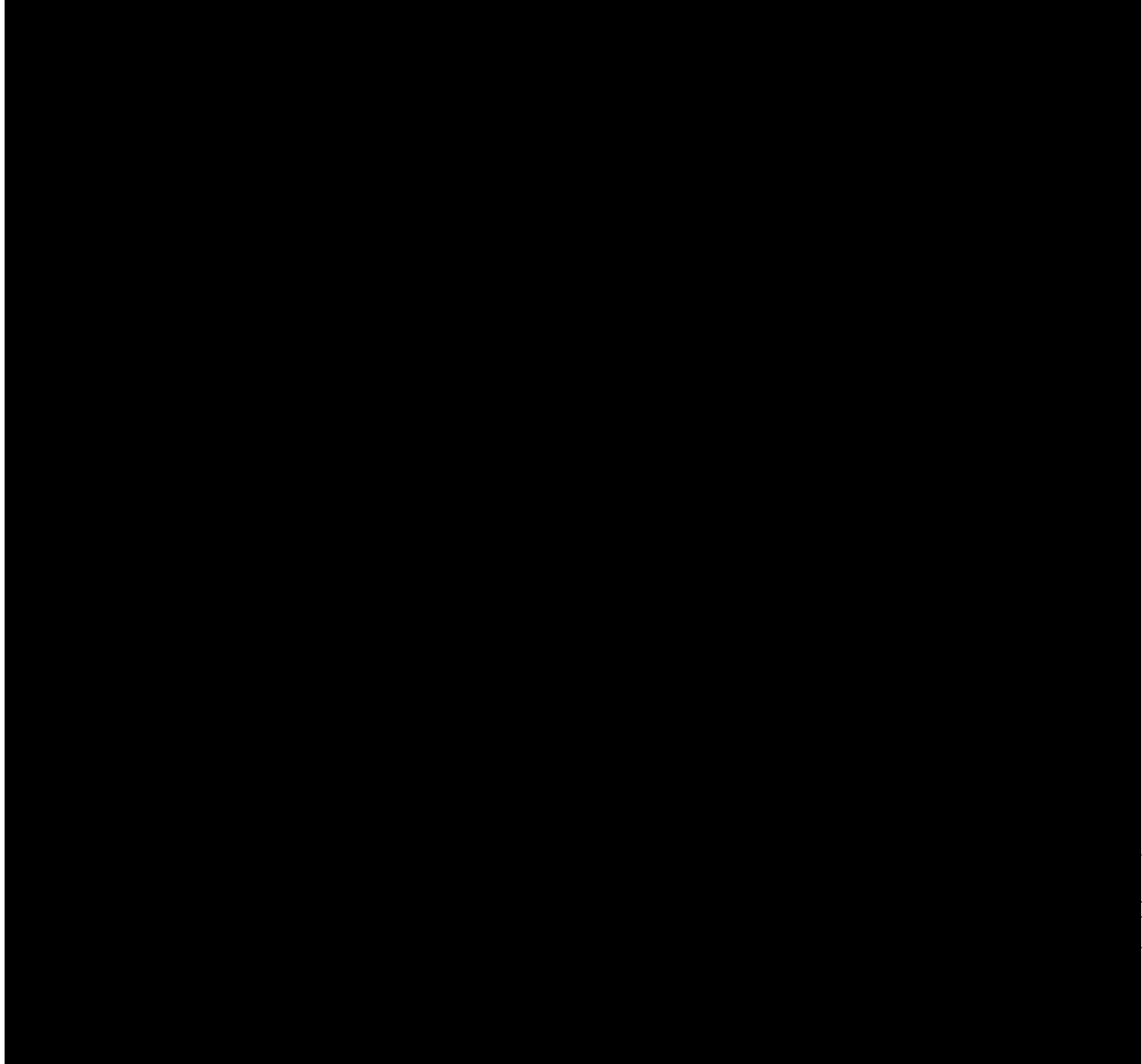


Figure B.18: Matlab code: Used HMC script Function to generate random phase wave train (3/4)

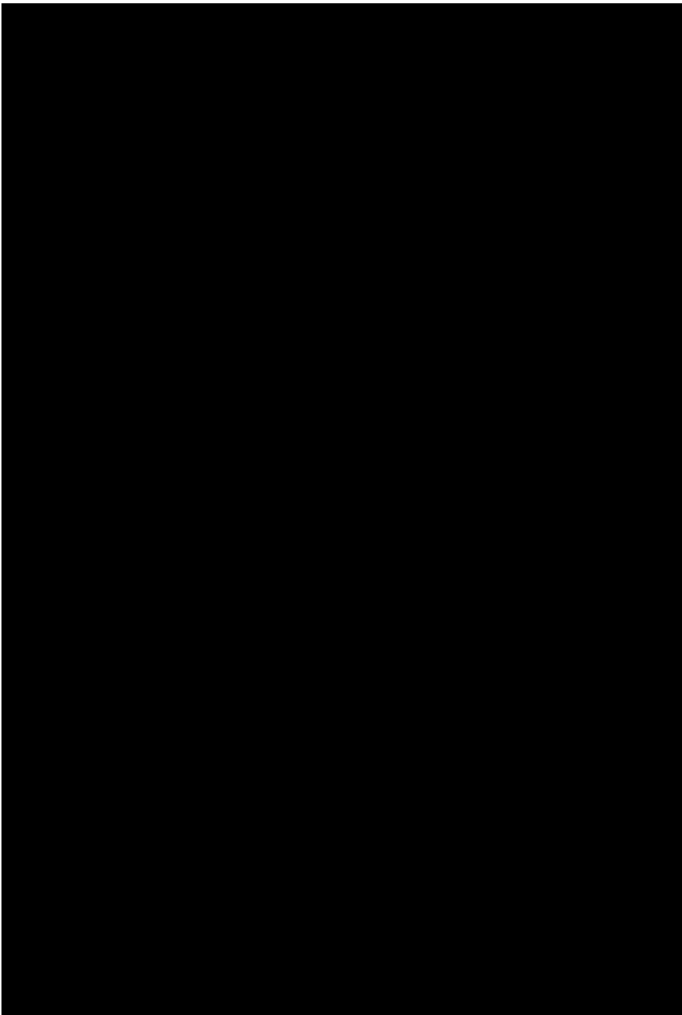


Figure B.19: Matlab code: Used HMC script Function to generate random phase wave train (4/4)



# List of Figures

1	Sign convention LiftDyn: Wave direction coming from, counter clock wise w.r.t. local body axis, 0 deg wave following vessel . . . . .	ix
2	Sign convention LiftDyn: Right handed coordinate system, Positive: Z up, x to bow, y to PS, yaw counter clock wise, roll SB down, Pitch bow down . . . . .	ix
3	Sign convention OrcaFlex: Wave direction going to, counter clock wise w.r.t. local body axis, 0 deg wave following vessel . . . . .	ix
1.1	Aegir . . . . .	1
1.2	Balder . . . . .	1
1.3	Thialf . . . . .	1
1.4	Sleipnir . . . . .	1
1.5	Structure of report . . . . .	4
2.1	Theoretical framework of Porter’s Five Forces (red) and PESTLE model (blue) . . . . .	6
2.2	Cumulative and annual offshore wind installations in Europe (MW) [17] . . . . .	6
2.3	European market outlook for next five years [17] . . . . .	7
2.4	Possible 80% cut in greenhouse gas emissions in the EU (100%=1990) [22] . . . . .	8
2.5	Average water depth and distance to shore of bottom-fixed offshore wind farms [17] . . . . .	10
2.6	New offshore wind investments and capacity financed: 2010 – 2017 (€bn) [17] . . . . .	11
2.7	Sea Installer, A2SEA . . . . .	14
2.8	Aeolus, Van Oord . . . . .	14
2.9	Saipem 7000, Saipem SpA . . . . .	14
2.10	Orion, GeoSea . . . . .	14
2.11	Floating substructures: barge, semi-submersible, spar buoy and tension leg platform <i>f.l.t.r.</i> . . . . .	16
3.1	Logistical operations involved during installation phase offshore wind turbines . . . . .	20
3.2	Conceptual purpose-built installation vessel ‘The Shuttle’, Huisman . . . . .	21
3.3	Pre-assembly configuration: 5 Pieces separately, Bunny Ear, Pre-assembled Rotor, Complete WTG <i>f.l.t.r.</i> . . . . .	21

3.4	All-in-one system: WTG installation in which components supplied by installation vessel . . . . .	22
3.5	Feeder vessel logistics: WTG installation in which components supplied by feeder vessel . . . . .	22
4.1	Top view of WTG components on installation vessels or feeder barges . . . . .	25
4.2	Installation costs per WTG (M€) 10 MW . . . . .	26
4.3	Installation costs (M€) 10 MW WTG, depending on OWF size . . . . .	27
4.4	Installation costs (M€) 10 MW WTG, depending on distance to port . . . . .	28
4.5	Installation costs (M€) 10 MW WTG for Doggersbank, changing installation time and day-rate . . . . .	29
4.6	Single-lift installation with floating vessel . . . . .	30
5.1	Clearance between tower and transition piece . . . . .	32
5.2	Hookload curve and maximum lifting heights Thialf . . . . .	34
5.3	Frequency areas with respect to motional behavior [53] . . . . .	38
5.4	LiftDyn Model . . . . .	38
5.5	Operability Curve . . . . .	40
5.6	Operability Curve with WTG mass increase (factor 2) . . . . .	40
5.7	Operability Curve with sling stiffness increase (factor 100) . . . . .	40
5.8	Operability Curve with sling stiffness increase (factor 10000) . . . . .	40
5.9	Mating procedure of connection tower to transition piece . . . . .	41
5.10	Representation of docking pin and bucket . . . . .	42
5.11	Representation of spring and dampers in TP (yellow) and buckets (red) . . . . .	42
5.12	Sign convention OrcaFlex model . . . . .	43
5.13	Impact load on buckets & TP [kN], sea state $H_s : 2.5m, T_p : 6s$ . . . . .	44
5.14	Rotations of Tower bottom [deg], sea state $H_s : 2.5m, T_p : 6s$ . . . . .	45
5.15	Total number of failed simulations (left bar) and successful simulations (right bar) . . . . .	46
5.16	Distribution of failed simulations per sea state (mean) . . . . .	46
5.17	Maximum impact load on left bucket [kN] (P90) . . . . .	47
5.18	Distribution of maximum impact load on left bucket, $H_s : 1m, T_p : 7s$ . . . . .	47
5.19	First maximum impact load on TP [kN] (P90) . . . . .	47

5.20	Maximum impact load on TP [kN] (P90) . . . . .	47
5.21	Zoomed-in time-series of impact load TP (a) and velocity Tower (b), sea state: $H_s = 1.5m, T_p = 6s$ . . . . .	48
5.22	First maximum impact load vs. vertical velocity, sea state = $H_s : 1.5m, T_p : 6s$ . .	49
5.23	First maximum impact load vs. vertical velocity, sea state = $H_s : 1m, T_p : 10s$ . .	49
5.24	First maximum impact load vs. vertical velocity . . . . .	49
5.25	Zoomed-in plot of first maximum impact load vs. vertical velocity . . . . .	49
5.26	Contact forces on buckets with sea state $2.5 H_s 6 T_p$ . . . . .	50
5.28	Docking system with 3 units . . . . .	51
6.1	Delay determined in sequence tool . . . . .	53
6.2	Datapoints in environment . . . . .	53
6.3	Average waiting on weather per installation step . . . . .	54
6.4	Time-series of Z-motion of $Tower_{bottom}$ (based on $H_s = 1.5 m, T_p = 6 s, \text{wavedir} = 0 \text{ deg}$ ) . . . . .	56
6.5	Time-series of Z-velocity of $Tower_{bottom}$ (with 22% uptime, time-frame = 90 s) .	56
6.6	Time-series of Z-acceleration of $Tower_{bottom}$ (with 100% uptime, time-frame = 90 s) . . . . .	56
6.7	Scatter diagrams of uptime [%], with varying time-frame . . . . .	57
6.8	Average waiting time before a time-frame occurs depending on uptime percentage	57
6.9	Average WoW per installation step, WTG set-down = 65 s . . . . .	58
6.10	Total installation time incl. WoW . . . . .	59
6.11	Total installation time incl. WoW, shorter time-frame . . . . .	59
A.1	5 Pieces Separately with Tower in 1 Piece, SeaInstaller – SeaJacks . . . . .	65
A.2	Bunny Ear, Haliade - Alstom . . . . .	65
A.3	Rotor Star with Tower in 2 Pieces, Senvion . . . . .	65
A.4	Bolted connections between WTG components . . . . .	66
A.5	Costs per vessel type, based on known JUV day-rate . . . . .	66
A.6	Example sailing route: from Vlissingen port to Borselle I & II ( $\approx 70 \text{ km}$ ) . . . . .	68
A.7	New shipping route for sailing in offshore wind farms . . . . .	68
A.8	Conceptual design of lift-frame for single-lift installation of WTG . . . . .	70
A.9	Time-series of vertical impact load on TP (kN) . . . . .	72

A.10	Time-series of vertical impact load on right bucket (kN) . . . . .	72
A.11	Time-series of impact load on cone of right bucket (kN) . . . . .	72
A.12	Time-series of impact load on cylinder of right bucket (kN) . . . . .	72
A.13	Time-series of impact load on cone of right bucket in x-direction (kN) . . . . .	73
A.14	Time-series of impact load on cone of right bucket in y-direction (kN) . . . . .	73
A.15	Time-series of impact load on cylinder of right bucket in x-direction (kN) . . . . .	73
A.16	Time-series of impact load on cylinder of right bucket in y-direction (kN) . . . . .	73
A.17	Time-series of tension in hoist wire on port side crane(kN) . . . . .	74
A.18	Time-series of tension in hoist wire on star board crane (kN) . . . . .	74
A.19	Time trace of Hs,environment (orange) and Hs,limit (blue) . . . . .	75
A.20	Zoomed-in time trace of Hs,environment (orange) and Hs,limit (blue) . . . . .	75
B.1	Matlab code: Create OrcaFlex input data files = 50 simulations per defined sea state . . . . .	77
B.2	Matlab code: Uptime analysis (1/6) . . . . .	78
B.3	Matlab code: Uptime analysis (2/6) . . . . .	79
B.4	Matlab code: Uptime analysis (3/6) . . . . .	80
B.5	Matlab code: Uptime analysis (4/6) . . . . .	81
B.6	Matlab code: Uptime analysis (5/6) . . . . .	82
B.7	Matlab code: Uptime analysis (6/6) . . . . .	83
B.8	Matlab code: Modify environment with unity check inserted, based on uptime (%) limit . . . . .	84
B.9	Matlab code: Create dataset from OrcaFlex simulations . . . . .	85
B.10	Matlab code: Function for retrieving data of OrcaFlex simulations (1/2) . . . . .	86
B.11	Matlab code: Function for retrieving data of OrcaFlex simulations (2/2) . . . . .	87
B.12	Matlab code: Create scatterplot from OrcaFlex simulations . . . . .	88
B.13	Matlab code: Used HMC script for Inverse Fourier Transformation (1/3) . . . . .	89
B.14	Matlab code: Used HMC script for Inverse Fourier Transformation (2/3) . . . . .	90
B.15	Matlab code: Used HMC script for Inverse Fourier Transformation (3/3) . . . . .	91
B.16	Matlab code: Used HMC script Function to generate random phase wave train (1/4) . . . . .	92
B.17	Matlab code: Used HMC script Function to generate random phase wave train (2/4) . . . . .	93

---

B.18 Matlab code: Used HMC script Function to generate random phase wave train (3/4) . . . . .	94
B.19 Matlab code: Used HMC script Function to generate random phase wave train (4/4) . . . . .	95



# List of Tables

3.1	Pros and cons per type of installation vessel . . . . .	20
3.2	Pros and cons per pre-assembly strategy [46] . . . . .	22
5.1	Operational limits and weather restrictions per step for one WTG installation . . . . .	31
5.2	Critical path of steps for installation of 4 WTGs . . . . .	33
5.3	Thialf crane specifications per lift operation . . . . .	34
5.4	Mode shapes of free-hanging WTG computed by LiftDyn . . . . .	38
5.5	Environment used in OrcaFlex . . . . .	42
5.6	Measured impact loads during set-down . . . . .	43
5.7	Impact loads for optimal set-down moment . . . . .	50
5.8	Reduction in impact loads with 3 pins (average values of 8 simulations) . . . . .	51
5.9	Reduction in maximum rotations of wind turbine tower . . . . .	51
6.1	Total WoW days, OWF size = 80 WTGs . . . . .	58
A.1	Duration per installation step of a jack-up vessel . . . . .	67
A.2	Dimensions of 10 MW RWT . . . . .	69
A.3	COG per component of 10 MW RWT . . . . .	69
A.4	Example of three mode shape mass with distribution factors of the Thialf and three components of WTG . . . . .	71



# Bibliography

- [1] “Heerema marine contractors history,” Aug 2017. [Online]. Available: <https://hmc.heerema.com/about/history/>
- [2] (2018, Apr) Crude oil prices. [Online]. Available: <https://oilprice.com/>
- [3] Reuters. (2018, Jan) Oil prices are set for their strongest january in 5 years. [Online]. Available: <http://fortune.com/2018/01/29/oil-prices-high-january-2018/>
- [4] C. Krauss, “Oil prices: What to make of the volatility, new york times,” Sep 2017. [Online]. Available: <https://www.nytimes.com/interactive/2017/business/energy-environment/oil-prices.html>
- [5] R. Arezki and J. Yao, *Oil prices and the global economy*. International Monetary Fund, 2017.
- [6] I. Slav, “Oil and gas could see the longest period of declining investment in the history of the industry, business insider,” Sep 2017. [Online]. Available: <http://www.businessinsider.com/oil-and-gas-industry-investment-decline-2016-9?international=true&r=US&IR=T>
- [7] Oil and G. V. Publication, “Heerema to axe 250 jobs,” Nov 2017. [Online]. Available: <https://oilandgasvision.com/heerema-to-axe-250-jobs/>
- [8] M. Centraal, “Kolen, olie en gas,” Sep 2017. [Online]. Available: <https://www.milieucentraal.nl/klimaat-en-aarde/energiebronnen/kolen-olie-en-gas/>
- [9] S. Bley, M. Hametner, A. Dimitrova, R. Ruech, A. De Rocchi, and K. Gschwend, E. and Umpfenbach, “Smarter, greener, more inclusive? indicators to support the europe 2020 strategy-2017 edition,” 2017.
- [10] I. Pineda, P. Tardieu, and L. Mir, “The european wind industry in 2016 financing and investments trends clean energy pipeline global,” 2017.
- [11] T. R. O. CBS, “Offshore supply industry dynamics, business strategies in the offshore supply industry,” 2017.
- [12] F. G. Nielsen, “Hywind: Deep offshore wind operational experience,” 2013.
- [13] IRENA, “Innovation outlook: Offshore wind,” 2016.
- [14] OffshoreWIND.biz, “Heerema to handle borkum riffgrund 2 substation,” Aug 2017. [Online]. Available: <https://www.offshorewind.biz/2016/03/25/heerema-to-handle-borkum-riffgrund-2-substation/>
- [15] T. T. Netherlands, “Tki wind op zee cost reduction options for offshore wind in the netherlands fid,” 2010.
- [16] W. Europe, “Unleashing europe’s offshore wind potential a new resource assessment,” 2017.
- [17] —, “Offshore wind in europe, key trends and statistics,” 2018.
- [18] GWEC, “Global wind market annual market update,” 2016.

- [19] M. P. Financial Times, "Chinese steel production to slow sharply in 2018," Feb 2018. [Online]. Available: <https://www.ft.com/content/7dfb918e-f087-11e7-b220-857e26d1aca4>
- [20] U. N. F. C. C. Change, "Paris agreement," Aug 2017. [Online]. Available: [http://unfccc.int/paris\\_agreement/items/9485.php](http://unfccc.int/paris_agreement/items/9485.php)
- [21] C. from the Commission *et al.*, "A policy framework for climate and energy in the period from 2020 to 2030," Aug 2014. [Online]. Available: [http://unfccc.int/paris\\_agreement/items/9485.php](http://unfccc.int/paris_agreement/items/9485.php)
- [22] —, "2050 low-carbon economy," Jan 2018. [Online]. Available: [https://ec.europa.eu/clima/policies/strategies/2050\\_en](https://ec.europa.eu/clima/policies/strategies/2050_en)
- [23] Accenture, "Changing the scale of offshore wind examining mega-projects in the united kingdom," 2013.
- [24] C. from the Commission *et al.*, "The investment plan for europe and energy: making the energy union a reality," Jun 2016. [Online]. Available: [https://www.europa-nu.nl/id/vk4xdvzuvby6/nieuws/the\\_investment\\_plan\\_for\\_europe\\_and?ctx=vhsjd8w6pdvc](https://www.europa-nu.nl/id/vk4xdvzuvby6/nieuws/the_investment_plan_for_europe_and?ctx=vhsjd8w6pdvc)
- [25] J. Peeringa, R. Brood, O. Ceyhan, and G. d. W. W. Engels, "Ecn study - upwind 20mw wind turbine pre-design blade design and control," Nov 2011.
- [26] M. Gainsborough, "Offshore wind and the wider energy system," *Offshore Wind Energy London*, Jun 2017.
- [27] U. Report, "Design limits and solutions for very large wind turbines," Mar 2011.
- [28] J. De Decker and A. Woyte, "Review of the various proposals for the european offshore grid," *Renewable energy*, 2013.
- [29] J. Carrillo-Hermosilla, P. R. del Gonzalez, and T. Konnolo, "What is eco-innovation?" 2009.
- [30] C. from the Commission *et al.*, "Eu emissions trading system (eu ets)," Aug 2017. [Online]. Available: [https://ec.europa.eu/clima/policies/ets\\_en](https://ec.europa.eu/clima/policies/ets_en)
- [31] C. C. A. . I. Licence, "Eu parliament's ets reform met with praise and chagrin in germany," Feb 2017. [Online]. Available: <https://www.cleanenergywire.org/news/power-taxes-levies-reach-all-time-high-views-ets-reform-split/eu-parliaments-ets-reform-met-praise-and-chagrin-germany>
- [32] D. E. Authority, "A simple and effective eu ets seven general strategies and numerous practical measures for simplifying the eu ets," May 2015.
- [33] E. Dupont, R. Koppelaar, and H. Jeanmart, "Global available wind energy with physical and energy return on investment constraints," *Applied Energy*, 2018.
- [34] G. P. H. R Camilla Thomson, "Life cycle costs and carbon emissions of wind power," *University of Edinburgh*, 2015.
- [35] "European marine observation and data network," Jan 2018. [Online]. Available: [https://ec.europa.eu/budget/euprojects/european-marine-observation-and-data-network\\_en](https://ec.europa.eu/budget/euprojects/european-marine-observation-and-data-network_en)
- [36] D. M. of infrastructure and water management, "White paper on offshore wind energy," Sep 2014. [Online]. Available: <https://www.government.nl/documents/reports/2015/01/26/white-paper-on-offshore-wind-energy>
- [37] , "Blue piling technology," Oct 2017. [Online]. Available: <https://fistuca.com/technology/>

- [38] T. Verfuß, "Noise mitigation systems and low-noise installation technologies," 2014.
- [39] S. Eurobarometer, "Public awareness and acceptance of co 2 capture and storage," *Special Eurobarometer*, 2011.
- [40] N. E. A. RVO, "Offshore wind energy in the netherlands - the roadmap from 1,000 to 4,500 mw offshore wind capacity," Jan 2015. [Online]. Available: <https://www.rvo.nl/sites/default/files/2015/03/Offshore%20wind%20energy%20in%20the%20Netherlands.pdf>
- [41] , "Bold & brave tern install areva 5mw..." dec 2017. [Online]. Available: <http://windcarrier.com/blog/case-studies/global-tech-i/>
- [42] , "A2sea fleet," Feb 2018. [Online]. Available: <https://www.a2sea.com/fleet/sea-installer/>
- [43] I. F. Vis and E. Ursavas, "Assessment approaches to logistics for offshore wind energy installation," *Sustainable energy technologies and assessments*, 2016.
- [44] D. Energy, "Burbo bank extension owf environmental statement," 2013.
- [45] B. Associates, "Offshore wind: A 2013 supply chain health check," Nov 2013.
- [46] E. Uraz, "Offshore wind turbine transportation & installation analyses planning optimal marine operations for offshore wind projects," Jun 2011.
- [47] Y. T. Muhabie, J.-D. Caprace, C. Petcu, and P. Rigo, "Improving the installation of offshore wind farms by the use of discrete event simulation," *Improving the Installation of Offshore Wind Farms by the use of Discrete Event Simulation*, 2015.
- [48] C178-AIB-V-CA-50001, "Internal source hmc," 2016.
- [49] RoymechX, *Mass Moment of Inertia Hollow Cylinder*, Oct 2018. [Online]. Available: [http://www.roymech.co.uk/Useful\\_Tables/Form/Dynamics\\_inertia.html](http://www.roymech.co.uk/Useful_Tables/Form/Dynamics_inertia.html)
- [50] Efundu, *Mass Moment of Inertia Block*, Oct 2018. [Online]. Available: [http://www.efunda.com/math/solids/solids\\_display.cfm?](http://www.efunda.com/math/solids/solids_display.cfm?)
- [51] H. Goldstein, *Classical mechanics*. Pearson Education India, 2011.
- [52] A. Haas and T. Verschoyle, *Introduction to theoretical physics*. Constable & company ltd., 1928. [Online]. Available: <https://books.google.nl/books?id=VavvAAAAMAAJ>
- [53] J. M. Journée and W. Massie, "Offshore hydrodynamics," *Delft University of Technology*, 2001.
- [54] M. Webster, "Merriam webster's collegiate encyclopedia: The ultimate desk reference," 2000.
- [55] S. E. Ramberg and O. M. Griffin, "Laboratory study of steep and breaking deep water waves," *Journal of Waterway, Port, Coastal, and Ocean Engineering*, 1987.
- [56] S. Hillenius. (2017, nov) Msc thesis - deterministic vessel motion prediction based on a wave radar forecast. [Online]. Available: [file:///C:/Data/Downloads/Thesis\\_Stijn\\_Hillenius\\_09\\_01\\_17\\_FINAL\\_TU.pdf](file:///C:/Data/Downloads/Thesis_Stijn_Hillenius_09_01_17_FINAL_TU.pdf)
- [57] Vestas, "The world's most powerful available wind turbine gets major power boost," Jan 2018. [Online]. Available: <http://www.mhivestasoffshore.com/category/v164-9-5-mw/>
- [58] —, "Brochure v164-8.0mw," Mar 2018. [Online]. Available: [http://www.homepages.ucl.ac.uk/~uceseg/Fluids2/Wind\\_Turbines/Turbines/V164-8MW.pdf](http://www.homepages.ucl.ac.uk/~uceseg/Fluids2/Wind_Turbines/Turbines/V164-8MW.pdf)
- [59] N.-A. Bak, C., "The dtu 10-mw reference wind turbine," May 2013. [Online]. Available: [http://orbit.dtu.dk/files/55645274/The\\_DTU\\_10MW\\_Reference\\_Turbine\\_Christian\\_Bak.pdf](http://orbit.dtu.dk/files/55645274/The_DTU_10MW_Reference_Turbine_Christian_Bak.pdf)